RHEOLOGY OF THICKENED GOLD TAILINGS FOR SURFACE DEPOSITION

A thesis submitted to

the Faculty of Graduate Studies and Research

in partial fulfillment of the requirements for the degree of

Master of Applied Science

by

Shabnam Mizani

B.Sc., University of Tehran, 2007

Department of Civil and Environmental Engineering

Carleton University

Ottawa-Carleton Institute for Environmental Engineering

September 2010

©Shabnam Mizani, 2010

Library and Archives Canada

Published Heritage Branch

395 Wellington Street
Ottawa ON K1A 0N4
Canada

Bibliothèque et Archives Canada

Direction du Patrimoine de l'édition

395, rue Wellington
Ottawa ON K1A 0N4
Canada

Your file Votre référence
ISBN: 978-0-494-71570-3
Our file Notre référence
ISBN: 978-0-494-71570-3

NOTICE:

The author has granted a non-exclusive license allowing Library and Archives Canada to reproduce, publish, archive, preserve, conserve, communicate to the public by telecommunication or on the Internet, loan, distribute and sell theses worldwide, for commercial or non-commercial purposes, in microform, paper, electronic and/or any other formats.

The author retains copyright ownership and moral rights in this thesis. Neither the thesis nor substantial extracts from it may be printed or otherwise reproduced without the author's permission.

AVIS:

L'auteur a accordé une licence non exclusive permettant à la Bibliothèque et Archives Canada de reproduire, publier, archiver, sauvegarder, conserver, transmettre au public par télécommunication ou par l'Internet, prêter, distribuer et vendre des thèses partout dans le monde, à des fins commerciales ou autres, sur support microforme, papier, électronique et/ou autres formats.

L'auteur conserve la propriété du droit d'auteur et des droits moraux qui protège cette thèse. Ni la thèse ni des extraits substantiels de celle-ci ne doivent être imprimés ou autrement reproduits sans son autorisation.

In compliance with the Canadian Privacy Act some supporting forms may have been removed from this thesis.

While these forms may be included in the document page count, their removal does not represent any loss of content from the thesis.

Conformément à la loi canadienne sur la protection de la vie privée, quelques formulaires secondaires ont été enlevés de cette thèse.

Bien que ces formulaires aient inclus dans la pagination, il n'y aura aucun contenu manquant.

Canada

Abstract

Slope and stack geometry are critical parameters affecting the performance of thickened tailing deposits. The geometry of these stacks is in part influenced by the rheological behaviour of the tailings, as well as by depositional parameters such as flow rate. Previous studies on small scale laboratory simulations in flumes showed that the topography of simple geometries can be predicted using equation derived from the Navier-Stokes equation using Lubrication Theory.

One of the difficulties of applying this theory at the field scale, is the potential for change in the rheology of the tailings as they flow. This research investigates this possibility by slowly depositing tailings using single and multilayer tests in a flume. Changes in the rheological properties were quantified by best-fitting the lubrication theory equations to equilibrium profiles.

Results indicate that the yield stress can substantially increase while the tailings are still flowing due to settling and by capillary induced flow into underlying desiccated tailings. This can potentially be used as an advantage by mine operators to reduce the pumping costs related to transportation of thickened tailings.

Acknowledgments

First and foremost I would like express my deep gratitude and sincere thanks to my supervisor, Professor Paul Simms, for his immense guidance, support, and encouragement during the course of my thesis. Thanks to him I learned the skills necessary to conduct research in a professional manner. This work would not have been possible without his continuous direction and feedback.

I would like to thank the Natural Science and Engineering Research Council, Golder Paste Tec and Barrick Gold for funding and providing the tailings.

Finally, I would like to express sincere appreciation to my family for their constant encouragement and support which have allowed me to reach this stage of my life.

To

my parents

Table of Contents

List of Tables

List of Figures

List of Symbols

C_v	Solid concentration by volume
D_{10}	10% passing of cumulative weight of particle size distribution
D_{50}	50% passing of cumulative weight of particle size distribution
D_{60}	60% passing of cumulative weight of particle size distribution
F_r	Froude number
g	Acceleration due to gravity
K	Consistency coefficient
n	Flow behavior index
p	Pressure
Q	Flow rate
R_e	Reynolds number
R_H	Hydraulic radius
S'	Dimensionless slump height
T	Torque
V_t	Transition velocity
γ	Shear rate
η_p	Plastic viscosity
θ_r	Deposition slope
θ	Angle of inclined surface

μ	Viscosity
μ_∞	Limiting viscosity at high shear rate
ρ	Density
τ	Shear stress
τ_y	Yield stress
τ_y'	Dimensionless yield stress

Chapter 1

Introduction

1.1 Introduction

Mining is an integral component of the Canadian and world economies. In Canada, the mining industry contributes $40 billion to the country's Gross Domestic Product (GPD) (MAC 2009). The economic and environmental liabilities associated with conventional management of mine waste are, unfortunately, vast and increasingly unsustainable. The Canadian public is more and more conscious of the risks of improper mine waste management, especially with regards to the oil sands industry. Tailings storage facilities in Northern Alberta are some of the very few man-made structures visible from space.

Mining can be defined as the excavation of subsurface material for the purpose of extracting a valuable mineral. The subsurface material may be excavated by open-pit

mining or underground mining. In "open-pit" mining, a very large pit, sometimes kilometers deep, is excavated to locate veins of the desired ore body. Underground mining involves the excavation of vertical shafts and intersecting horizontal tunnels to access an ore body when open-pit mining is not feasible.

Rock from the ore body is subsequently sent to the mill. The first step in milling or mineral processing is to crush and grind the extracted rock or soil to produce a water-borne suspension of fine particles less than 100 microns in diameter. This reduction in size facilitates the separation of the desired minerals, which is subsequently accomplished by various physical and /or chemical processes. In most kinds of mining, the extracted high value minerals compose less than 1 % of the ore body, leaving the remaining particles, the tailings, as waste. The flow sheet in Figure 1.1, shows a typical sequence of operations in mineral processing (Vick 1990).

Historically, tailings were deposited into rivers and streams, with sometimes the coarser fraction stacked on dry land. Modern practices include backfilling, in which some of the tailings are returned underground to fill the mined out voids (stopes) and to serve as ground support, facilitating greater ore recovery. For surface deposition, modern conventional practice is to deposit the tailings as a slurry, requiring containment in impoundments circumscribed by dams or dykes. Upon deposition, the coarser particles settle closer to the discharge point, whereas the finer and colloidal particles settle farther away from the deposition point. Due to the high water content of the tailings, settling produces a pond that submerges the tailings. Unfortunately, catas-

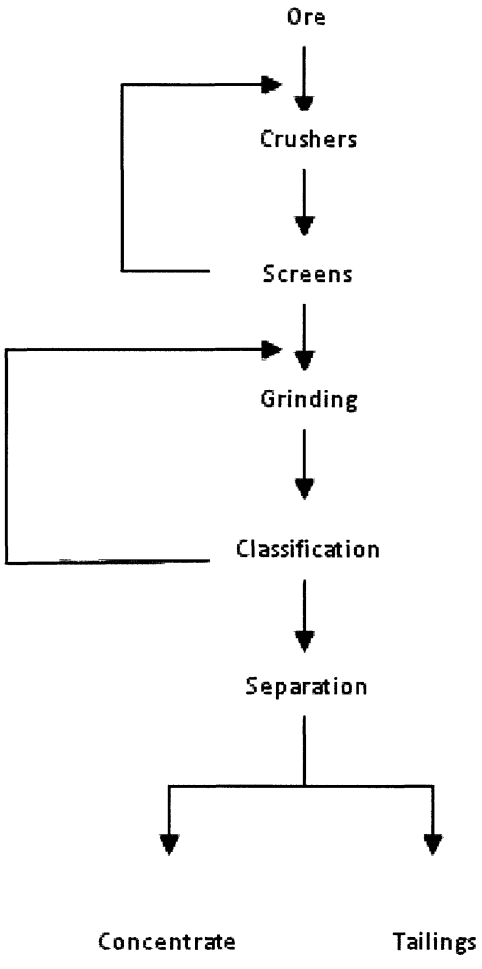

Figure 1.1: Schematic of general mineral processing organization (After Vick 1990)

trophic failures of tailing dams are not uncommon, and flooding of the downstream areas with tailings has resulted in severe economic and environmental devastation, and occasionally loss of life (ICOLD 2001). Accidents or failures often happen as a result of poor water control (dams over-topping) or earthquakes. For example, the failure of the 31m high Merriespruit gold tailing dam in February 1994 resulted in the death of 17 people and severe environmental damages. Approximately $600{,}000m^3$ of liquid tailings were released to the surrounding environment and traveled 3 km

downstream of the tailing dam (Fourie et al. 2001).

Depending on the type of mine the solids concentration (mass of solids / mass of total) of the slurry varies between 25 to 50%. Obtaining and / or treating this large amount of water can be expensive, especially for mines located in arid climates. Also, the escape of polluted water into the environment is another concern associated with conventional deposition. Contaminated water may escape by seepage out of the base of the impoundments (Chalkley et al. 1989).

Another common issue associated with the tailing deposition is Acid Rock Drainage (ARD). Iron-bearing sulphide minerals, which are present in many kinds of ore bodies, tend to react with oxygen, generating acidity. This acidity promotes the dissolution of other minerals present in the tailings. The end result is the generation of acidic pore-waters with high levels of heavy metals and other pollutants such as Arsenic. Acid rock drainage has led to ecological and human health damages and multimillion dollar cleanup costs at hundreds, if not thousands of mine sites in North America (Price 2003).

All these problems have led the disposal of tailings being a major environmental issue and also to increasing regulatory attention. These problems are becoming more serious as individual mining operations are increasing in size. Therefore, the mining industry has been investigating alternative methods for the deposition of mine tailings to reduce environmental liabilities and operational costs.

One such alternative method is called thickened tailings disposal, or TTD. This

technique was pioneered at the Kidd Creek Mine in Northern Ontario in the early 1970s by geotechnical consultant Eli Robinsky (Robinsky 1979). In TTD, the tailings are dewatered before transport to the storage facility, and are then deposited from one or several points, forming stacks of roughly conical geometry. The tailings must be dewatered to the extent where they exhibit some strength or yield stress sufficient to form these gently sloped self-supporting stacks. Thickening is usually achieved by the use of high-density high-rate thickeners, which are similar in concept to sludge thickeners but generally much larger, or in some operations by the use of vacuum filtration. TTD has several advantages over the conventional method as it eliminates the need for high dams and if deposition is cycled between a number of points stability is promoted by both self-weight consolidation and dessication (Sofra and Boger 2002, Thriault et al. 2003, Suttleworth et al. 2005) . Also, water recovery is maximized, which is especially important in areas where water is in short supply (Scola and Landriault, 2007).

Thickened tailings may include relatively wet tailings that are transported as a turbulent flow, and require a minimum pipeline velocity to inhibit settling of particles in the pipe invert. TTD may be also dewatered to the point that they can be transported as a slow moving laminar flow, often called paste tailings (Cincilla et al., 1997). Paste tailings require a certain fraction of fines (20% less than 15 microns) to minimize settling during transport.

One highly studied example of a TTD system is at the Bulyanhulu Gold mine.

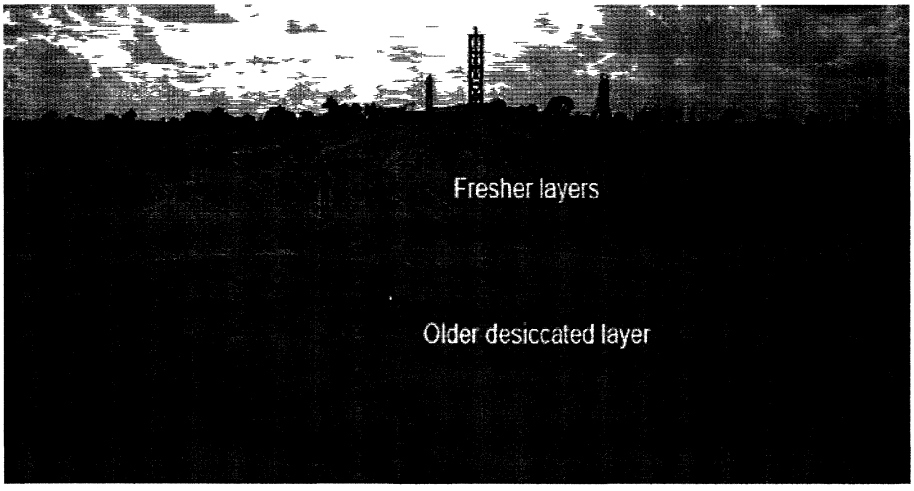

Figure 1.2: Surface deposition of thickened tailings at the Bulyunhulu mine (Picture taken by Jason Crowder)

This mine is located in Northern Tanzania and in a semi-arid climate. The chief economic reason for implementing this technique for this site was to conserve water. Tailings deposition at Bulyanhulu is cycled between multiple towers as shown in Figure 1.2, allowing strength gain and consolidation of the deposited layer and also controlling the evolution of the stack (Theriault et al. 2003).

In a TTD system it is important to understand the rheology of the tailings in order to optimize the disposal and transportation operations. The overall slope of the stack determines the maximum storage capacity, stability, and susceptibility to the stack erosion. The slope is a function of the rheological properties such as yield stress and viscosity as well as operational parameters such as flow rate and topography of underlying layer (Sofra and Boger, 2002).

The deposition geometry of individual layers also controls densification by desiccation, as the thickness of individual layers deposited in a cyclic deposition scheme

regulates the rate of drying (Fisseha et al 2009, Simms et al. 2007). In overly thick layers, non-uniform drying may develop whereby the surfaces of the exposed tailings dry quickly, but the mass of tailings in the layer remain relatively wet and weak. This is due to the well-know regulation of evaporation by total suction (Wilson et al. 1997). Therefore, the rheology of the tailings, by influencing layer thickness also influences consolidation and desiccation, the phenomena responsible for the strength gain of the tailings.

Several investigators have attempted to predict the deposition geometry of these stacks, but as yet there exists no definitive method to predict the over-all beach angle of an impoundment and / or how stack geometry evolves. The state of practice, whereby such angles are predicted, is poor, and at present no reliable method exists for predicting the ultimate slope angle and hence the capacity of a TTD impoundment.

Henriquez and Simms (2009) discovered that simple geometries of surface deposited tailings could be well-described at the laboratory scale using lubrication Theory. Lubrication Theory (LT) is a simplification of the Navier-Stokes equations previously applied to problems such as mud flow analysis. Henriquez and Simms (2009) showed that the overall angle of a deposit is scale-dependent, an important result as field deposition angles are consistently lower than those extrapolated from laboratory tests. However, certain problems were not addressed by Henriqez and Simms (2009), including:

1. The application of lubrication theory to multiple layers and realistic 3-D geometries.

2. Independent measurement of the relevant yield stress used in the Lubrication Theory equations. The relevant yield stress must characterize the behaviour of the tailings as they slow down and stop flowing. The yield stress determined from conventional tests is often applied to calculate friction losses during pipeline transport. This yield stress did not match that value back-calculated from the Lubrication Theory equations.

3. Accounting for changes in yield stress as the tailings flow away from a deposition point.

1.2 Objectives and scope

In the field, new tailings are deposited on top of older desiccated layers. As tailings flow away from the deposition point, for a slow enough flow rate, there may be sufficient time for water loss due to settling and possibly capillary action by underlying desiccated tailings (Figure 1.3). The overall objective of this research is to see how settling and capillary action change the rheology of overland flow and deposition geometry.

To achieve this goal the following experimental work were conducted:

1. Characterization of the rheology of the tailings using several different rheometry

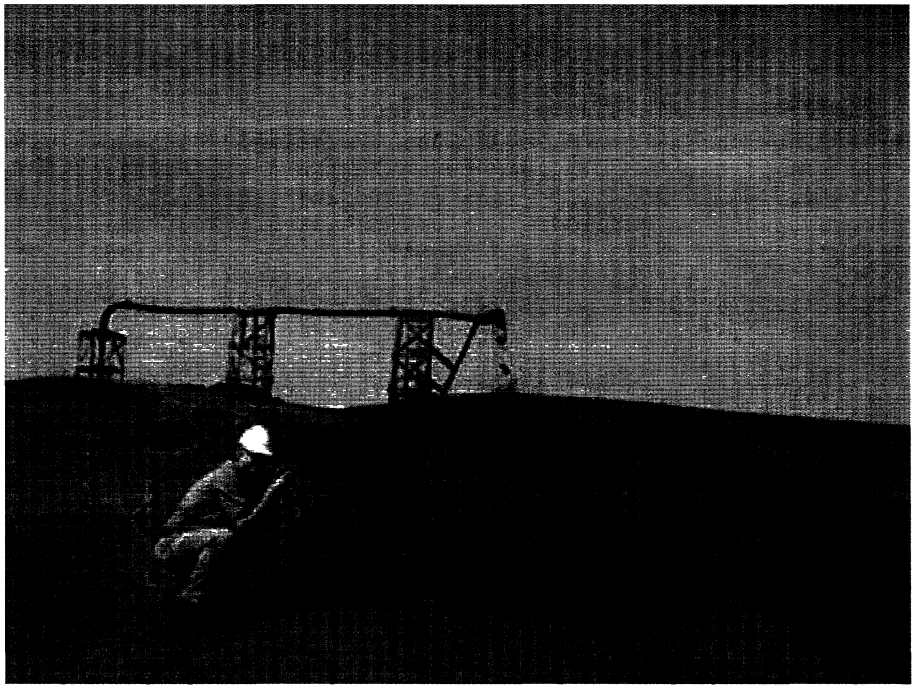

Figure 1.3: Fresh tailings deposited over an older desiccated layer (After Theriaultet al. 2003)

techniques.

2. Depositing tailings at slow flow rates into a flume. To evaluate the influence of settling, tailings were deposited as a single layer at a variety of flow rates. To evaluate the influence of adsorption of water by underlying tailings, fresh layers were deposited onto desiccated layers. The extent of desiccation was monitored using tensiometers. These tests were interpreted by fitting the Lubrication Theory (LT) equations to the equilibrium profiles of the fresh layer, to determine an average value of yield stress. This average yield stress quantifies the extent of "out of pipe" dewatering for each case.

1.3 Outline of the thesis

The outline of the thesis is presented as follow:

Chapter II: Presents a review of tailings and their management related to measurement of rheological properties, and different theories for predicting the geometry of the deposited stack.

Chapter III: Materials and methodology.

Chapter IV: Results and discussion.

Chapter V: Summary and conclusion drawn from the results.

Chapter 2

Literature Review

2.1 Definition of tailings and description of conventional disposal

The term "Tailings" refers to a waste product of mining, which comprises a suspension of fine grained (fine sand to clay size) particles and water. Tailings are generated either by milling of excavated rock, or by the extraction of minerals or bitumen from excavated overburden. Typical particle-size distributions of tailings are shown in in Figure 2.1.

As water is used in various mineral extraction processes, tailings are conventionally disposed as liquid slurry, necessitating confinement in ponds supported by one or more dams (Figure 2.2 picture of two tailings ponds). Typical solids concentrations (mass of solids / total mass) of slurried tailings at deposition are given in Table 2.1

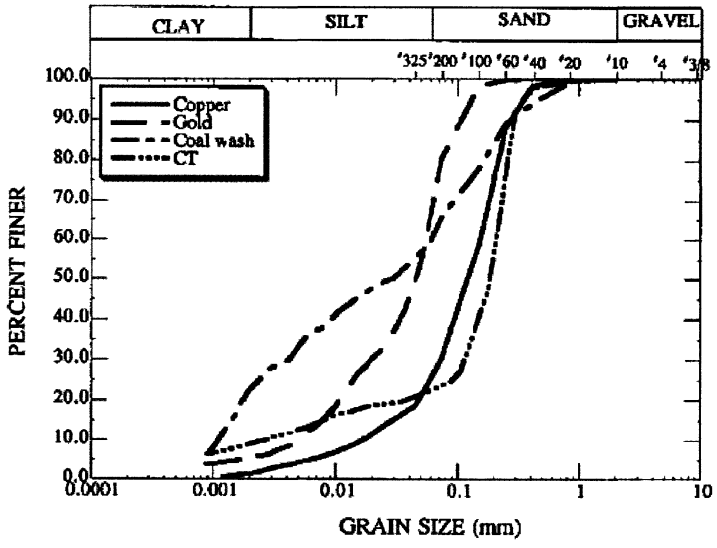

Figure 2.1: Grain size distribution of tailings (After Qui and Sego 2001)

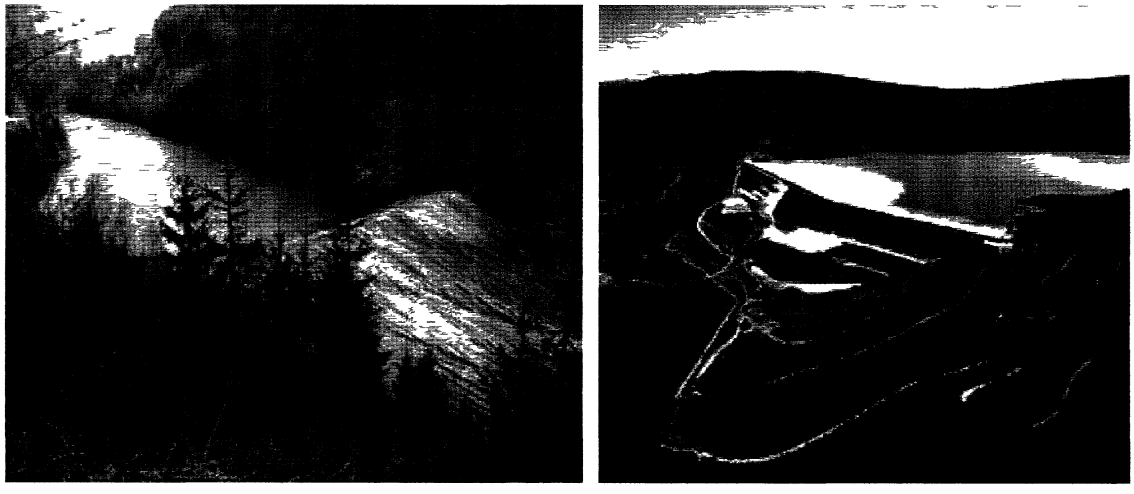

Figure 2.2: Example of tailing dams
(*www.mining-technology.com*)

Slurried tailings are typically transported from the mill to the tailings storage facility in a pressurized pipe, and a minimal velocity is usually required to prevent accumulation of fines in the pipe invert. Tailings may be deposited directly into

a pond, or they can be classified (separated) into "sands" (coarser particles) and "slimes" (finer particles smaller than 75 microns) using a hydrocyclone - the sand fraction is often used to construct the dike of starter dam for the tailings pond. Unclassified tailings will tend to grain-size segregate, the coarser fraction accumulating close to the deposition point. This phenonmenon is often utilized to facilitate dam construction, for example, by the upstream method (Figure 2.3), where the coarse fraction of the tailings are used as a foundation for the later dams due to their faster drainage and consolidation.

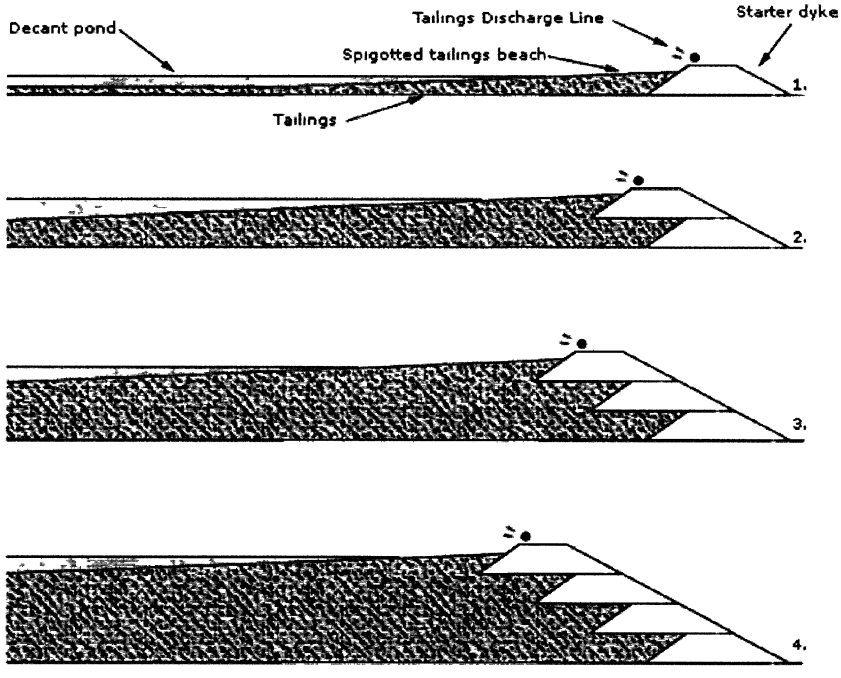

Figure 2.3: Upstream method of embankment construction (*tailings.info/conventional*)

Tailing Type	Slurry	Paste
Mineral sands/ slimes	15	24
Bauxite	27	45
Nickel (HPAL process)	35	45
Base metal	40	75
Gold	45	72

Table 2.1: Comparison of solid concentration of different types of tailings at deposition

2.2 Problems with conventional deposition

Catastrophic failure of tailing dams have unfortunately occurred with ongoing regularity and often with devastating results (ICOLD 2001). Very high dams (100 m+) and the positioning of tailings dams at topographic heights have led to very dramatic failures, in which the tailings flow several kilometers, essentially becoming a toxic landslide, resulting in severe economic and environmental devastation, and occasionally loss of life (Figure 2.4). The failure of tailings dams occur for several different reasons, one possibility being the susceptibility of the fine-grained unconsolidated deposits to static liquefaction. This may be potentially induced by, a rise in the phreatic surface or deposition of more material (Fourie and Tshabalala 2005). In addition, in wet climates tailings at the surface may remain in a soft condition and therefore untrafficable and difficult to reclaim.

Another important problem with conventional deposition involves the loss of water permanently to the tailings impoundment, and the potential for seepage out the base. Consider a typical gold mine that processes 200,000 tons of ore per day for slurry deposition at 50% solids concentration. Approximately 200,000 m^3/d of water is

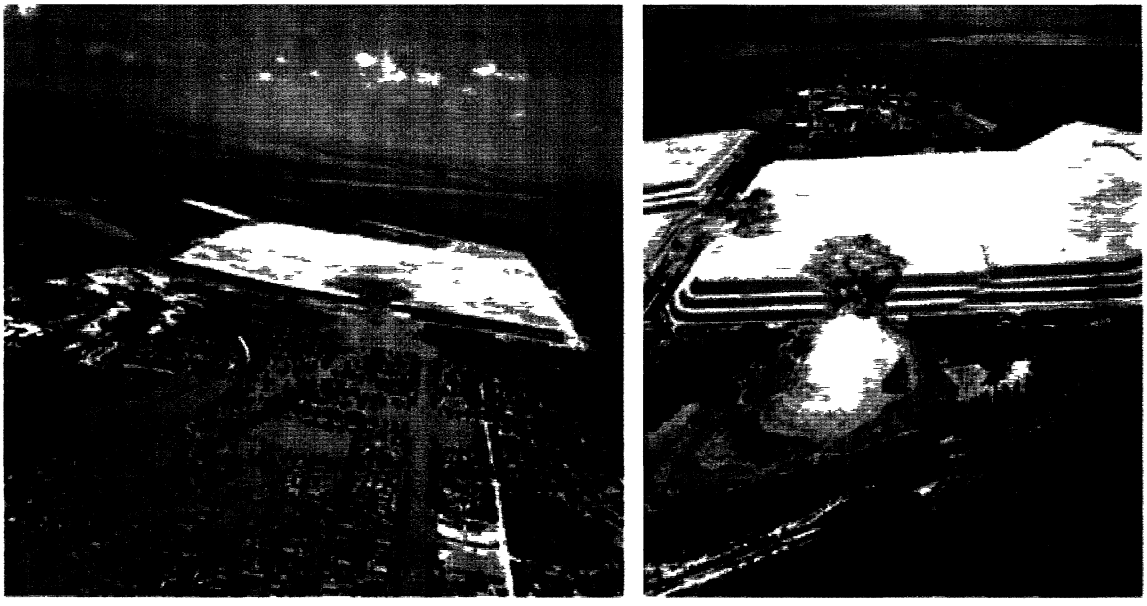

Figure 2.4: Tailings dam failure- Merriespruit tailings dam failure showing the path of the destructive mudflow (on the left). Failures at the Saaiplaas tailings dam (After Fourie et al. 2001).

deposited with the tailings. Some of this water may be recoverable by drawing off the consolidation water from the ponds surface, but this water may require treatment before it can be reused in the mine. The water consumption and water losses to the tailings are very large and represent one of the largest environmental and economic hurdles faced by a mining operation. The sustainability of all mines depends on the availability and cost of water, and in some cases is the crucial economic factor.

2.3 Acid Rock Drainage (ARD)

One of the common environmental issues not unique to conventional deposition, but a common problem for all sulphidic mine waste, is Acid Rock Drainage (ARD). Sulphide

minerals are stable under reducing anoxic conditions encountered deep underground, but when exposed to the atmosphere, will tend to react with oxygen, generating significant acidity, which in term facilitates the dissolution of many other minerals present in mine wastes. The end result is the generation of acidic pore-waters with very high ionic concentration and high levels of heavy metals and toxic non-metals such as arsenic. Acid drainage generation is driven by availability of oxygen, and therefore remediation techniques often focus on limiting the supply of oxygen to mine waste. Acid generation in mine waste and remedial measures such as soil covers and water covers are discussed extensively in the literatures (Jambor and Blowes 2003, Yanful et al. 2004, Wilson et al. 1998, etc.) .

2.4 Thickened tailings

Thickened tailings (TT) are dewatered to the point that they exhibit a minimal strength post-deposition, which allows them to be deposited in gently sloped self-supporting stacks. This reduces both water losses and reliance or elimination of dams and the associated risks of dam failure. It is also desirable that TT are at a sufficiently high solids concentration such that no grain-size segregation occurs during deposition. Tailings may be dewatered to different extents and by different methods. These methods include thickening, using high-density high-rate thickeners (Figure 2.5), similar in concept to sludge thickeners but generally much larger (Jewell and Fourie 2006). Self-compressive forces play a significant role in the thickeners and

therefore, deep beds are required. Comparatively lower moisture content or drier tailings could be gained through filtration. There are two types of filters: vacuum filters (where vacuum is applied for the separation of filtrate and slurry) and pressure filters (in which pressure is applied for this purpose) (Jewell and Fourie 2006).

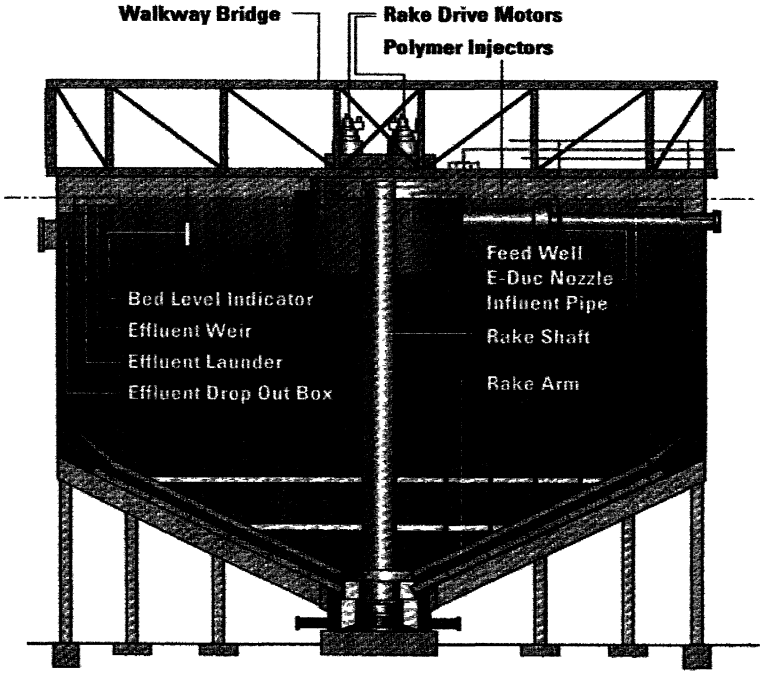

Figure 2.5: Ultra high-density paste thickener(After Jewell and Fourie 2006)

The concept of thickening tailings was suggested by Robinsky in 1965 and also by Shields (1975). Robinsky first implemented a thickened tailings deposition scheme at the Kidd Creek Mine of Timmins, in Northern Ontario in 1973 (Robinsky 1979). Due to the lack of equipment and technology for the dewatering and transportation of these high density tailings, this method was not widely implemented until in relatively recently. Thickened tailings has been frequently used in bauxite mining, but only in

a relatively small though increasing percentage for other kinds of mining. A notable exception is the oil sands, where many oil companies are implementing field trials for thickened tailings due to recent regulatory requirements mandating minimal shear strengths within set times post-deposition (ERCB Directive 074, Houlihan et al 2010). Although pumping technology and thickener designs have improved significantly, lack of familiarity with this technology seems to be the reason for holding back the wide implementation of surface deposition of thickened tailings.

Thickened tailings are ideally non-segregating during deposition, and are considered homogeneous or non-settling slurry where solids are evenly distributed and particle inertial effects are very small.

In order to avoid pipeline segregation of particles, the solid concentration by volume (C_v) must be in excess of 45% (Engman et al 2004). Moreover, 90% of the particles must be less than 80 microns in diameter. These fine particles will prevent segregation when flowing and by retaining colloidal water they avoid bleed water. Paste tailings, a subset of thickened tailings, are tailings that are non-segregating even at very low velocities, such that they can be pumped in the laminar range. This necessitates a sufficiently low solids concentration to manifest a significant yield stress, and that at least 15% of the particles are less than 20 microns in diameter. The transition between turbulent and laminar flow of concentrated suspensions can

be described by the following equation (Wilson, 2006):

$$V_t = 0.4 + 22.1 \left(\frac{\tau_y}{\rho_m} \right)^{0.5} \tag{2.1}$$

where:

τ_y is the yield stress of the flowing material.

ρ_m is the density of the mixture.

V_t is the transition velocity in (m/s)

Some of the advantages associated with TTD are: less demand for tailings pond territory, eliminating the need for tailing dams and associated catastrophic failures and a much shorter lag time before reclamation can begin (Ter-Stepanian,2000).

On the other hand, there are some concerns associated with this new disposal system. These high yield stress materials require high power consumption pumps and therefore high operational costs. Also, the materials should be dewatered to the point that there is a balance between the stability of the deposited tailings after they exit the pipeline and the spreadability of the thickened tailings into the disposal area. Finding the optimum value for the yield stress, which makes operating conditions economical remains a challenge.

Figure 2.6: Graphical representation of a fluid element being sheared

2.5 Rheology

As said earlier, TT is a high concentrated slurry. This material will flow continuously at high shear stresses but will stop at low shear stresses. It needs to flow when it is in pipes and pumps, but should stop when it is in place to allow for stacking. This is characteristic of non-Newtonian behaviour.

2.5.1 Newtonian fluids and Viscosity

Viscosity is the resistance that a fluid shows to flow due to internal friction. When a fluid element is sheared in one plane constantly, the shear strain angle will continuously grow (Figure 2.6); this strain rate is inversely proportional to the coefficient of viscosity. In other words viscosity resists deformation of the material when sheared. Many fluids including water are Newtonian, and show linear relation between shear stress and the strain rate, as given by Newton's law for fluids.

$$\tau = \mu \frac{\delta u}{\delta y} \tag{2.2}$$

Viscosity (μ) is expressed in Pascal-Second (Pa.s). Shear stress (τ) is the force

per unit area and has dimension of Pascal (Pa). Shear rate ($\frac{\delta u}{\delta y}$) is the instantaneous change in velocity across the fluid element perpendicular to the direction of shear and has units of (s^{-1}) (White 1986).

$$\tau = \frac{F}{A} \tag{2.3}$$

2.5.2 Non-Newtonian fluid

2.5.2.1 Yield stress

Yield stress exists in concentrated suspensions and is associated with the inter-particle forces and structure in tailings. The particles may aggregate due to inter-particle force of attraction to form flocs which are thought to form a three dimensional network. Yield stress is often conceptualized as the strength of this network structure and as the force per unit area needed to break this structure down followed by the rupture of the bonds connecting the units (Dzuy and Boger 1983).

At low stresses yield stress materials show solid-like behavior, whereas at high stresses they exhibit liquid-like behavior. That is, below the yield stress these types of fluid deform elastically and upon removal of stress there is a complete strain recovery. On the contrary, when the applied stress exceeds the yield stress, like a viscous material, the material continuously strains and there is no strain recovery. The transition between the solid-like behavior and liquid-like behavior takes place over a range which the material shows both elastic and viscous behavior (viscoelastic flow). The

yield stress may be defined as the transition from elastic to viscous behavior (Liddell and Boger 1996). In tailings, the yield stress increases exponentially with the solid concentration (Clayton et al. 2003).

2.5.2.2 Classification of non-Newtonian fluids

(i) Time-independent fluids:

In this type of fluid the structural changes with time could be ignored, the model is given by the form,

$$\frac{\delta u}{\delta y} = \gamma = f(\tau) \tag{2.4}$$

Which indicates that the rate of shear (γ) is a function of shear stress. These fluids are divided into three types as bellow:

a- Bingham plastics

b- Pseudo-plastic (shear thinning)

c- Dilatant (shear thickening)

Bingham plastic: Materials that exhibit yield stress and behave like solid at low stresses and like a Newtonian fluid at higher values. That is, flow starts when the yield stress is exceeded. Common examples of this type of fluid are slurries, toothpaste and sludge. In other words, when the fluid is at rest its structure has enough rigidity to overcome stresses less than yield stress and therefore deform elastically with complete

recovery when the stress is removed. When this stress is exceeded the fluid behaves as a Newtonian fluid. The rheological equation for a Bingham plastic is as bellow:

$$\begin{cases} \tau - \tau_y = \eta_p \gamma & \tau > \tau_y \\ \gamma = 0 & \tau \leq \tau_y \end{cases} \tag{2.5}$$

where:

τ is the shear stress,

γ is shear rate,

τ_y is the yield stress,

η_p is plastic viscosity representing the slope of the flow curve.

Figure 2.7 shows a typical flow curve of a Bingham flow. (Tanner, 2000)

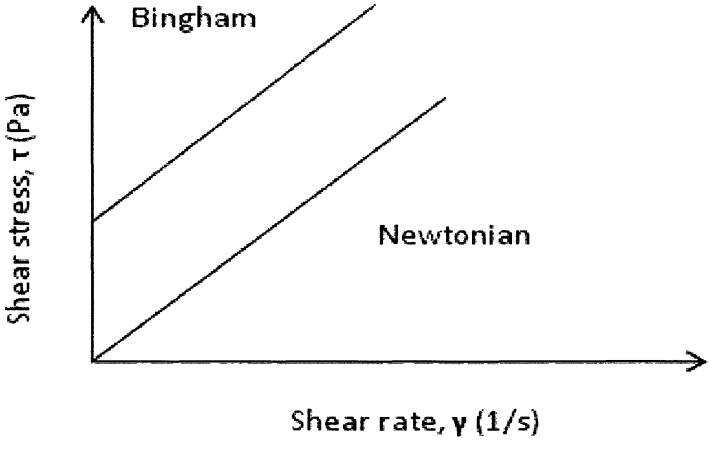

Figure 2.7: Shear stress versus shear rate for a Bingham body.

Pseudo-plastic: in these types of fluid viscosity falls with shear rate and the flow curve becomes linear only when the shear rates reach high values. Moreover,

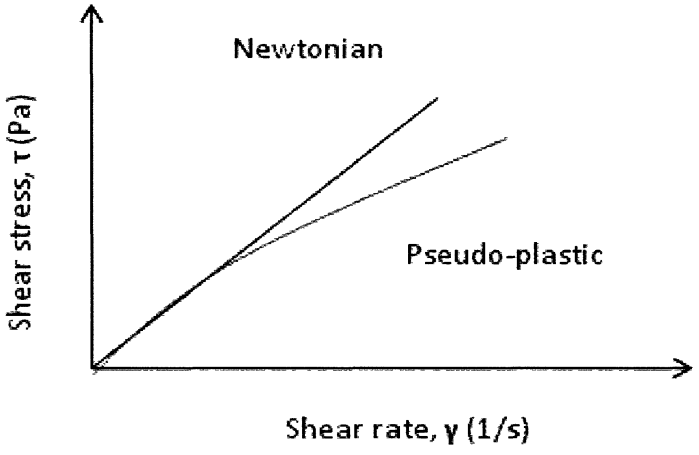

Figure 2.8: Shear stress versus shear rate for a Pseudo-plastic or shear thinning fluid.

these kinds of fluid do not show yield values. A physical interpretation of these phenomenons is that when the rate of shear increases the molecules progressively align in the direction of the shear and show lower resistance to flow and therefore the viscosity decreases.

A power law fluid is used to characterize fluids of this kind:

$$\tau = K\gamma^{n-1}\gamma \tag{2.6}$$

where:

K is the measurement of consistency or viscosity of fluid

n is the measure of degree of non-Newtonian behavior

Dilatant fluid: These fluids also do not show yield stress, however, as the rates

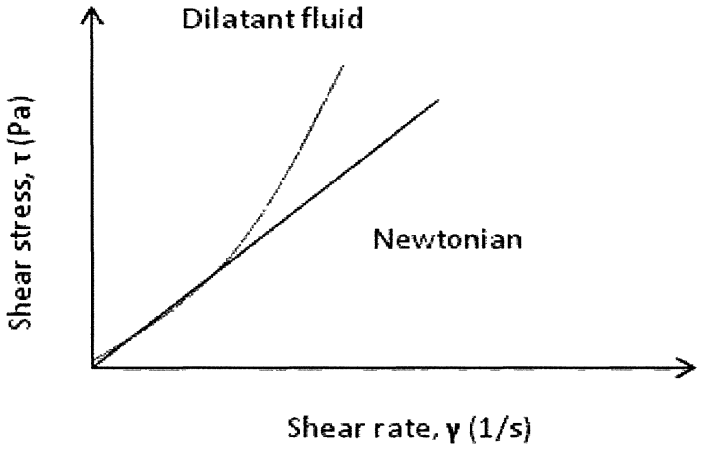

Figure 2.9: Shear stress versus shear rate for a Dilatant fluid.

of shear increase the viscosity of these materials increase. The power law is used for the characterization of these materials but the value for n is higher than unity. This kind of behavior can be explained according to Reynold (1885). He suggested that liquid lubricates the movement of passing one another when sheared in low rates of shearing. However, at higher rates these highly dense packing of particles broke up resulting in expansion or void increase. Now the amount of liquid in the new structure is not enough for lubricating the flow of particles. As a result this new structure is responsible for the viscosity increase with an increase in the shear rate.

(ii) Thixotropic fluids

The present internal structure of these kinds of fluid goes under changes for reasons like flocculation or deflocculation or other factors like chemical reactions. In the simplest case (symmetrical thixotropy), the fluids structure breaks down under

increasing duration of shearing, but will be built up when the shearing of the fluid has stopped. This could be called time-thixotropy as recovery of the structure depends on time alone. Therefore, these fluids exhibit a change in viscosity at constant shear rate with time like slurries (Harris, 1977). One example for a thixotropic fluid is red mud suspension (Nguyen and Boger 1998).

2.5.2.3 Flow curve

Flow curves graphically present the relationship between shear stress and shear rate. A sample of possible flow curves are illustrated in Figure 2.10:

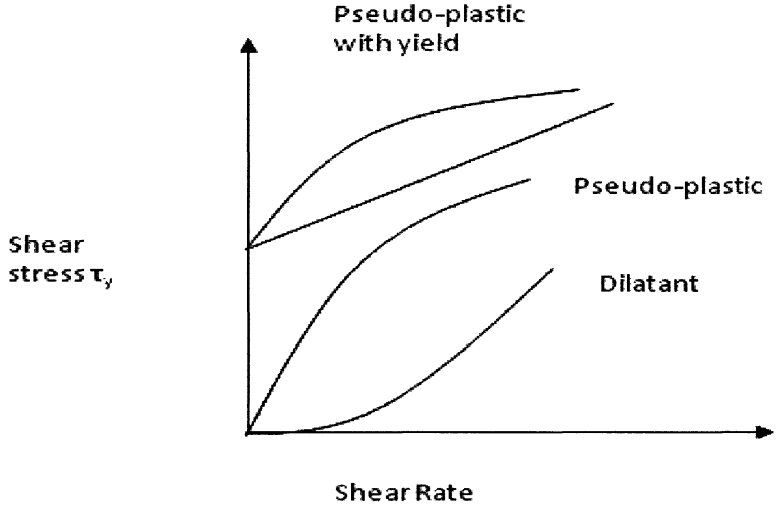

Figure 2.10: Different flow curves showing shear stress shear rate relationships (Rheology workshop, 2010)

2.5.2.4 Rheological Models

- Newtonian:

$$\tau = \mu \frac{du}{dy} = \mu\gamma \tag{2.7}$$

- Power law:

$$\tau = K\gamma^n \tag{2.8}$$

  - Pseudo-plastic: $n < 1$ (shear thinning)
  - Dilatant: $n > 1$ (shear thickening)

- Bingham plastic:

$$\tau = \tau_y + \eta_B\gamma \tag{2.9}$$

- Casson plastic:

$$\tau^{0.5} = \tau_y^{0.5} + (\eta_c\gamma)^{0.5} \tag{2.10}$$

$$\tau^{0.5} = \tau_y + \eta_c\gamma + (\sqrt{4\tau_y})\gamma^{0.5} \tag{2.11}$$

These constitutive equations can be grouped in two categories described by the following models:

1. Yield pseudo-plastic (Herschel- bulkley Model)

$$\tau = \tau_y + K\gamma^n \tag{2.12}$$

2. Yield plastic (Halborn 2008, Halborn and Klein 2009)

$$\tau^k = \tau_y^k + (\mu_\infty \gamma)^k \tag{2.13}$$

where:

τ is shear stress(Pa)

τ_y is yield stress (Pa)

K is consistency coefficient $(Pa - s^n)$

n is flow behavior index

μ_∞ is plastic viscosity (Pa-s), limiting viscosity at high shear rate

k is scaling factor

μ_B and μ_C are viscosity (Pa-s)

Flow curve of thickened tailings have been alternatively described by several different models: including the Bingham and Herschel and Bulkley model (Kwak et al. 2005, and Dzuy and Boger 1983).

2.6 Measurement of Rheological Properties

2.6.1 Types of Rheometer

The rheological characteristics of a fluid can be measured using a rheometer. There are many types of rheometer, including:

- Rotational Viscometer
- Yield stress measurement devices
- Tube viscometer
- Online viscometer
- Slump cylinder/cone

2.6.2 Rotational Viscometer

There are different types of rotational viscometer:

- Cone and plate
- Concentric cylinder
- Plate-plate
- Bob only (Brookfield)
- Vane

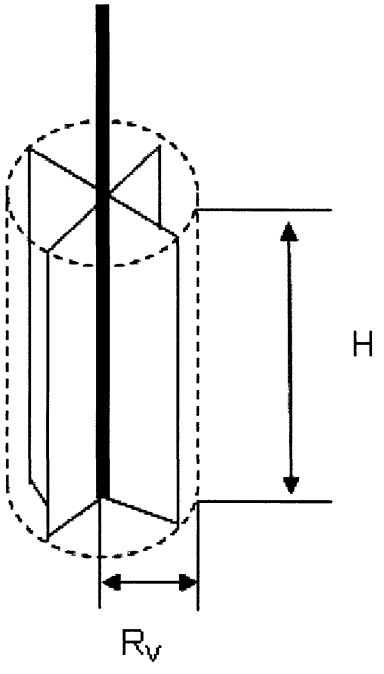

Figure 2.11: Schematic diagram of a vane fixture

A rotational viscometer with a vane fixture was used in this research.

2.6.2.1 Vane

A vane consists of 2 to 8 thin blades arranged at equal angles around a shaft (see Figure 2.11). The vane has been used previously by different authors J. L. Russell (1936), Hobson (1940) and M. Keentok (1982) (Dzuy and Boger 1983). The torque required to turn the vane is related to the static yield stress on the cylinder that is cut through. This instrument is suitable for concentrated slurries and paste that have significant values of yield stress as it eliminates the effects of wall slip observed with rotating viscometers.

The two other advantages of the vane geometry over other conventional geometries

are: (Dzuy and Boger 1983)

- Allowing the material to yield under static conditions, and within itself.
- Keeping the errors associated by the intrusion of the vane into the material to a minimum value (the intrusion does not break the internal structure).

2.6.3 Yield Stress measurement

The common techniques used for measuring the yield stress are the "direct" and "indirect" methods. The indirect methods are based on fitting the shear stress/shear rate data to one of the rheological model equations and extrapolating the fitted curve to zero shear rate. The yield stress gained from this method is very dependent on the applicability of the assumed model to the behavior of the material. Due to problems related to slip flow, fracture and expulsion of sample in the low shear rates, extrapolation of shear stress is difficult in this range (Lideell and Boger 1996). Moreover, low shear rate data are required which are rather hard to achieve. For this thesis it will be seen that the low shear rate zone is of the most interest.

Common examples of direct measurement of the yield stress, where the measurement of the yield stress depends on the assessment of the stress which the fluid starts to flow, are stress growth, creep/recovery, and stress relaxation.

i) Rate controlled mode (Stress Growth)

In the stress growth technique, a low and constant shear rate is applied to the vane and the torque is measured as a function of time. The torque is then converted to shear

stress assuming that the stress is distributed uniformly along the sheared cylindrical surface. In many materials, four distinct stages can be identified from the stress-time profile: a linear increase in the shear stress followed by a non-linear behavior, a peak stress and finally a stress decay region (Figure 2.12). The linear region is assumed to correspond to elastic deformation while the non-linear region represents the viscoelastic flow where the breaking of the network bonds occurs and they get stretched above their elastic limits (Liddell and Boger 1996). After the maximum stress the material starts to flow like a viscous liquid and the stress decreases after this peak as the fluid disintegrates completely.

Three yield stresses may be defined for some materials. The static yield stress, (τ_{y1}), corresponds to the transition from an elastic fluid to a viscoelastic behavior, the dynamic yield stress, (τ_{y2}), corresponds to the change between viscoelastic and viscous behavior, and residual stress τ_{y3} , which happens at equilibrium state (Kwak et al. 2005 and Liddell and Boger 1996).

Analysis

In the vane method when the torque reaches its highest value it is said to be the yielding moment. Therefore, for determination of the yield stress from the maximum torque it is assumed that the total torque is the combination of shearing on the cylindrical surface circumscribing the vane and the two end surfaces.

$$T = (2\pi R_v H)\tau_w R_v + 2[2\pi \int_0^{R_v} \tau_e(r) r dr r] \tag{2.14}$$

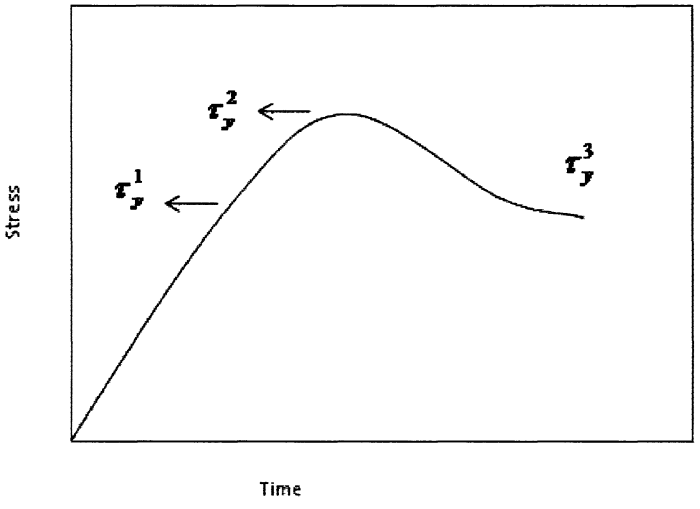

Figure 2.12: A typical stress-time profile in a rate controlled mode with possible definitions of yield stress (After Liddell and Boger 1996)

where,

T is the measured torque

R_v is the radius of the vane

τ_w is the shear stress at the cylindrical wall

τ_e is shear stress at the end surface as a function of radial position

H is length of the vane

For small diameter vanes, it can be assumed that the shear stress at the ends is uniformly distributed and that it is equal to the shear stress at the cylindrical wall. As a result Equation 2.14 reduces to:

$$T = \frac{\pi D_v^3}{2}\left(\frac{H}{D_v} + \frac{1}{3}\right)\tau_y \tag{2.15}$$

From the measured torque and the vane dimensions the materials yield stress can be easily calculated.

ii) Stress controlled mode

This mode could be operated in two ways. First, a constant stress is exerted in steps and the strain is measured as a function of time for each step. The material shows elastic behavior below the yield stress and the strain increases towards a constant value. Whereas, it increases indefinitely with time when the stress goes above the yield stress. In the second method a constant stress-rate is exerted to the vane while the strain is measured as function of stress. When a sudden increase in the strain is observed it is said that the yield stress is reached.

iii) Stress Relaxation Method

In this technique the suspension is first sheared at a constant shear rate. The speed is then reduced slowly or suddenly to zero, the yield stress is equal to the value of the shear stress exerted by the material on the rotating body. It is said that the material has a true yield stress if the residual stress remains constant for a relatively long time of relaxation, in stopping the vane from returning to its original position (Dzuy and Boger 1983). A schematic of this procedure is shown in the following Figure 2.13.

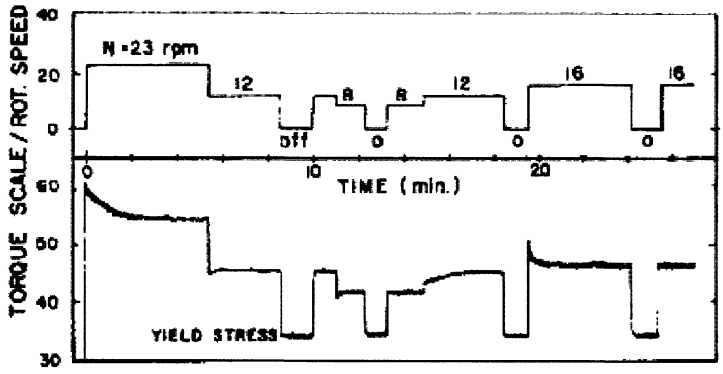

Figure 2.13: Schematic of the stress relaxation method procedure (After Duzy and Boger1983).

2.6.4 Slump Test

The ASTM standard cone slump test (ASTM 1998) was originally developed to evaluate the workability or consistency of concrete. The slump test has since been adapted to measure the workability of other time-independent materials such as mineral tailings suspensions. The slump test is applicable in surface and underground tailing disposal as a mean to measure the yield stress, where it is an important parameter in tailings transport design.

Both the cylindrical and cone shaped containers have been used for the slump test for mine tailings. A cylindrical geometry has been found to be more practical than the cone. Previous studies (Clayton et al. 2003) have shown that yield stresses measured from slump tests on titanium dioxide pigment suspension and a Cannington paste sample (a mineral tailings paste) using a cone model did not show good agreement with yield stresses using a vane technique, whereas better agreement was found using a cylinder. Using a cylinder has other advantages over the cone slump test; the

simple geometry makes it easy to fill. The complex geometry of the cone leads to air bubbles while filling it, which can then affect the result. Furthermore, at high yield stresses the shape of the slumped material is less consistent for the cone. In addition, the cylinder-based slump could be easily completed with a part of a pipe or even a can. Finally, cylindrical geometry slump test are easier for a single person to use. When a cone is filled from a small opening in the top, hydrostatic forces lift the cone, therefore the cone needs to be held down during filling (Hallborn, 2010). There are several models for relating the slump value (drop height) to a corresponding yield stress.

Analysis

In the model developed by Pashias et al. (1996) it is assumed that the maximum shear stress is the same as half the hydrostatic pressure; therefore, the stress increases linearly with depth from zero at the top to its maximum value at the bottom (Figure 2.14). After lifting the cylinder and cessation of flow the height stops decreasing at the depth where the shear stress drops below the yield stress. The geometry of the material above the yield surface is assumed to remain cylindrical and sink as the material beneath it flows. A dimensionless slump can then be related to yield stress by the following equation:

$$S' = 1 - 2\tau_y' \lfloor 1 - Ln(2\tau_y') \rfloor \tag{2.16}$$

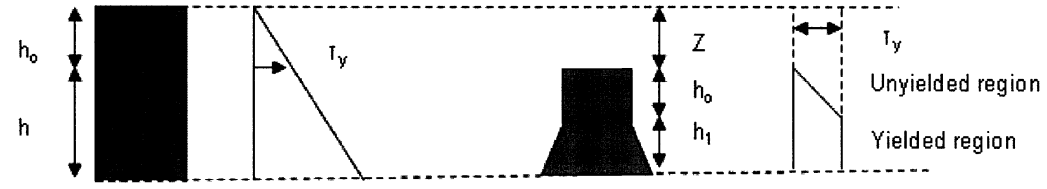

Figure 2.14: Example of a Slump test, where z is the settling height and H is the height of the cylinder (After Pashias et al. 1996)

This equation can be simplified by expanding $Ln(2\tau')$ into the infinite series

$$\tau'_y = \frac{1}{2} - \frac{1}{2}(\sqrt{s'}) \tag{2.17}$$

where

τ'_y is dimensionless yield stress

s' is dimensionless slump height $S' = \frac{Z}{H}$

The yield stress is then calculated by multiplying the dimensionless yield stress by the unit weight and height of the cylinder

$$\tau'_y = \frac{\tau_y}{\rho g H} \tag{2.18}$$

Combining the above equations gives:

$$\tau_y = \rho g H 0.5(1 - \sqrt{\frac{z}{H}}) \tag{2.19}$$

It should be pointed that in the derivation it is assumed that the horizontal planes

remain horizontal, the friction between the material and the walls of the cylinder are ignored; also,the relation assumed between the pressure to stress distribution is that for an elastic solid.

2.7 Comparison of yield stress measurement methods

As presented earlier, indirect methods are based on fitting the shear stress shear rate data to one of the rheological model equations and extrapolated the fitted curve to zero shear rate. The yield stress gained from this method is very dependent on the applicability of the assumed model to the behavior of the material. For example, a lot of researchers have used the Bingham model, though in concentrated suspensions this model overestimates the yield stress and even sometimes predicts a yield stress where one does not exist (Crowley and Kitzes, 1957). Therefore, for suspensions showing nonlinear plastic behavior, the Casson or Herschel Bulkley equations may better predict the yield stress. Values gained for the yield stress of titanium dioxide suspension in a study conducted by Dzuy and Boger by different methods are compared in the following Table.

Method	Yield stress(N/m^2)
Bingham	(234+282)/2=258
Herschel-Bulkley	125
Casson	128
Stress Relaxation (Concentric cylinder)	106+/- 10
Vane (Stress growth)	126

Table 2.2: Yield stress results with 37.3%TiO2 suspension (Nguyen and Boger 1983)

2.8 Physical properties affecting rheology of tailings

The flow behavior of the tailings is strongly influenced by its rheological properties like viscosity and yield stress. On the other hand these parameters themselves are affected by the physical properties:

2.8.1 Carrier fluid viscosity

For some fluids even a small change in the temperature could result in significant variation in the viscosity of the fluid (Wright, 1977). Crowder (2004) performed flume tests on tailings for a range of temperatures and found significant differences in the behavior when the temperature was increased from 20 to 40^0C.

2.8.2 Solid content

As the slurry concentration increases the particles interaction (viscosity) increases due to hydrodynamic and granuloviscous effects. A material with high solid concentration

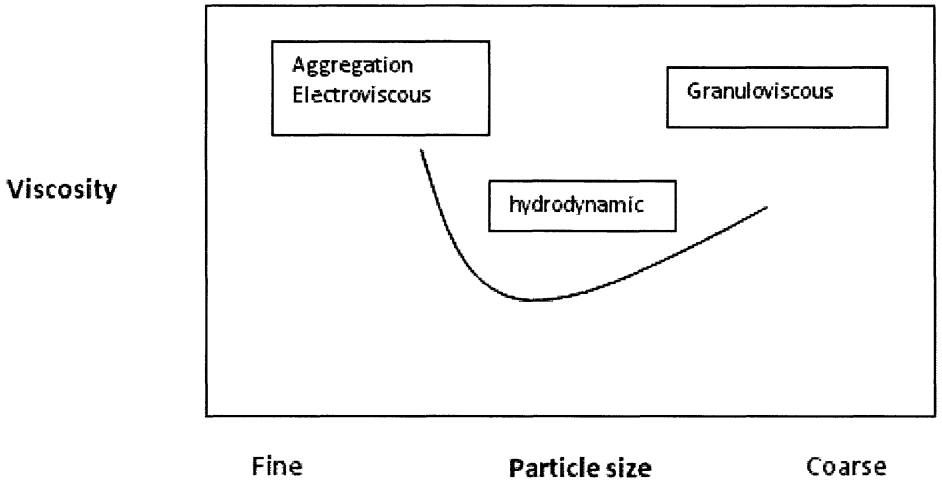

Figure 2.15: The influence of particle size on viscosity (Rheology workshop, 2010)

will exhibit higher yield stress.

2.8.3 Particle size and size distribution

Aggregation, electroviscous and hydrodynamic effects increase as the particle size of the material decreases. On the other hand, as the particle size increases the granuloviscous effects become higher. For example, the minimum viscosity for quartz particle occurs at a particle diameter of 16 μm (Clarke 1967).

Rheology is also dependent on the particle size distribution. For example, suspensions with wide distributions show lower viscosity in comparison to the ones with a narrow distribution. That is probably due to the particle packing effects (Rheology workshop, 2010).

2.8.4 Surface properties of particles

2.8.4.1 Chemical additives (coagulant, dispersants, flocculants)

Yield stress is defined as the maximum force that the particle network of a suspension can withstand before rupturing (Mpofa, 2003); therefore, it is related to the inter-particle forces. The inter-particle forces such as the van der Waals and electrostatic forces are responsible for flocculation or dispersion of the suspension. Figure 2.16 shows the combined surface effects. The magnitude of the various inter-particle forces are related to the pore water chemistry as well as temperature.

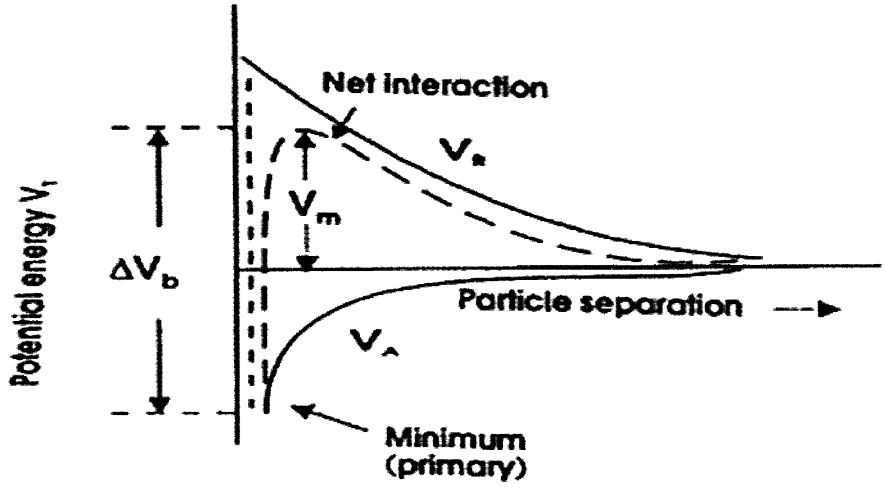

Figure 2.16: Combined surface charge effects (Modified from Rowe et al. 1995)

2.8.4.2 ph and Dissolved ions

ph- For a given material, there is a ph such that the surface charge is minimum, called the Iso-electric point (iep), where the Van der Waals forces overcome the repulsion forces leading to aggregation. As the ph becomes lower or higher, viscosity and yield

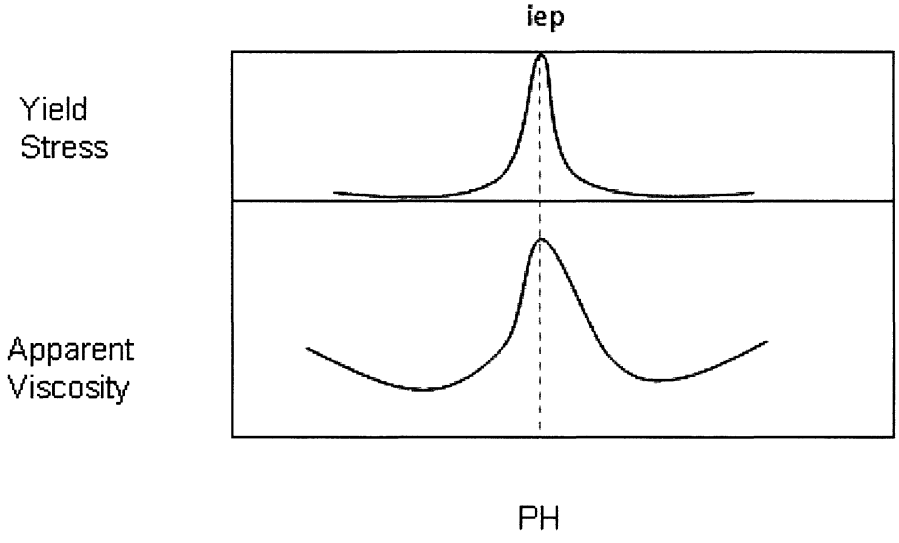

Figure 2.17: Effects of Ph on rheological properties (Rheology workshop, 2010)

stress decreases. This is, due to the particles increased dispersion as electrostatic repulsion increases (Figure 2.17). Extreme repulsive interaction results in highly dispersed suspensions which do not exhibit yield stress but rather Newtonian behaviour (Leong and Boger 1990).

Dissolved ions- Dissolved species, in a similar way, affect the rheology by enhancing or reducing aggregation as a result of reducing or increasing the surface charge on particles.

2.9 Post-deposition behavior of tailings

The flow of thickened tailings away from the deposition point and the consequent geometry of the stack have important consequences for the management of these

facilities. The geometry of the stack and in particular the overall slope determines the footprint, storage capacity, susceptibility to erosion and slope stability. Moreover, these tailings should be reclaimed and for purposes such as revegetation, soil covers should be installed. If the slope is too steep then the design and installation will be more challenging. Also, the perimeter bonds (dams) are designed based on the predicted slope and it is necessary for them to be able to retain rain runoff and decant water. Rheology also indirectly controls densification by desiccation and oxidation during deposition (Figure 2.18), as the thickness of individual layers deposited in a cyclic deposition scheme regulates the rate of drying (Fisseha et al 2009, Simms et al. 2007).

Previous studies (Henriquez 2008) have shown that the geometry of freshly deposited tailings cannot be characterized by a single angle and that the geometry is dependent on the scale (Figure 2.19). That is the reason why there is not a good correlation between the angle measured in the laboratory flume tests and in the field scale (Oxenford and Lord 2006, Engman et al. 2004).

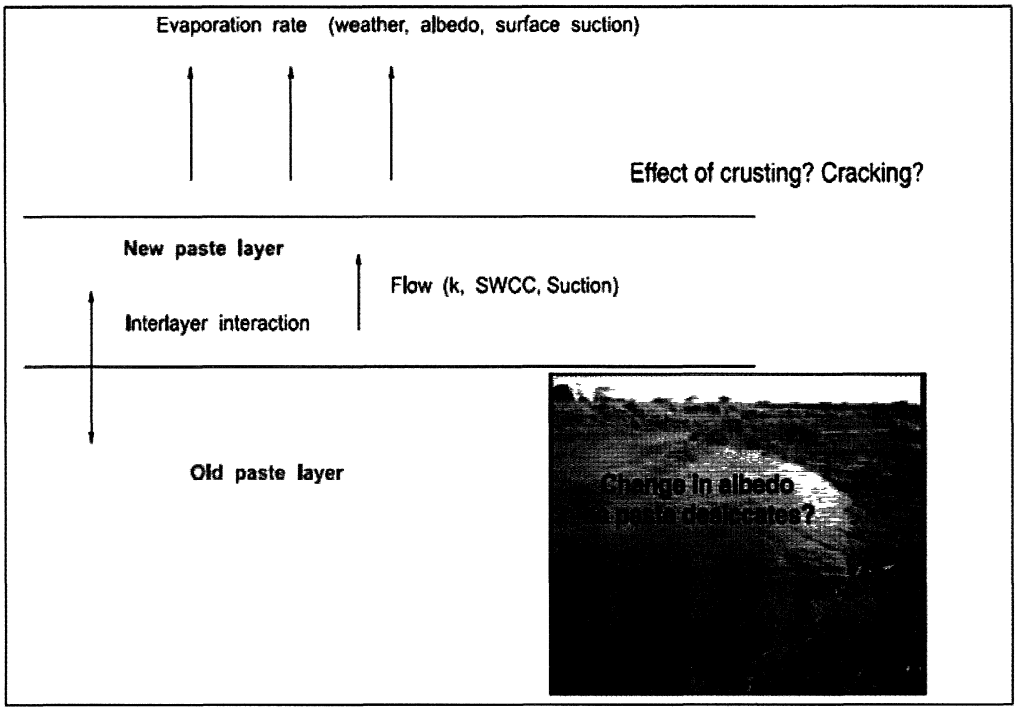

Figure 2.18: Factors affecting drying of freshly deposited layer (After Simms et al. 2007)

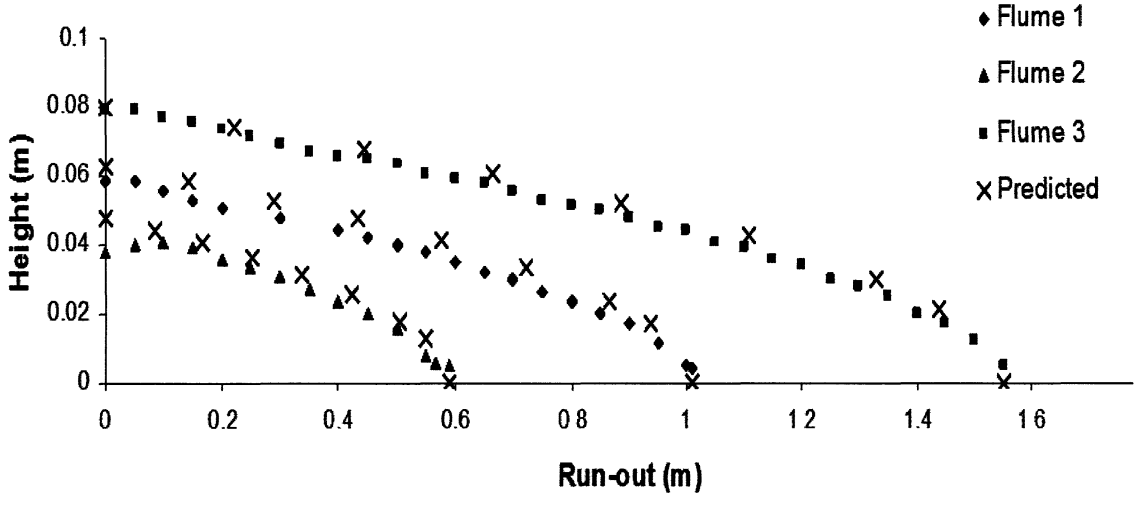

Figure 2.19: Three different single layer flows at 40% gravimetric water content at different volumes (After Henriquez and Simms, 2008).

In general, the final angle of the stack is a function of dewatering of the tailings, material properties, the scale of deposition, the deposition plan (cyclic versus continuous) and climate. For example, in the cyclic deposition plan, thinner layers will be formed leading to steeper slopes. An increase in the slope of the deposition will allow more tailings to be stored and therefore a more efficient use of the disposal area (Heniquez and Simms 2009).

As this thesis studies the evolution of the rheological properties of the tailings after they emerge from the pipe, it is important to understand the phenomena that may contribute to dewatering of the tailings while they are still flowing.

It is known for hard rock thickened tailings that the volume reduces post-deposition by both hindered settling and desiccation. Even for highly thickened paste gold tailings, hindered settling can result in a substantial decrease in void ratio- from one site where gold tailings were deposited at 40% gravimetric water content the void ratio decreased from 1.4 to 1.0 due to settling alone in 2 days (Fisseha, 2008). Also, dewatering post-deposition may be maximized by aggregate-promoting materials, such as polymers or lime (Matthews et al. 2002 and http://www.suncor.com/en/newsroom/2625.aspx?id=3233).

Desiccation, which may occur by both evaporation, drainage or capillary action by underlying layer, can further reduce volume to the shrinkage limit of the material. Evaporation-driven desiccation and subsequent desaturation of thickened gold tailings has been studied by Simms et all. (2007), Fisseha et al. (2010), Simms et al. 2010,

Dunmola and Simms (2010).

Consequently a drier tailings will be gained if the thickness of the layer is reduced or the drying time increases. The thickness of the deposited tailing depends on tailings rheology and deposition time. Generally, as the tailings become drier they will occupy less volume and become stronger. However, excess evaporation and drying will lead to an increase in the risk of oxidation and therefore acid generation. At water contents lower than the Air Entry Value the risk of acid generation increases. As a result, the optimal drying time requires the knowledge of unsaturated hydraulic and volume change behavior as well as the top and bottom boundary (Fahey and Newson, 2003).

2.9.1 Theories on stack geometry

By studying the different theories proposed by different authors it seems that a uniform view of the mechanism which governs the tailing deposition and beach formation does not exist. Some studies have concentrated on the behavior of the tailings in the laminar region and estimating the beach slope once the flow becomes stationary (Henriquez and Simms, 2009). By contrast, other authors such as Fitton et al. (2006), Pirouz and Williams (2007), have built their theories assuming a more complex system of sheets and fans.

Fitton et al. (2006), for example, predicted the equilibrium slope of a tailing channel based on a semi-empirical turbulent open channel. The empirical fit gives the relation between depth and flow under equilibrium condition, which has been

shown to be in turbulence flow condition and therefore nonsegregating.

$$d = 12.2Q^{0.6} \tag{2.20}$$

Where:

Q is the flow rate in liters per second.

d is the depth of flow in millimeters.

This relation is then used for the beach slope calculation using a critical velocity (V_t).

$$i = 100 \tan(\arcsin 0.073V_T^2 / \left(\frac{8\rho V_T^2}{\tau_y + K(2V_T/R_H)^N}\right)^{0.25} 2R_H g) \tag{2.21}$$

Where:

ρ is the slurry density.

V_T is the average velocity in the channel below which sedimentation will occur

τ_y is the yield stress of the slurry

R_H is the hydraulic radius

K is the fluid consistency index from Herschel and Bulkley model

i is the channel bed angle (equivalent to slope ($i\%$))

Pirouz and Williams (2007), predicted the overall slope of the beach based on the slope of self-formed tailing channels, where the flow in the channel is a "steady state total transport uniform turbulent flow". The overall beach slope is determined based on the minimum slope required in order to create the steady state turbulent total

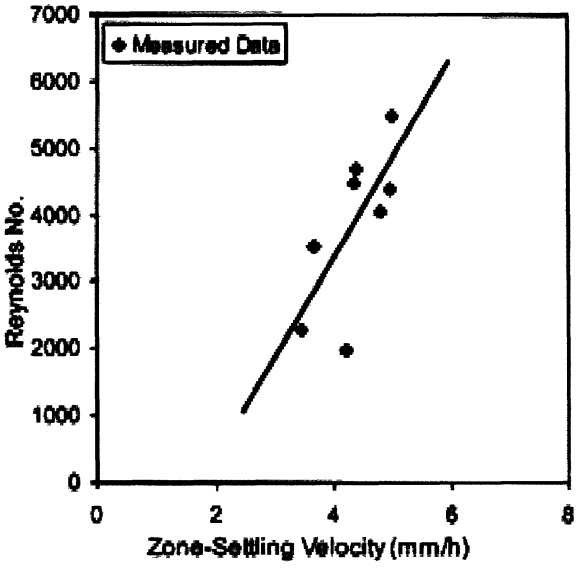

Figure 2.20: The relation between the Reynolds number and the zone settling velocity from the full scale flume tests (After Pirouz and Williams 2007).

transport flow condition. The level of turbulence should be enough to overcome the zone settling velocity of the tailing particles (Figure 2.20) using the empirical relation which exists between the zone settling velocity and the Reynolds number or the level of turbulence. The zone settling velocity is a function of initial solid percent and rheology which could be determined using a special laboratory technique.

McPhail et al (1995) advanced a scaling technique based on energy dissipation of velocity head of the material as it flows away from the pipe.

Kwak et al (2005), using a flume apparatus and under laboratory conditions, showed that the angle of repose increases linearly with yield stress. This relation was similar to the findings of Sofra and Boger(2001). Sofra and Boger(2001) presented a model which the deposition slope is presented as a ratio of factors resisting the flow

to the factors generating the flow.

$$\theta_r = f\left(\frac{\tau_y F_r}{R_e}\right) \tag{2.22}$$

Where:

$$R_e = \frac{wv\rho}{\eta_p} \tag{2.23}$$

$$F_r = \frac{v^2}{wg} \tag{2.24}$$

and,

w is the flume width

v is the flow velocity

ρ is the density

2.9.2 Lubrication Theory

In this theory, a yield stress fluid model is used for describing the equilibrium geometry of the stack. Several assumptions are used in order to simplify the Navier-Stokes momentum and continuity equations, such as: very small thickness to length ratios, homogeneous fluid and a very small velocity such that the ratio of inertia to viscous forces will vanish from the equations. These simplified momentum and continuity equations have been solved analytically for yield stress fluids under special geometries and special conditions by several researchers, for applications such as mud or lava flow

(Yuhi and Mei, 2004; Liu and Mei, 1990; Coussot and Proust, 1996).

$$\rho g \sin\theta - \frac{\partial p}{\partial x} + \frac{\partial \tau}{\partial z} = 0 \tag{2.25}$$

Where,

ρ is density

g is acceleration due to gravity

p is the pressure

τ is shear stress

θ is the angle of inclined surface

If it is further assumed that the pressure distribution is hydrostatic (Figure2.21):

$$P = \rho g(h - z)\cos\theta \tag{2.26}$$

Then differentiating Equation 2.26 to substitute it into the left-hand side of Equation 2.25 , and solving for the shear stress:

$$\tau = \rho g(h - z)\cos\theta \left(\tan\theta - \frac{\partial h}{\partial x}\right) \tag{2.27}$$

When the bed stress exceeds the yield stress fluid flow starts. The yield surface is where shear stress equals the yield stress. Assuming a flat bed and putting $z = 0$

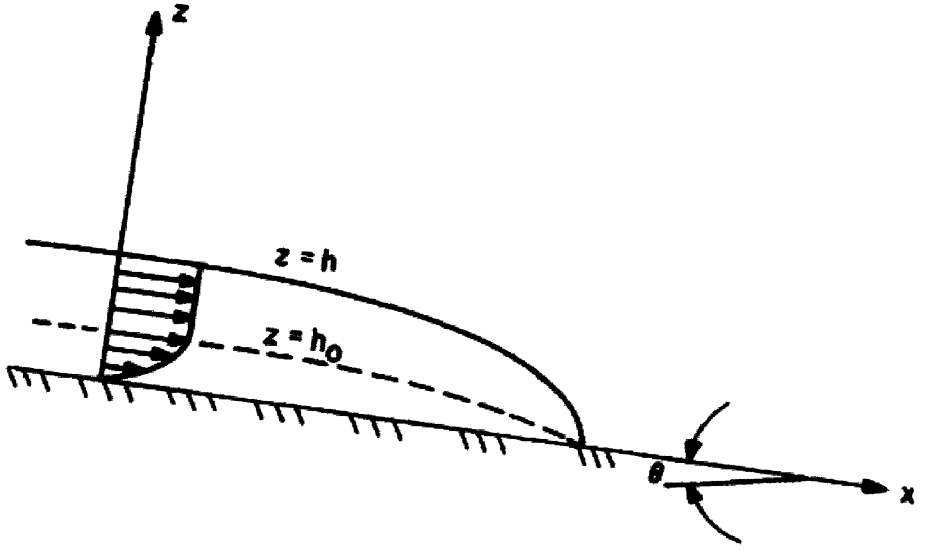

Figure 2.21: Geometry used in description of Lubrication Theory equations for spreading on an inclined plane (After liu and Mei 1990).

the following expression can be gained for a steady state profile of a Bingham fluid:

$$\tau_y(x - x_0) = \frac{\rho g}{2}(h^2 - h_0^2) \tag{2.28}$$

where h_0 is the height at x_0

Yuhi and Mei (2004), described the two and three dimensional slow spreading of fluid mud over a gently sloped conical surface as bellow:

$$h' - h'_0 + Ln(1 - h') = x' - x'_0 \tag{2.29}$$

Where

$$h = h' \left(\frac{\tau_y}{\rho g \sin \theta} \right) \tag{2.30}$$

$$x = x' \cot \theta \left(\frac{\tau_y}{\rho g \sin \theta} \right) \tag{2.31}$$

Note that here z and x are the vertical and horizontal directions, not along the slope or perpendicular to the slope.

Simms (2007) and Henriquez and Simms (2009) examined the applicability of Equations 2.28 and 2.29, the results showed a good agreement for small scale tests in laboratory flume for kaolinite and gold tailings, for single and two-layer deposits. This thesis will use the Lubrication Theory Equations to evaluate changes in the rheological properties during deposition.

Chapter 3

Materials and Methods

3.1 Characteristics of tailings

Gold tailings were obtained from the Bulyanhulu mine located in the North West of Tanzania, Africa. Tailings were collected from the site at the tailings plant before pumping and were then shipped to Carleton University in plastic buckets. They were shipped at a geotechnical gravimetric water content (GWC) of 38%, corresponding to a solid concentration of 70%, but undergone settling due to vibration during transport. The tailings arrived with a layer of water on top, giving the settled tailings a GWC of 25%. The bleed water (water on top) was then mixed with the settled tailings to increase the water content. The predominant dissolved ionic species in the bleed water were calcium, magnesium and sulfate. The electric conductivity of the pore-water was $4ms/cm$.

3.2 Particle Size Distribution

The particle size distribution of the gold tailings were determined according to the ASTM standard D422-63 (1990) "Standard Test Method for Particle Size Analysis of Soils". Particle size distribution of the tailings is shown in Figure 4.1.

3.3 Settling Test

Two sets of settling tests were conducted were tailings were poured into columns with a diameter of 15 cm and initial heights of 0.5 and 0.25 m at 70% solid content. The vertical settlement was recorded over 8 days. Measurement of tailings settlement was done by hand (using a ruler), while tailings were allowed to drain through a hole in these columns, protected by a filter paper. Evaporation was minimized using a cap.

3.4 Rheological Properties

The rheology of the tailings was characterized using slump tests and an Anton Paar Physica MCR301 model rheometer while they were prepared at geotechnical gravimetric water contents ranging from 25%-50%.

3.4.1 Slump Test

Material

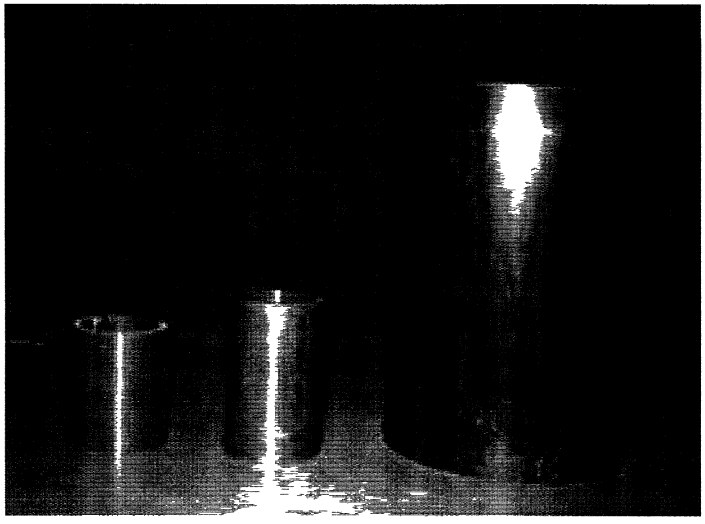

Figure 3.1: Cylinders used in slump test

- Open ended cylinders with different height and diameters as shown in Table 3.1 and Figure 3.1
- Tailings sample
- Smooth flat surface
- A paint mixer
- Measuring tape
- Personal protective equipment

Cylinder	**Height(cm)**	**Diameter(cm)**	**Construction Material**	**Aspect Ratio(H/D)**
1	19.1	15.4	PVC	1.24
2	7.9	4.8	PVC	1.64
3	6	4.8	PVC	1.25

Table 3.1: Dimension of cylinders used in slump test

Experimental Procedure

Before the test, tailings were mixed with a stirring machine for about 10 minutes. After placing the cylinder on a smooth flat plate it was filled with sample and it was lifted quickly and evenly, the change between the cylinder and deformed material was measured. The midpoint of the slumped material was taken as the representive height due to the uneven top surface. Also, the diameter of the outward flow was recorded.

Several slump tests were done using three different cylinder sizes while the water content of the material was varied between 26%-45%. The aspect ratio used for these sets of tests were in the range in which other authors ie. Pashias et al. 1996, Clayton et al. 2003, and Henriquez and Simms (2009), used. All the tests were performed at room temperature (22-24^0).

3.4.2 Rheometry using a Vane fixture

The rheology of the tailings was investigated using An Anton Paar Physica Rheometer (Figure3.2), using a vane fixture. The vane fixture has been thought to minimize errors associated with the wall-slip phenomena, less sample disruption and allowing the material to yield within itself (Gawu and Fourie, 2004, Dzuy and Boger 1983, Liddle and Boger 1996).

The rheometer uses an air bearing fixture together with a synchronous motor to virtually eliminate system compliance problems. Magnets mounted on the rotor disc produce a constant magnetic field, providing delay-free coupling of the fixture to the

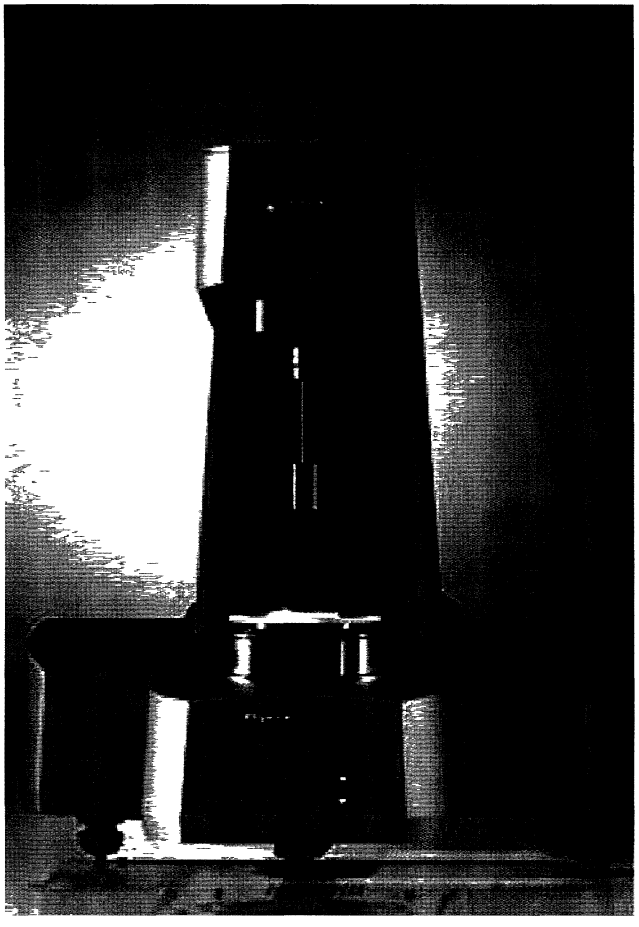

Figure 3.2: The Anton Paar Physica Rheometer
www.anton-paar.com/Rheometers

rotor.

A variety of techniques were employed for the yield stress measurement of the tailings, such as flow curves, stress relaxation, stress growth and creep recovery. The theory of these techniques was previously described in Chapter II.

3.4.2.1 Flow curves

Material

- An Anton Paar Physica Rheometer (MCR301)
- Tailings sample
- Vane geometry (ST 224V-4L)
- A paint mixer
- A computer
- Personal protective equipment

Experimental Procedure

Tailings were poured into the CC27 cup provided for this geometry. The vane which was used had a diameter of 22 mm and the depth of 40 mm (Figure 3.3). Prior to the measurement of the flow curve the suspension was sheared by stirring with a spatula in order to remove any thixotropically recovered structure to produce a homogeneous structure. The cup is then placed into a depression in the rheometer base (See Figure 3.2). The vane fixture was then lowered by the rheometer into the centre of the sample, submerging the fixture beneath the sample surface. Measurements were initiated no later than 1 minute after the submersion of the vane fixture.

During the measurement of each flow curve the shear rate will be that commanded and the shear stress is calculated from the average torque measured over the measuring point duration. For a shear rate sweep, the measuring point duration for each measurement is as follows. When commanding a specific speed or rate there

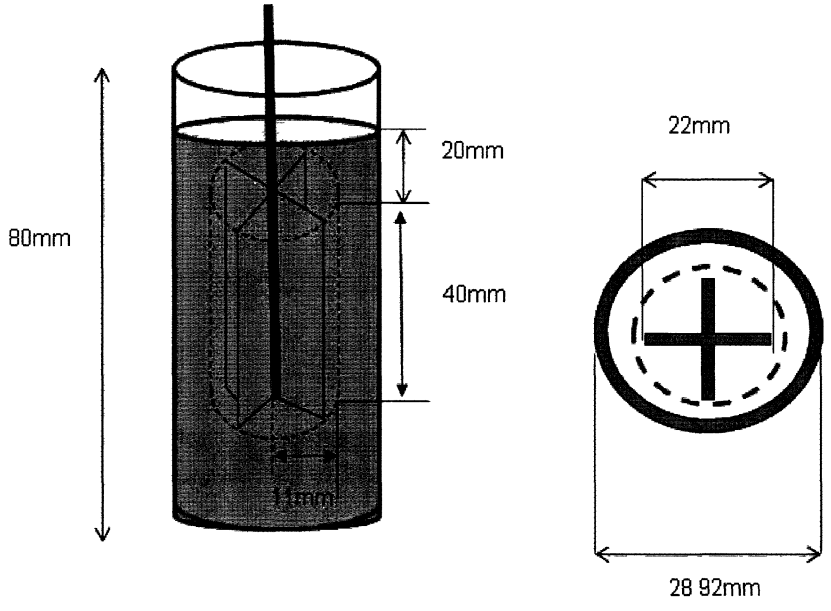

Figure 3.3: Schematic of the vane geometry

is a required time to reach steady state. The time required to reach steady state is approximately the measuring duration for that particular shear rate. The software ignores the first 50% of the measuring time due to adjusting the set speed/shear rate. The final 50% of the data is averaged for the measuring point. It is assumed that an equilibrium has been reached in the last 50% of the measuring time. If the measuring time is changed (lowered or raise), this may affect the results. If the measuring duration is lowered too much the average may incorporate the start up behavior and thus discrepancies. Based on the results gained in section 4.3.1.1 a minimum of 0.5 seconds was used for the flow curve measurements.

3.4.2.2 Vane in rate controlled mode

Experimental procedure

A volume of suspension was raised into the sample container (cup) such that the vane was fully immersed in the material. Carefully the vane was placed in the center of the sample and it was then rotated at a constant velocity. The torque needed in order to keep the constant movement of the vane is measured as a function of time. In the beginning as the network bonds are stretching the sample shows linear behavior from itself, but as it goes on the torque must increase in order to overcome the more stretched bonds so that it could keep the rotational constant. Eventually all of these bonds will break and the material will yield. The yield stress is then calculated from the maximum torque.

3.4.2.3 Vane in stress controlled mode

Experimental procedure

This experiment was operated in two ways. First, a constant torque was exerted to the vane immersed in the tailings for a certain time and the strain was measured as a function of time. This procedure was repeated with different stresses. In the second mode a constant stress-rate was exerted to the vane up to a certain value of stress, while the strain was measured as function of stress.

3.4.2.4 Shear Stress Relaxation Method

Experimental procedure

After the sample was loaded into the cylinder the vane was rotated at a chosen speed and the evolution of the torque was measured as a function of time. When an equilibrium condition was reached the vane was brought to a sudden stop and the shear stress remaining on the rotating device in the relaxed condition was taken as the yield stress. In order to ascertain the results the procedure was repeated a few more times and at other rotational speeds.

3.5 Flume Test

For simulating the depositional behavior of thickened tailings under laboratory conditions, a flume apparatus was used. Previously, several authors have utilized this technique. For example, Henriquez and Simms (2009), Sofra and Boger, (2001), Kwak et al. (2004) used a flow channel with a reservoir at one of its ends, after filling the reservoir the gate was lifted allowing the material to flow down the channel.

3.5.1 Material

- Flume apparatus with acrylic side walls and with the dimension shown in Table 3.2 and Figure 3.4
- Tailings sample

- A high speed camera, model IN250
- A paint mixer
- Tensiometer-type T5-2.5
- A computer
- A measuring tape
- A 7.3mm tube
- A pump (Masterflex model 77410-10)
- Personal protective equipment

Length(cm)	**Height(cm)**	**Width(cm)**
243	30	15.2

Table 3.2: Flume apparatus

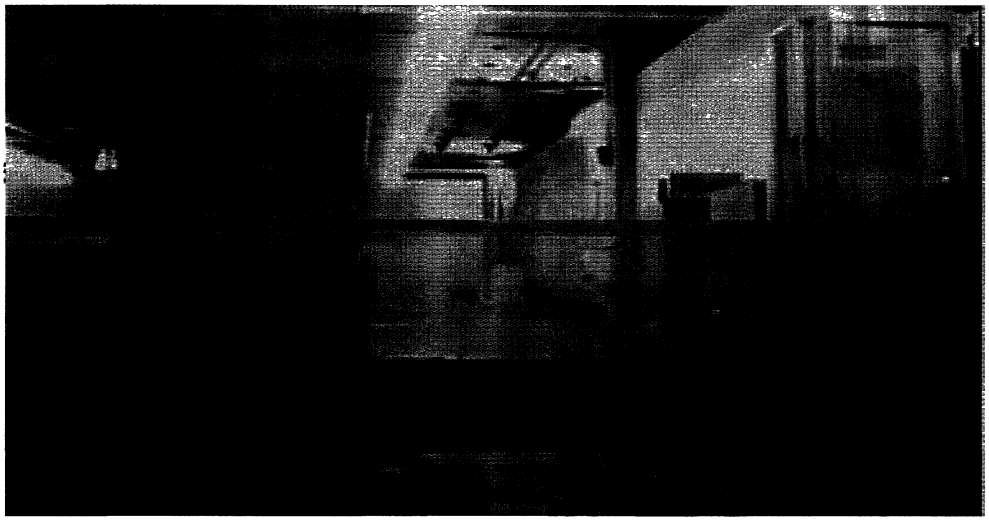

Figure 3.4: Flume apparatus

3.5.2 Experimental Procedure

Flume tests were performed on horizontal surface in both single and successive layers and with different volumes. The materials were thoroughly mixed before each test and during any test in the pump reservoir, to simulate the shearing of the material that would occur during transport. The tailings were then pumped through a tube with a diameter of 7.3 mm which was installed at a height of 10 cm from the bottom of the flume. The tailings were pumped at constant flow rates between 0.4 to 8 liters per minute (LPM). The length of the flow and the depth were measured at different locations (every 5cm) for the determination of the resulted profile. The geometry of the flows was visualized using high speed cameras, Model IN250 from High Speed Imaging. Using the data from two different locations the overall angle is calculated from:

$$\theta_r = tan^{-1}\left(\frac{H_1 - H_2}{L}\right) \tag{3.1}$$

where,

L is the distance between H_1 andH_2

H_1 is the is the depth near at the deposition point

H_2 is the is the depth the toe

Flume tests on successive layers were conducted while the tailings were pumped

with the flow rate of 0.4 LPM and through the tube. The older layer was left to dry for several days to generate a significant matric suction. The water flux between the two layers was tracked by tensiometers installed in the underlying older layers, and by sampling the fresh layer for water content after it had stopped moving. Run-out and the depth at different locations (every 5cm) was measured after the flow came to rest. The variability in yield stress was evaluated by best-fitting Equation 2.28 or 2.29 to the flume profiles.

Note that all the tests were performed in the room temperature (21-24^{0}C)

3.6 Pouring Test

These sets of tests were also conducted on a flat 1 m by 1m Plexiglas surface (Figure 3.5). Certain volume of tailings were pumped out the end of a 0.1 cm diameter rubber above the deposition point, which was deposited less than 5 cm above the tailings surface allowing it to flow radially resulting in roughly axi-symmetric deposits. Layers are deposited after the previous layer has stopped settling but before desiccation occurs (30% GWC for this material). Topography is visualized by dropping plumb lines from an overlying grid with maximum intervals of 5 cm. Most of these tests were carried out by undergraduate student, Lucy He, under the supervision of the author. The author interpreted the results using the Lubrication Theory.

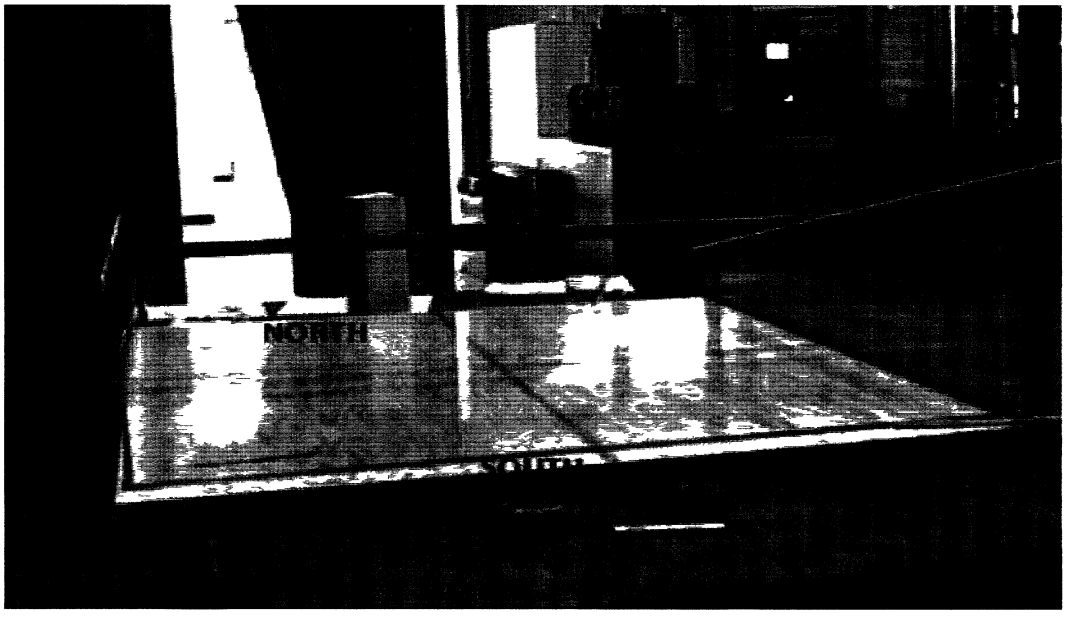

Figure 3.5: Pour test setup

3.6.1 Material

- Tailing paste sample
- A high speed camera, model IN250
- A PAINT MIXER
- Plexiglas box of 1m by 1m (Figure 3.5)
- A computer
- A measuring tape
- A 10mm tube
- A pump (Masterflex model 77410-10)

- Personal protective equipment
- A funnel

Chapter 4

Experimental Results and Discussion

4.1 Material characteristics

4.1.1 Geotechnical properties

The geotechnical properties of the tailings are shown in Table 4.1.

Properties	Value
Specific Gravity	2.77
D_{10},D_{50},D_{60} (microns)	1,35,70
$Cu(D_{60}/D_{10})$	70
Liquid limit (%)	20
Plastic limit (%)	19
Hydraulic conductivity (m/s)	2×10^{-7} (at e=0.8)

Table 4.1: Properties of tested Tailings.

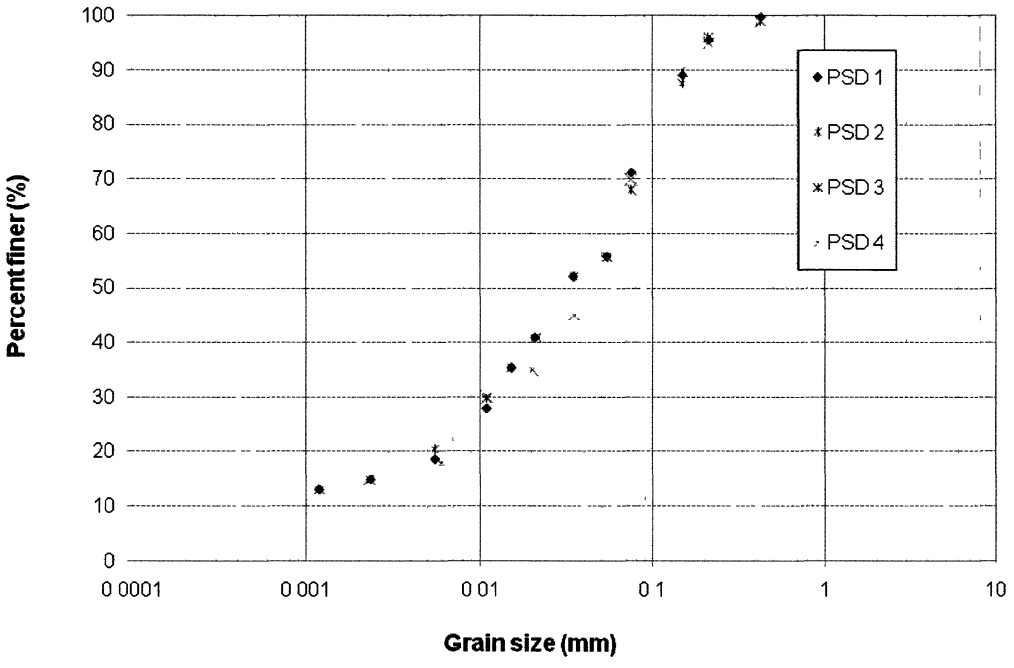

Figure 4.1: Particle size distribution of gold tailings from hydrometer and sieve analyses

4.1.2 Particle Size Distribution

Figure 4.1 presents the particle size distribution of the tested tailings in terms of percentage of fines by weight versus diameter of particles.

From Figure 4.1, it could be seen that the tailings contained particles as fine as or finer than 1 μm up to 400 μm. Also, around 40% by weight corresponds to the particles finer than 20 μm; therefore, they can be considered as non-segregating and could be pumped in the laminar range even at low velocities. The average size or the D_{50} was approximately 35 μm.

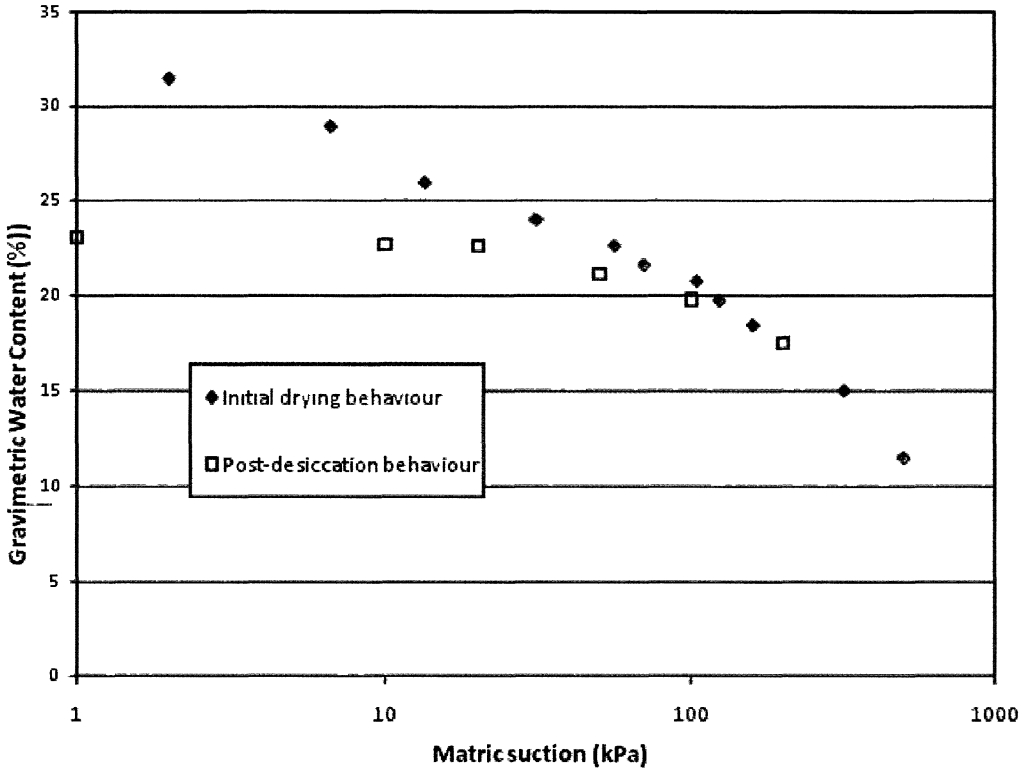

Figure 4.2: Water retention curves for initial drying, and for drying subsequent to desiccation and rewetting (After Fisseha et al. 2010)

4.1.3 Water-retention curve

As the capillary effects on flow behavior is been investigated, it is of interest to show the water-retention characteristics of the material. The water-retention curve (WRC), is shown in Figure 4.2. This shows equilibrium water-content of the material at given constant pore-water pressures. Water-retention is a function of the particle size distribution of the material, that is, the finer the grain size, the greater the capacity for water-retention. The water retention curve was attained by others (Fisseha et al. 2010), for both initial drying path and second drying path after rewetting.

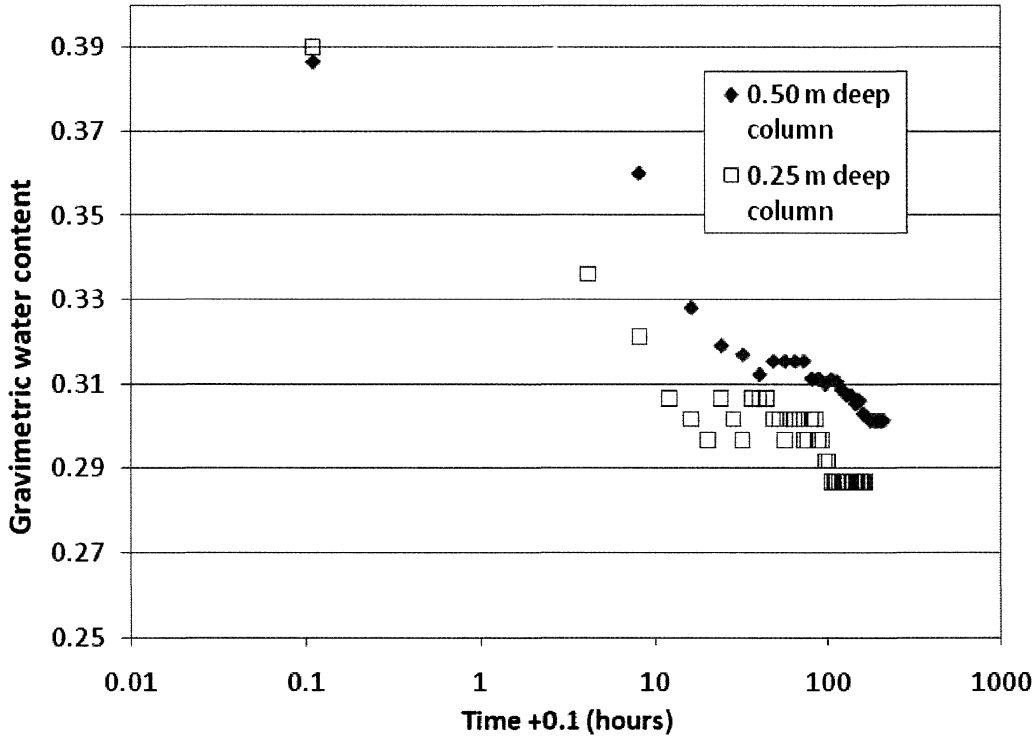

Figure 4.3: Settling behaviour of thickened gold tailings in columns.

4.1.4 Settling curves

As mensioned in chapter II an important behaviour of the material is that it undergoes hindered settling subsequent to deposition or even during deposition. An examples of hindered settling curves for tailings are illustrated in Figure 4.3.

4.2 Slump Test

Several slump tests were conducted on the Bulyunhulu gold mine tailings at gravimetric water contents between 26 to 45% and using three different cylinder sizes. Figure 4.4 presents the dimensionless slump height versus the water content.

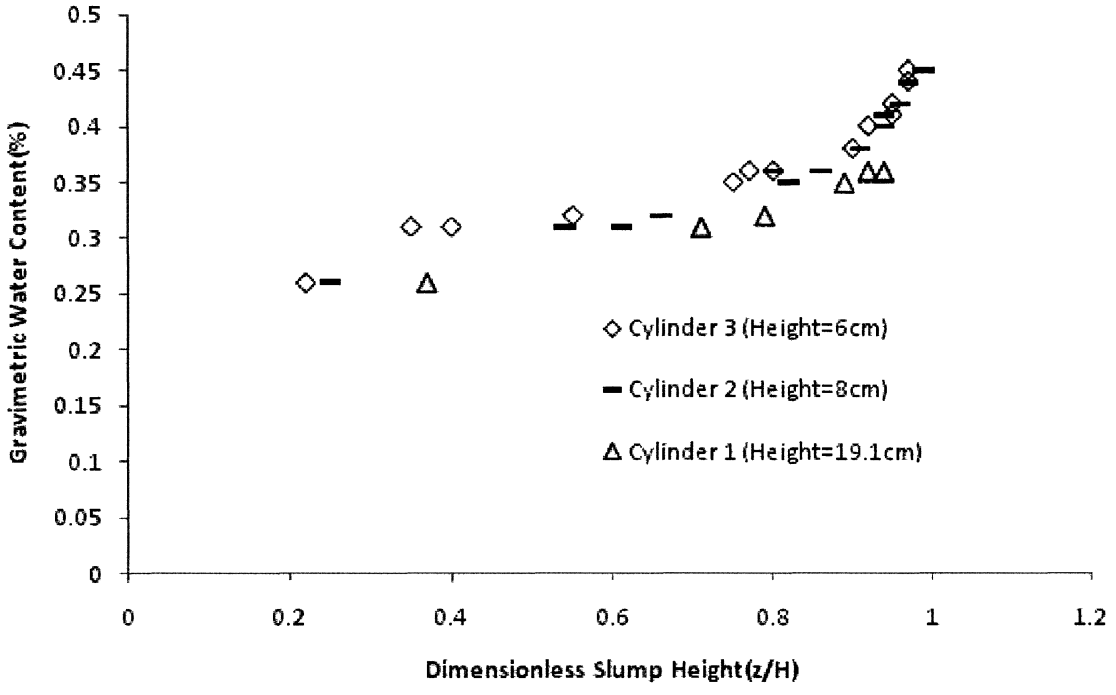

Figure 4.4: Dimensionless slump height versus water content.

It can be seen that the height of the cylinder somewhat affects the results. For instance, the dimensionless slump height for the larger cylinder (Cylinder 1 in graph) is higher at the same water content relative to the smaller cylinders. It is rather difficult to conclude that whether the scatter in the data is due to the experimental errors or the aspect ratio (H/D).

The yield stress can be obtained by multiplying the dimensionless yield stress by the ρgH. Figure 4.5 presents the yield stress values for each water content using Equation 2.18 .

As observed from the previous Figures, yield stress is very sensitive to the changes in the water content. One of the possible reasons for the deviation of the larger

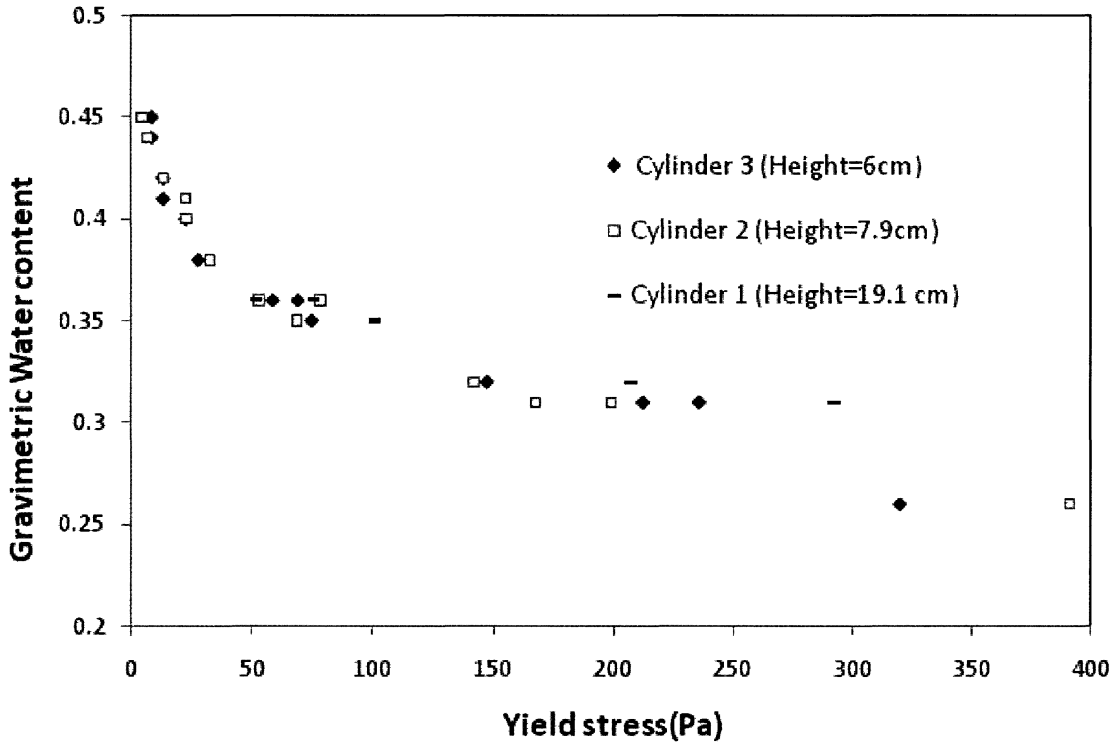

Figure 4.5: Yield stress values versus gravimetric water content

cylinder results from the other ones is that the effects of friction would be more for larger volumes (in the derivation of the equation the effects of friction between the wall and base and the suspension is ignored).

4.3 Rheological characterization

4.3.1 Flow curves

4.3.1.1 Sensitivity of flow curves to measuring point duration

The appropriate measuring point duration time or the time required to get to the steady state at a given shear rate was investigated on the tailings at the gravimetric water content of 38%. The results indicate that a measuring point duration below 0.5 seconds (.25 and .15 seconds) leads to unrealistic results. This is evident in the behaviour between shear rates 100 and 150, where a drop in shear stress is observed. As it takes a finite amount of time for the vane fixture to be accelerated to the next shear rate, lowering the measurement time will lead to increasing bias by shear stress values measured before equilibrium is reached. This error becomes more obvious as the measuring point duration decreases.

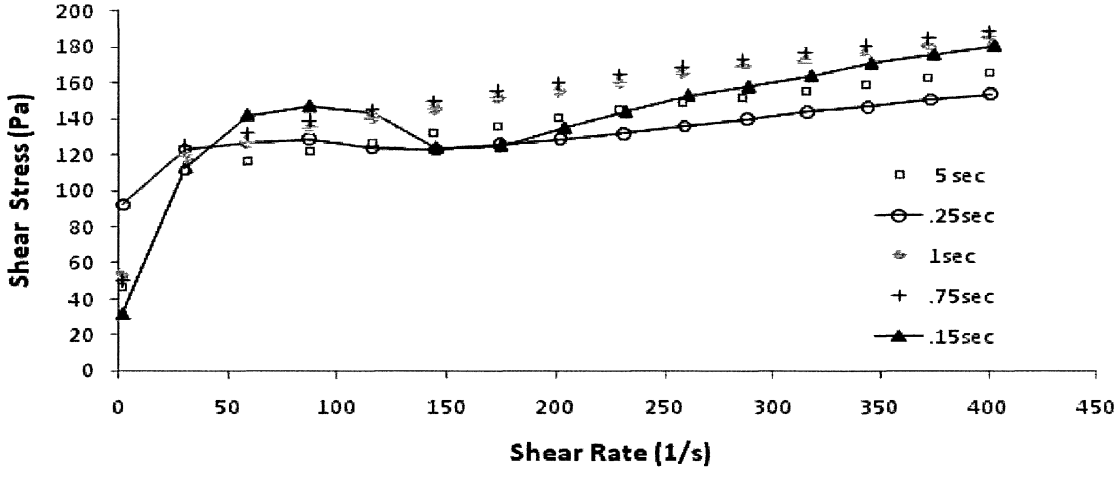

Figure 4.6: Flow curves for a 38% GWC sample at different measuring point time durations

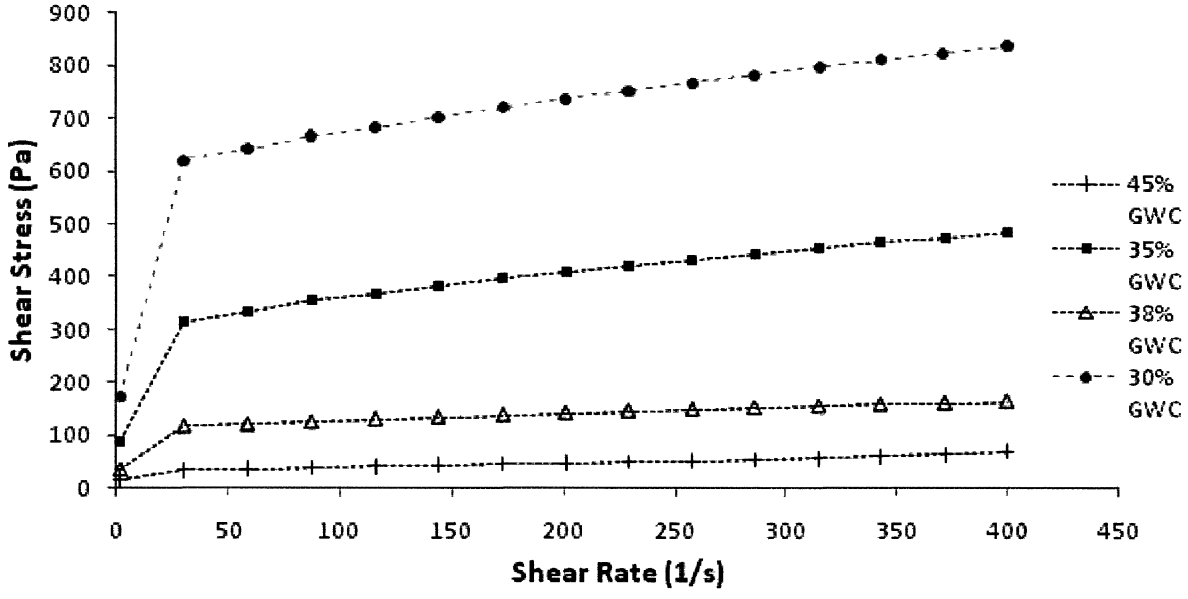

Figure 4.7: Flow curves for different water content tailing samples.

4.3.1.2 Flow curves from shear rates 0 to 400 and at low shear range

Flow curves over a wide range of shear rates for tailings prepared at different water contents are shown in Figure 4.7. The data presented in Figure 4.7 show that tailings exhibit a measurable yield stress at all water content studied.

For dilute samples a straight line could be reasonably drawn through the data to estimate yield stress based on a Bingham model. On the other hand, for more concentrated samples, the relation between the shear stress and shear rate becomes nonlinear at low shear rates. The accuracy of the yield stress determined from the direct extrapolation is highly dependent on the availability and reliability of the data at very low shear rate region.

Figure 4.8 presents the flow curve results conducted in the low shear rate region.

The same sample was used during this test while the shear rate went up to the maximum values of 5, 10 and 15 s^{-1} . In this plot some data pertain to an increasing shear rate and some to a decreasing rate, and as observed the up and down segments are not the same. For the increasing segments the initial shear stress recorded by the rheometer is around 25 Pa while the final shear stress on the decreasing shear rate path varied between 46 to 52 Pa. A possible explanation for this hysteresis is that stress depends on the shear rate history and time is required for the stress to change from one steady state to another. Similar behavior is also observed by Blakley et al. (2003) on a laterite slurry.

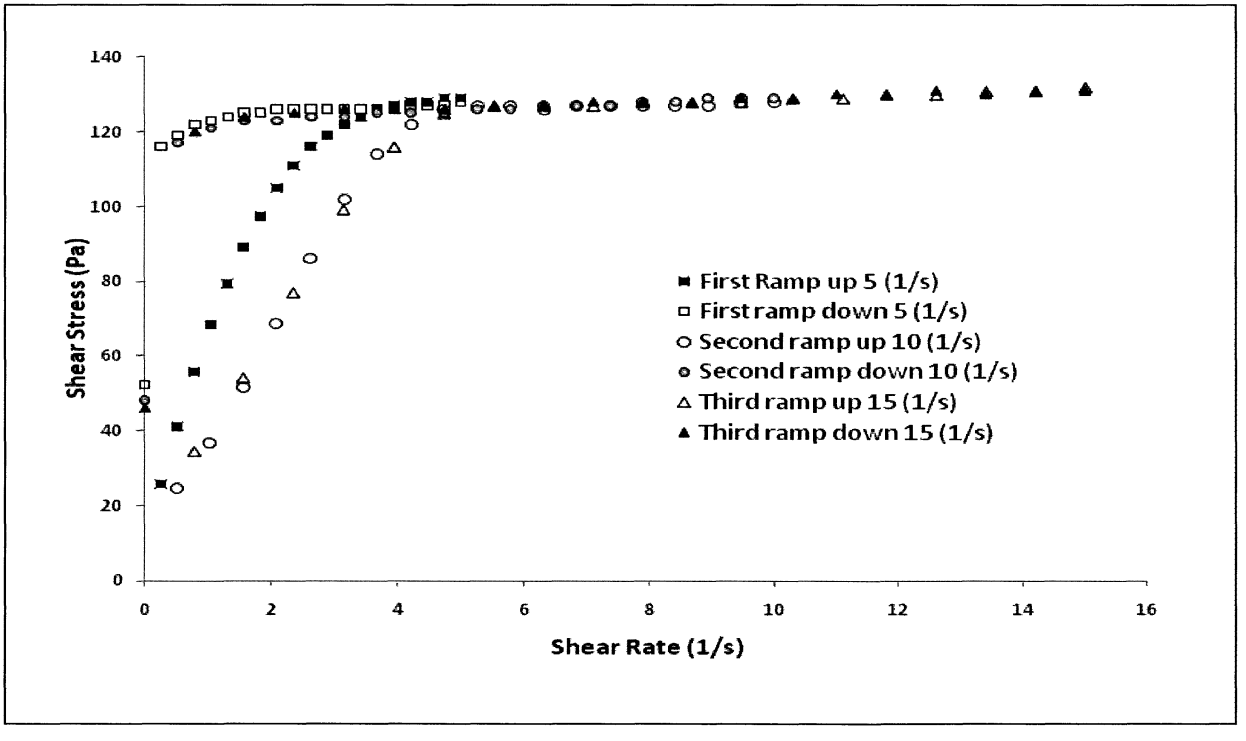

Figure 4.8: Flow curves for a sample prepared at 38% GWC and at low shear rate region

4.3.1.3 Model fitting

As mentioned in Chapter II, one of the rheological models that have been applied to describe the behaviour of thickened tailings is the Bingham model (Kwak et al. 2005, Boger 2009).

The Bingham model is fitted to flow curves of samples at 38% gravimetric water content in the following figures. Figures 4.9 and 4.10 show the data over a period of 7.5 and 60 seconds respectively. Total measurement time did not appreciably change the flow curves.

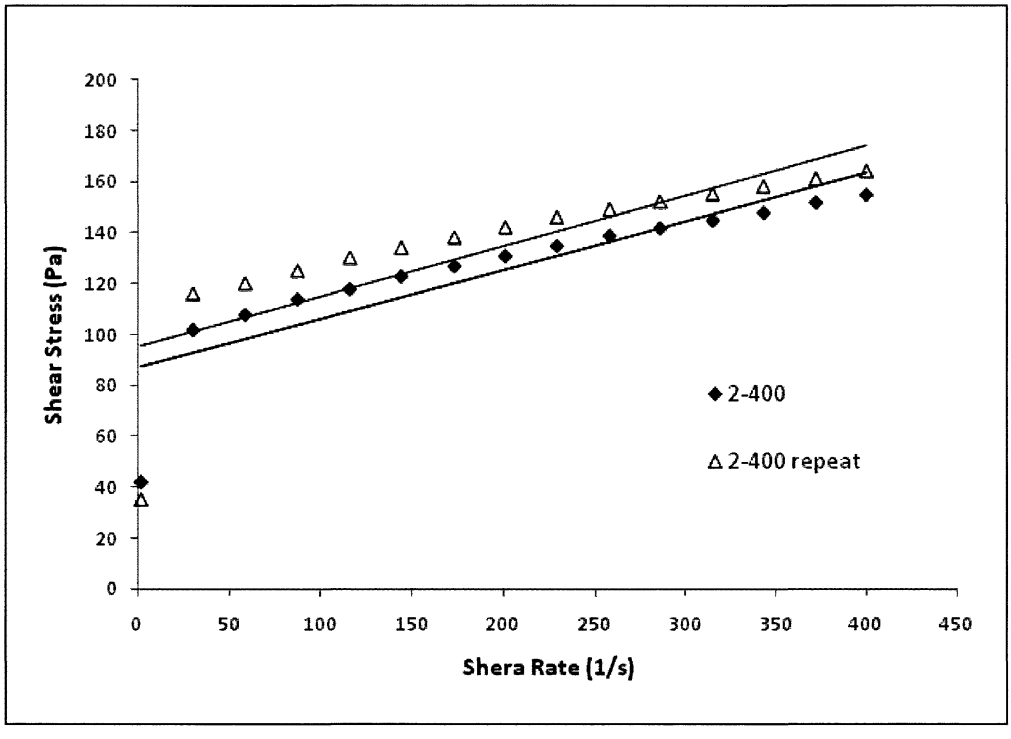

Figure 4.9: Flow curves measured over 7.5 s

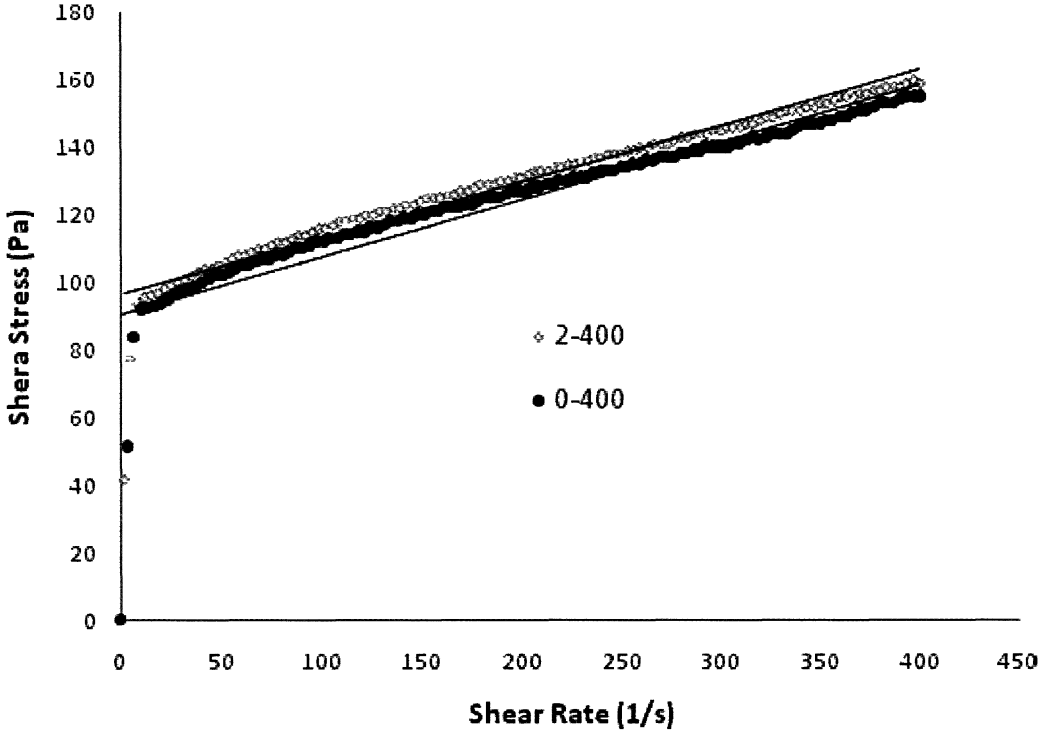

Figure 4.10: Flow curves measured over 60 s

When the Bingham model is applied to estimate friction losses in pumping, a dynamic yield stress is usually evaluated by best fitting the flow curve excluding the data below a shear rate of 100 s^{-1} (DIN 53019). For this material, the dynamic yield stress is much greater than the yield stress evaluated from the slump test (30 Pa for 38% GWC). In fact, the shear stress measured at the lowest shear rate by the rheometer (Figures 4.7 to 4.10) gives the best agreement with the yield stress extrapolated from the slump test, though there is significant variability. Unfortunately, data at low shear rates are usually discounted because of errors that arise at this level

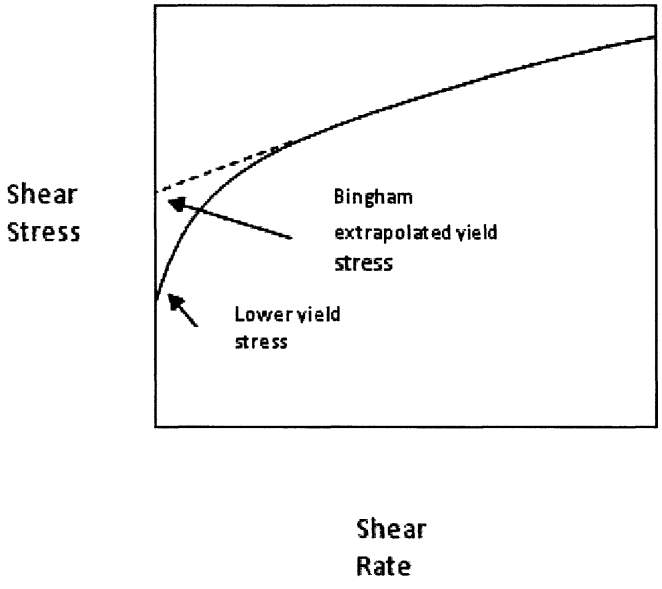

Figure 4.11: Typical stress-rate behaviour for a Pseudo-plastic fluid

of shear stress (Boger 2009 and Lideell and Boger 1996). Nevertheless, it must be stressed that the yield stress of interest is the yield stress that characterizes where the material stops flowing, and therefore it should not be surprising that the slump yield stress (static yield stress) lies significantly below the dynamic yield stress.

As can be observed from the previous figures, it seems that the Bingham model leads to an over estimation of the yield stress. Figure 4.11 shows a shear stress-shear rate behavior often observed with yield stress materials. Bingham yield stress is gained by extrapolating from a linear region at higher shear rate and therefore has no meaning in terms of the true yield stress (Boger 2009). It seems that the flow curve describes a yield Pseudo-plastic behavior rather than a perfect Bingham Fluid.

To account for the observed non-linear behavior, the Casson and Herschel and Bulkley equations were fitted to the flow curves. For the Casson model only a plot of

$\tau^{0.5}$ versus $\gamma^{0.5}$ is required. Figure 4.12 shows all the Casson plots for different water contents and for flow curves at different water contents.

The Herschel and Bulkley equation were fit by a trial and error until the best fit with the recorded data is obtained. Figure 4.13 illustrates the results for this model.

As seen in Figures 4.12 and 4.13, the nonlinear equations correlates better with the experimental data. However, as the concentration of the sample increases the correlation is poorer.

Yield stress and viscosity results obtained by model fits are compared in Table 4.2.

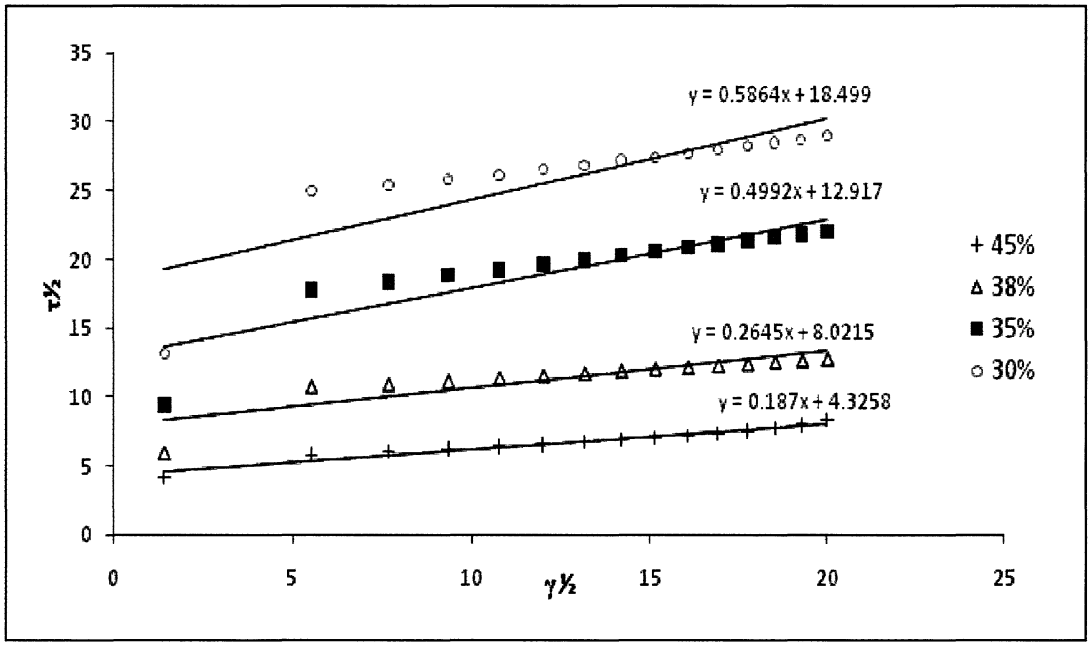

Figure 4.12: Casson plots of $\tau^{0.5}$ versus $\gamma^{0.5}$ for tailings at different gravimetric water content.

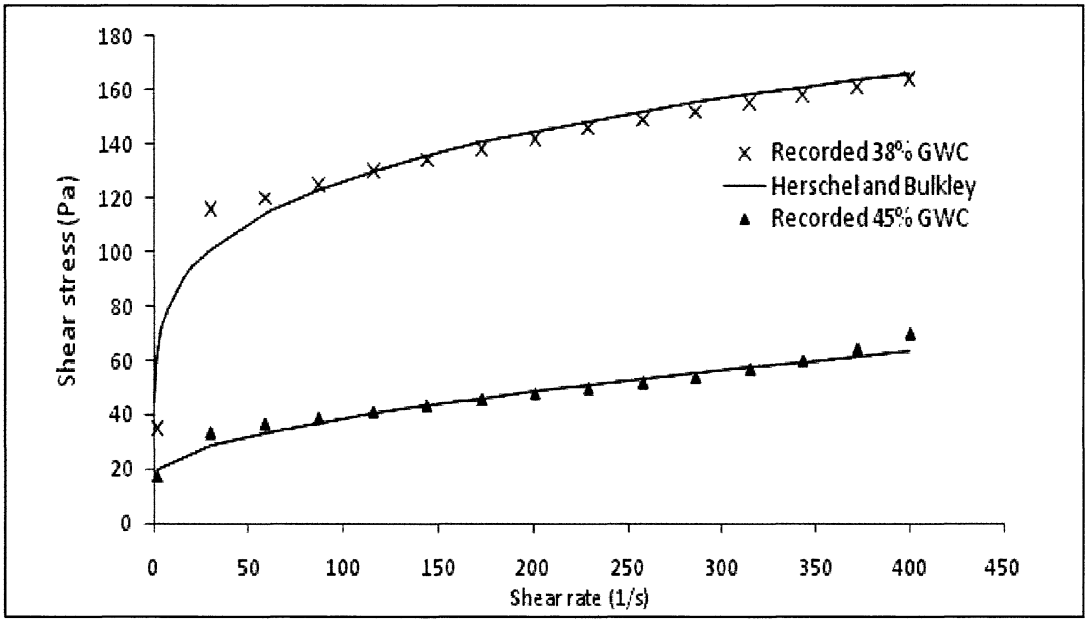

Figure 4.13: Herschel and Bulkley model fit to flow curve at 38% and 45% GWC

GWC	30%		35%		38%		45%	
Method	$\tau_y(Pa)$	$\eta(Pa.s)$	$\tau_y(Pa)$	$\eta(Pa.s)$	$\tau_y(Pa)$	$\eta(Pa.s)$	$\tau_y(Pa)$	$\eta(Pa.s)$
Bingham Model	506	.97	260	.64	95	.19	27	0.1
Casson Model	342	.34	166	.24	64	.06	18	.03
Herschel Bulkley	75	-	40	-	25	-	18	-

Table 4.2: Yield stress at different water content obtained by model fits

4.3.2 Direct Measurement

4.3.2.1 Stress Relaxation

The results obtained with the stress relaxation method at different water contents are presented in Figures 4.14 through 4.18.

In this suite of tests the vane was rotated at a constant speed and when an equilibrium condition was reached the vane was brought to a sudden stop. The test was repeated with different shear rates in order to investigate the applicability of this technique. The stress exerted on the vane prevents the vane from going back to its original zero stress and therefore is the shear stress which defines the limit between flow and nonflow condition (Dzuy and Boger 1983).

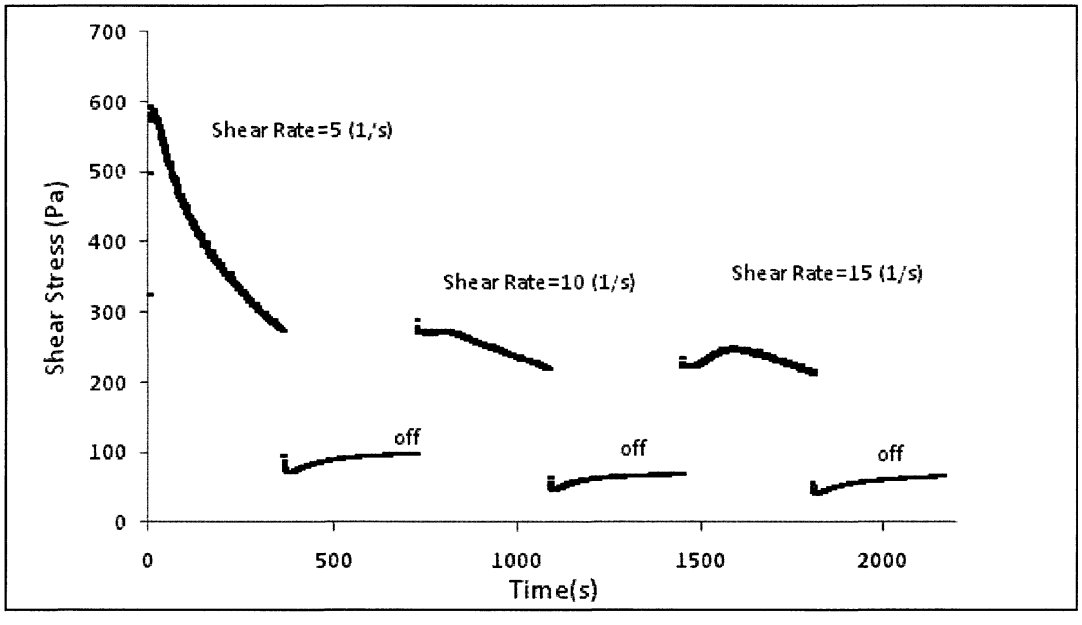

Figure 4.14: Stress relaxation method for tailings at 30% GWC

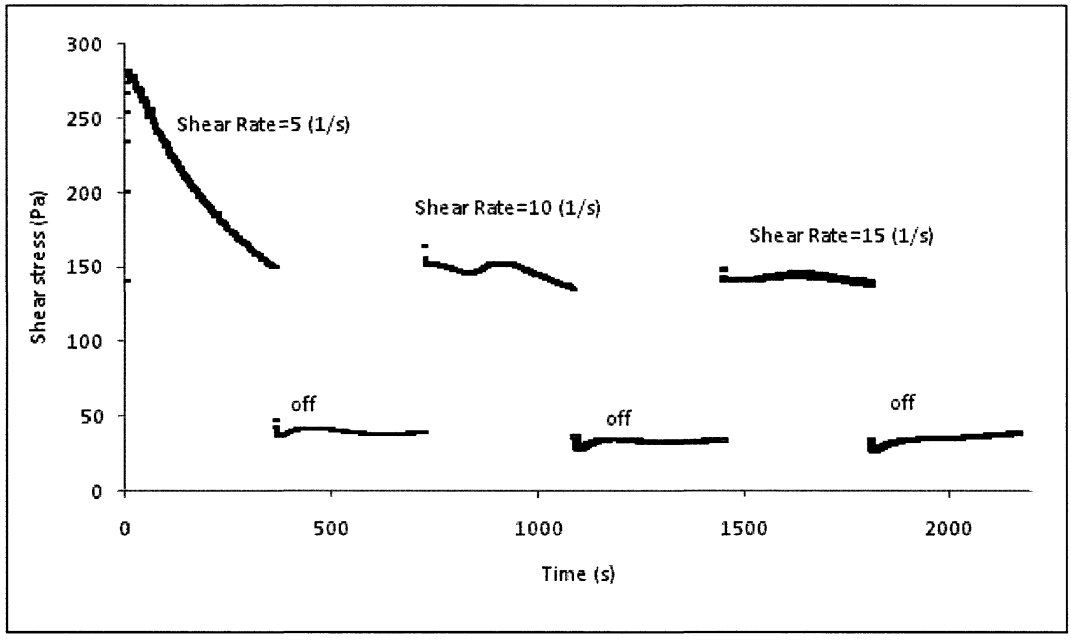

Figure 4.15: Stress relaxation method for tailings at 35% GWC

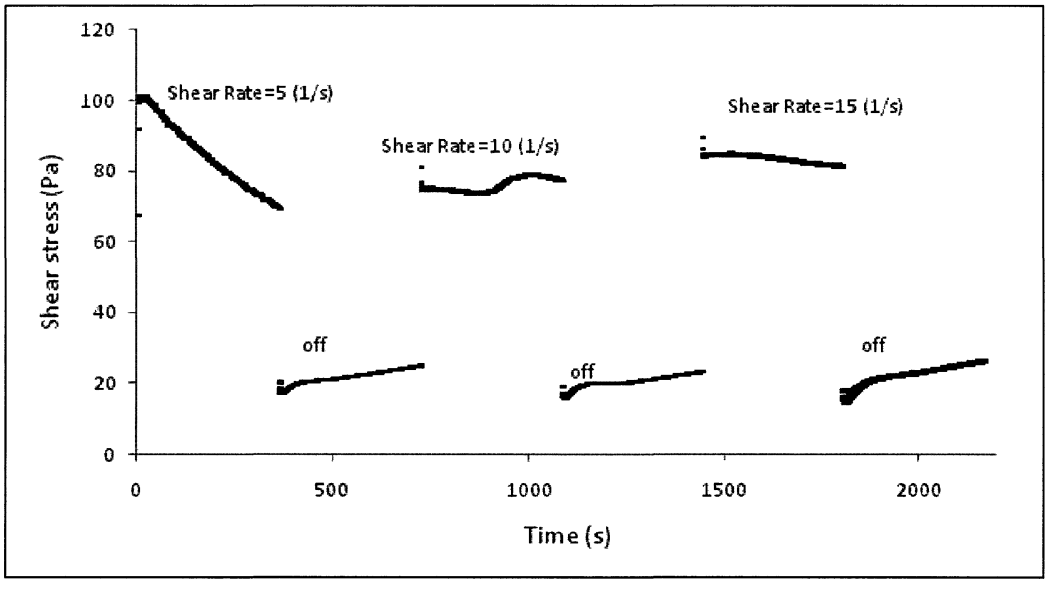

Figure 4.16: Stress relaxation method for tailings at 38% GWC

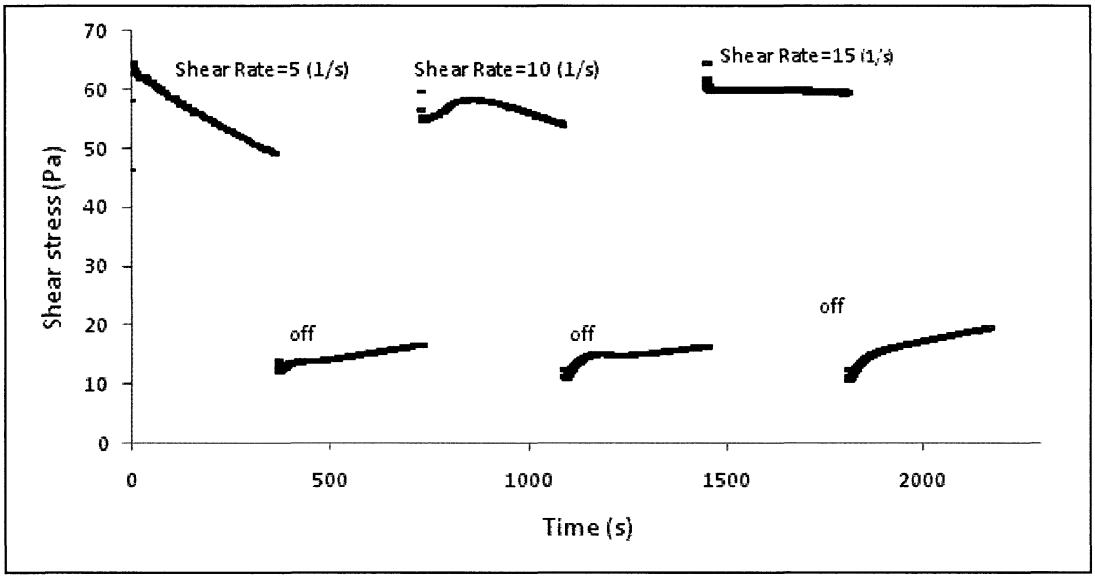

Figure 4.17: Stress relaxation method for tailings at 40% GWC

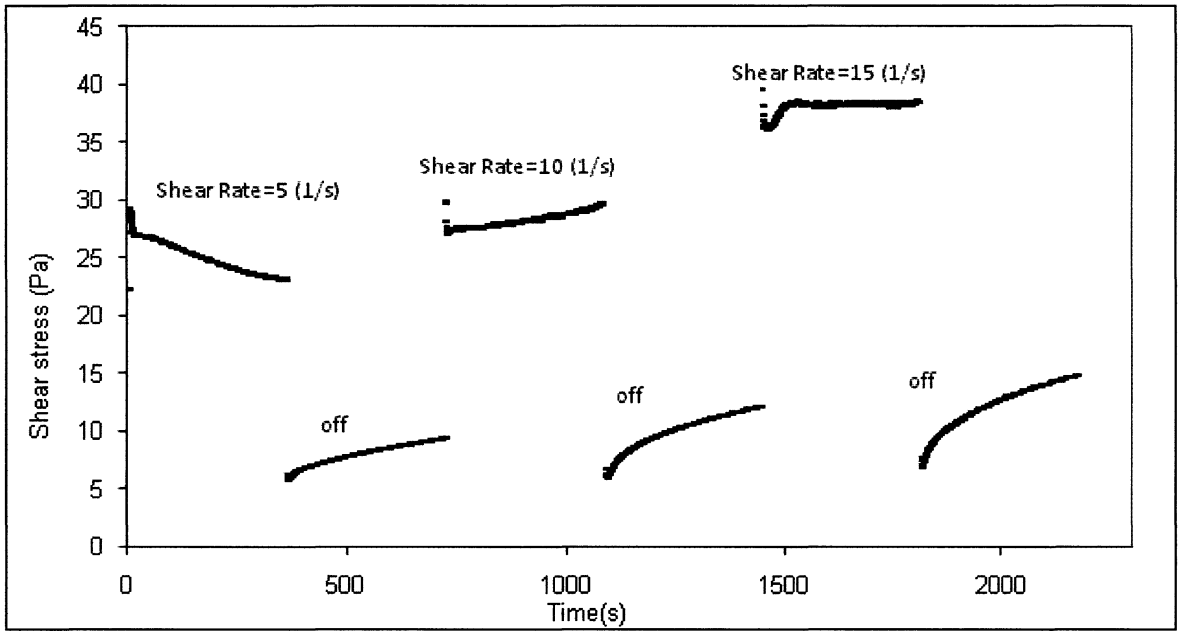

Figure 4.18: Stress relaxation method for tailings at 45% GWC

As can be observed from the previous figures, an equilibrium state is not achieved in the lower shearing phase, for all water contents except 45% GWC, which is probably due to thixotropic build up. This behavior is further discussed in section 4.3.2.3.

Also, although the residual shear stress after shearing at different rotational speed was in the same range but the value increased with time. This is likely due to settlement over the long required time for the experiment, resulting in increase in the shear stress. Moreover, the discrepancy between the residual stress and the results from the slump test seems to increase as the GWC of the sample decreased. Similar behavior has been observed with red mud samples (Dzuy and Boger 1983).

4.3.2.2 Creep recovery

4.3.2.2.1 Application of a constant stress in steps Figure 4.19 illustrates the strain-time profile for tailings at 38% GWC. These profiles were measured with the vane in stress controlled mode. Constant stresses varying from 20 up to 150 Pa were applied in steps to the sample for 1 minute. Strain is calculated from strain rate (revolutions per minute) times by time (in seconds).

Figure 4.19 shows that the material does not strain when a shear stress of 20 Pa is applied however it starts flowing at the shear stress of 50 Pa and reaches a constant level of strain. This indicates that the static yield stress lies somewhere between 20 to 50 Pa. In this region some of the network bonds are broken, however some bonds are reformed due to thixotropic structural build up of the suspension. Eventually,

the rate at which the network bonds are reformed exceeds the rate at which they are broken at this level of stress resulting in a constant level of strain. As the shear stress exerted on the material increases the magnitude of the strain rate (shear rate) also increased (Figure 4.20). These results indicate that the stress required for the continuous rotation of the vane is around 120 Pa.

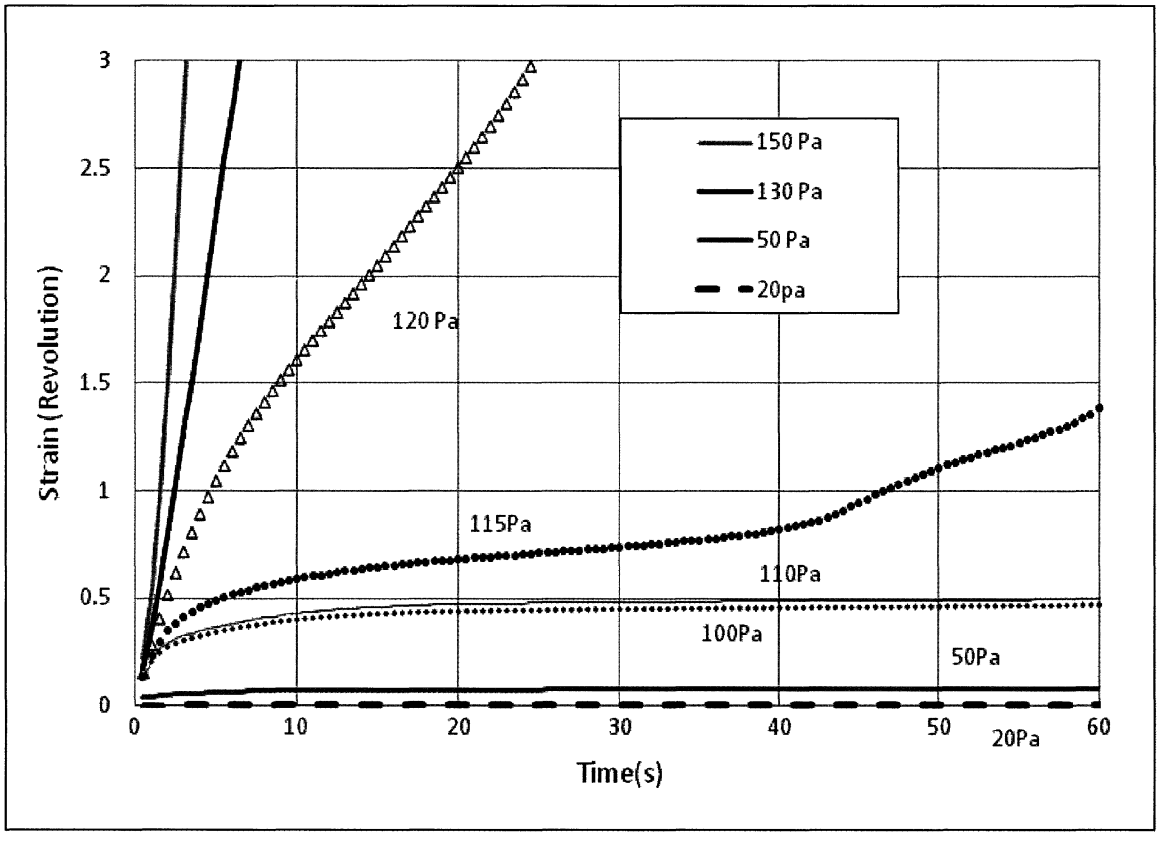

Figure 4.19: Strain-time profile for sample prepared at 38% gravimetric water content for constant stress levels

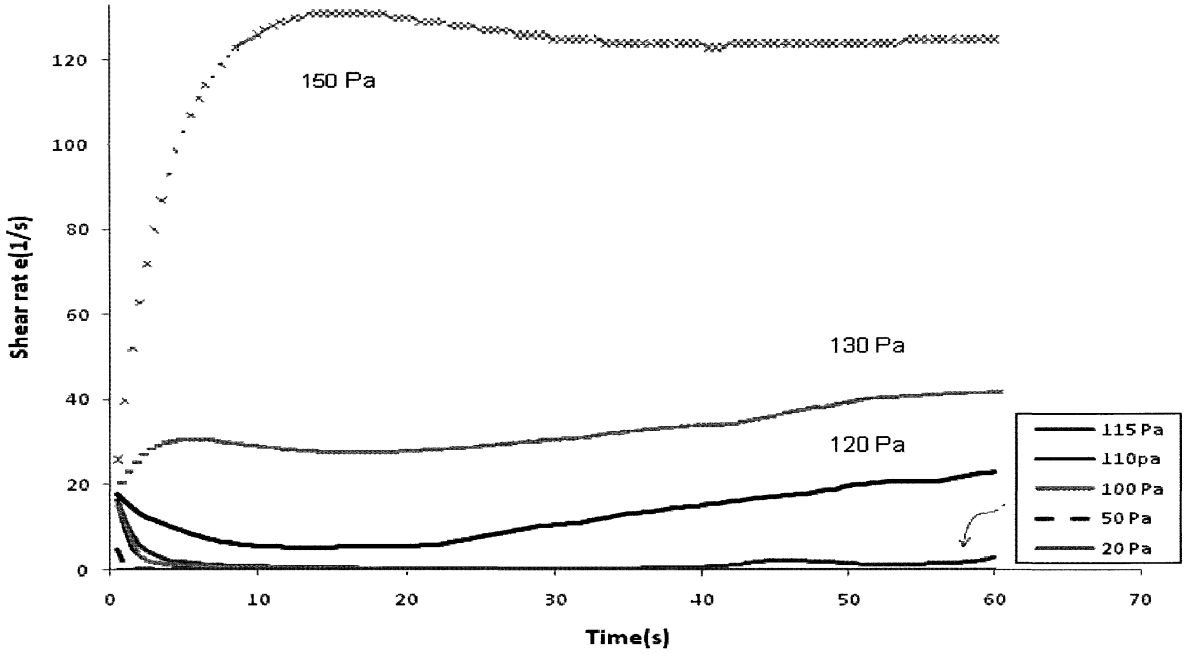

Figure 4.20: Strain rate(shear rate)-time profile for sample prepared at 38% gravimetric water content.

4.3.2.2.2 Application of a constant increasing stress rate Figure 4.21 presents the strain-stress profile for a sample prepared at 38% GWC. The profiles were measured with the vane while a constant stress-rate of 2.5 and 5 $Pa.s^{-1}$ were applied to the suspension. There is no maximum in the stress-strain profile because the stress increases with time; therefore, it is rather difficult to determine the critical stress since it depends on the experimenter's judgment of when an appreciable movement of the vane is observed. However, interesting results were observed when looking at the viscosity of the tailings during this test (Figure 4.22). Two separate zones of more or less constant values were detected; 10 Pa.s from 30 Pa to 90 Pa, and then 1 Pa.s above 100 Pa. From this data and from following comparisons with lubrication

theory, this lower yield stress best characterizes when the material stops moving.

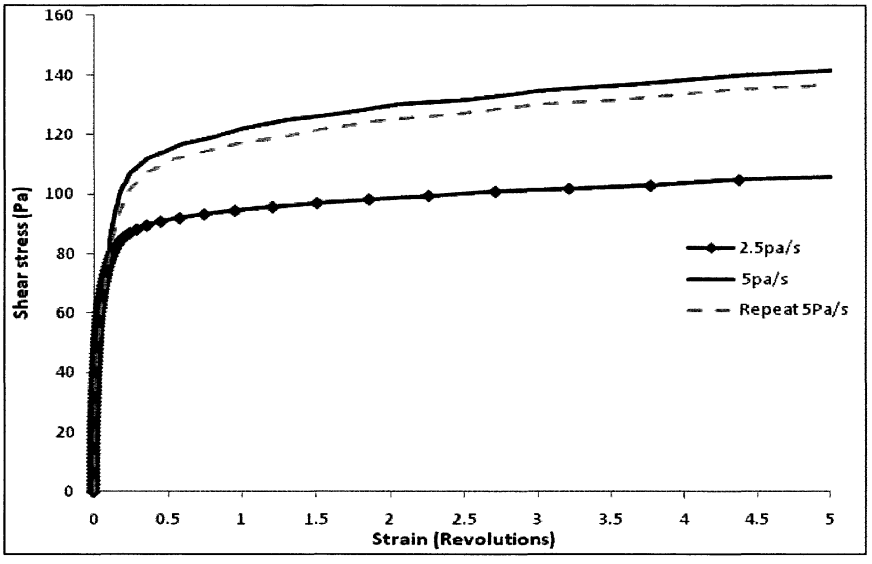

Figure 4.21: Stress-strain profiles for sample prepared at 38%GWC measured at 5 $Pa.s^{-1}$ and 2.5 $Pa.s^{-1}$

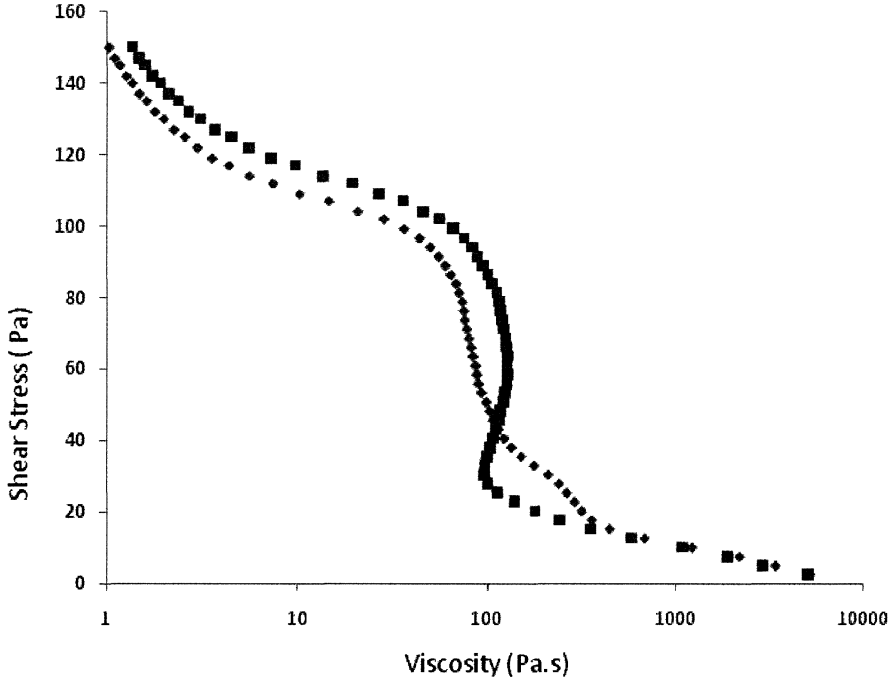

Figure 4.22: Viscosity -shear stress profile for sample prepared at 38 % GWC measured at 5 $Pa.s^{-1}$

4.3.2.3 Stress Growth

Table 4.3 and Figure 4.23 presents the yield stress as a function of applied rotational speed (constant shear rate) for tailings prepared at 38% GWC. The yield stress corresponds to the maximum yield stress measured in the stress-time profile with the vane and in the rate controlled mode.

Rate (s^{-1})	.006	.01	.1	1	2	10
Maximum stress (Pa)	Not observed	Not observed	64.8	63.3	75.9	82.9

Table 4.3: Maximum stress versus rotational speed at 38% GWC .

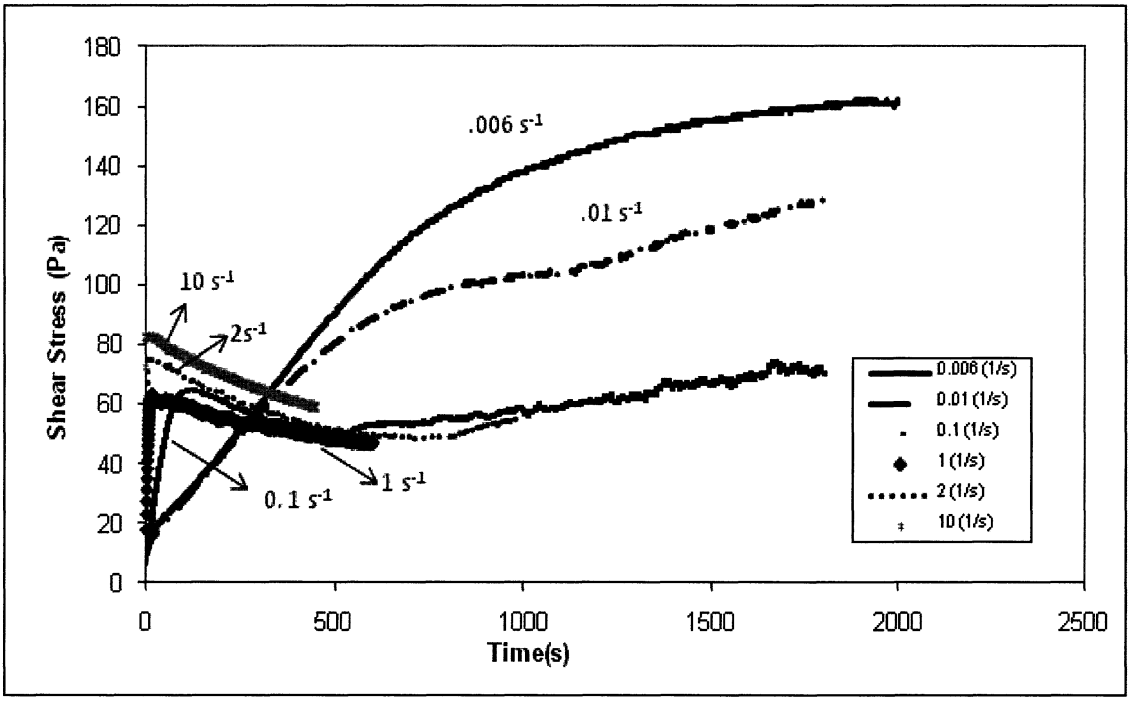

Figure 4.23: Stress-time profiles of tailings of 38% GWC for different rates.

The results from the table show that there is a region (between 0.1 and 1 s^{-1}) where the maximum stress measured is independent of rotational speed. That is above the rate of $1(s^{-1}$) the maximum stress increases with increasing speed. Also, it seems that below 0.1 (s^{-1}) a maximum stress could not observed within the time frame of the test. However, this limit can differ between different instruments. For example, Nguyen and Boger (1983) result with the Haake Rheometer on red mud suspension and Liddell and Boger (1996) result with Weissenberg Rheogonimeter on a TiO_2 pigment suspension showed similar trend.

The reason why the maximum stress increases with an increase in the rotational speed after a certain value is that, at higher rates, the network bonds are rapidly pulled apart not allowing the suspension the required time for the elastic response and the possibility of orientation. The reason for the lower limit and increase of stress with a decrease in the rotational speed is due to the thixotropic build up of the suspension in the relatively long time of shearing. That is, the rate at which the bonds are reformed is higher than the rate at which they are broken.

Figure 4.24 illustrates the strain-stress profile generated for the samples prepared at 38% GWC. The profiles shown are those measured with the rotational speed of 0.1 and $1(s^{-1})$. In this type of test, typically an elastic region is apparent where there is a linear relationship between strain and shear stress, and the yield stress demarks the change from elastic to viscoplastic behavior. Here, there are two linear regions, one from 0 to around 10 Pa, another from 10 Pa to around 40 pa. One can potentially

evaluate three different yield stresses from Figure 4.23 and 4.24, the lower yield stress of 10 Pa, the apparent limit of linear strain at 40 Pa, and the peak stress at 64 Pa.

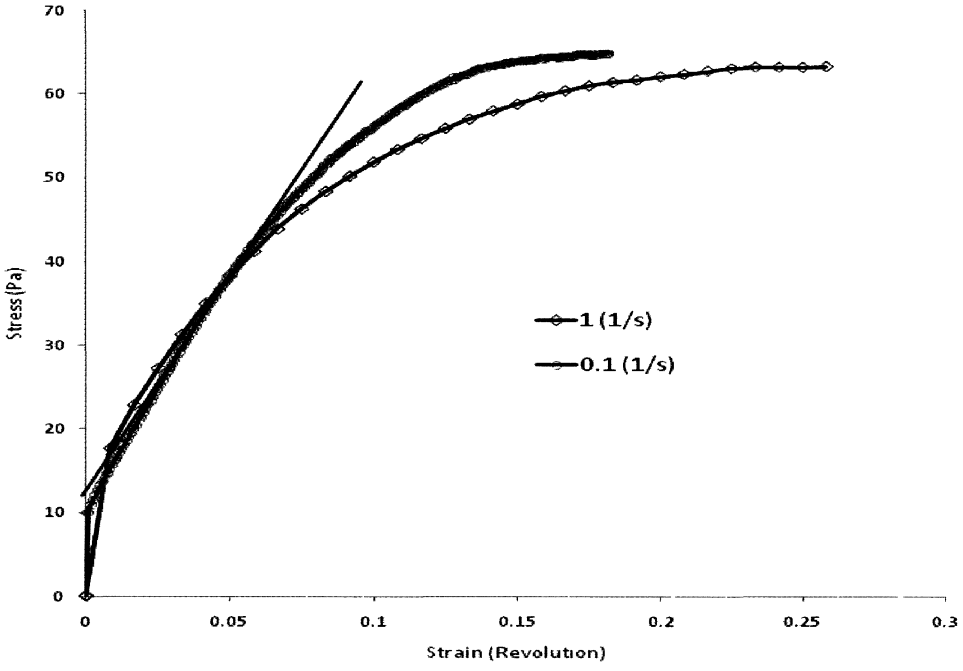

Figure 4.24: Stress-strain profiles of tailings at 38% GWC measured at shear rates of 0.1 and 1 (s^{-1}).

4.3.3 Comparison of yield stress measurement

Table 4.4 shows the yield stress for tailings prepared at 38% GWC using different methods. By comparing the different techniques used for the measurement of yield stress it could be seen that there was a good agreement between the direct measurement and the results from the slump test. More consistent results are obtained using a stress relaxation technique (Figure 4.25). This residual shear stress gives good agreement with yield stress determined from the slump test. Note that the average

value recorded for the stress is reported in this figure.

Methods	Possible yield stress
Slump test	30
Stress relaxation	22
Constant stress	20-50
Stress growth	10, 40, 64

Table 4.4: Yield stress at 38% GWC

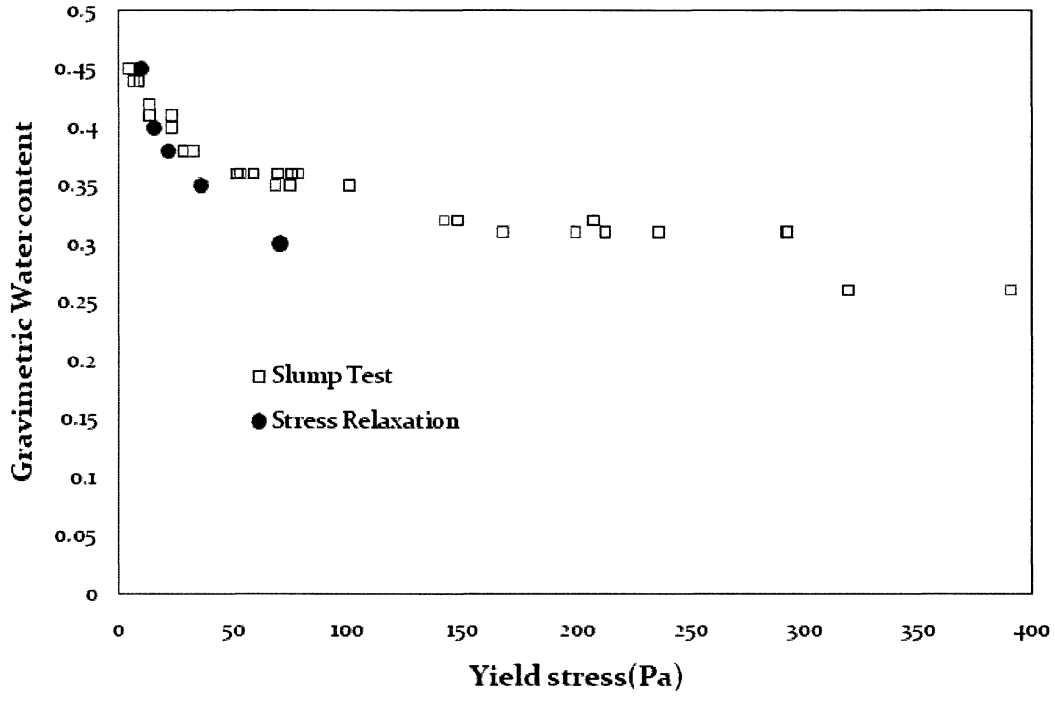

Figure 4.25: Yield stress from slump tests and stress-relaxation tests

4.4 Flume Test

The flume apparatus was used to study the changes in the rheological properties of the gold mine tailings during deposition. Flume test on horizontal planes and on successive layers with different flow rates were considered while the water flux out of

the flowing tailings into underlying desiccated tailings was tracked using tensiometers installed in the bottom layer. The tests are summarized in Table 4.5.

Test number	Description
1	Single layer deposition at flow rate of 1.6 LPM
2	Single layer deposition at flow rate of 0.8 LPM
3	Single layer deposition at flow rate of 0.4 LPM
4	Single layer deposition at flow rate of 0.4 LPM in 30 min
5	Single layer deposition at flow rate of 0.4 LPM in 40 min
6	Single layer deposition at flow rate of 0.4 LPM in 30 min at 47%GWC
7	Two layer deposition at flow rate of 0.4 LPM in 15 min
8	Two layer deposition at flow rate of 0.4 LPM in 18 min
9	Two layer deposition at flow rate of 0.4 LPM in 10 min
10	Two layer deposition at flow rate of 0.4 LPM in 35 min on flat plane
11	Single layer deposition at flow rate of 0.4 LPM in 15 min on slope plane

Table 4.5: Summary of flume tests

4.4.1 Flume tests on horizontal planes

Initial flume tests were conducted on horizontal planes to investigate the effects of deposition speed on the final profile. The results are presented in Figure 4.26. As expected, the run-out of the flow increased and the final slope decreased as the time of deposition decreased. It could therefore be concluded that as the deposition speed decreased, tailings had more time for settling resulting in an increase in the yield stress. Generally no difference in profiles was observed for tailings deposited at 1.6 LPM or higher, for this specific volume of material.

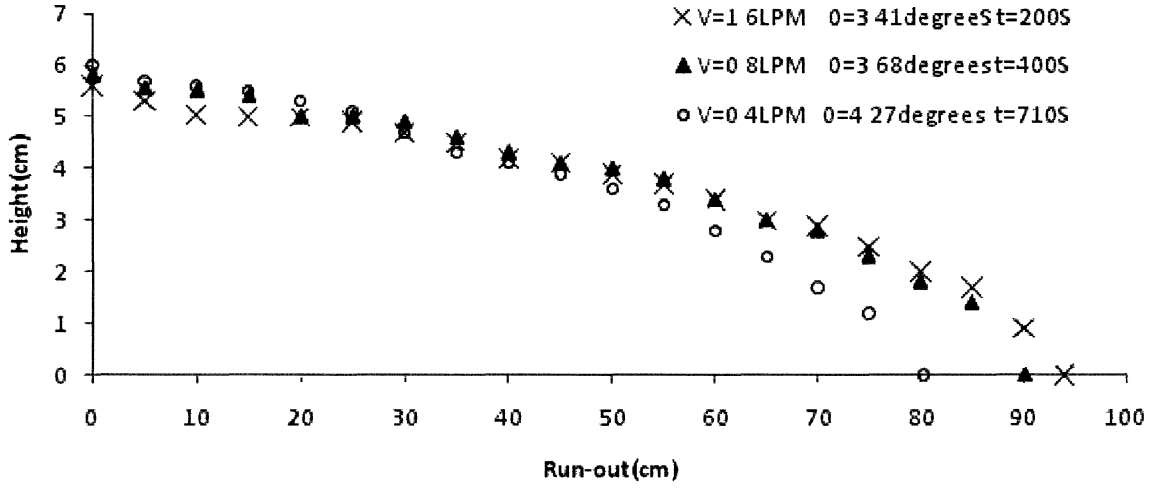

Figure 4.26: Three single layer flows at 38% gravimetric water content at different deposition rates.

Single layers deposited at rates higher than 1.6 LPM formed stable geometries. The profiles could be well fit using the yield stress extrapolated from slump tests for the pumping water content (30 Pa at 38% GWC) using Equation 2.28 as illustrated in Figure 4.27.

In order to quantify these changes, the variability in yield stress was evaluated by best-fitting Equation 2.28 to the flume profiles (Figure 4.28 through 4.30). Although the actual yield stress probably varies within these layers, this at least gives an indication of the change in the rheological properties as the tailings flow.

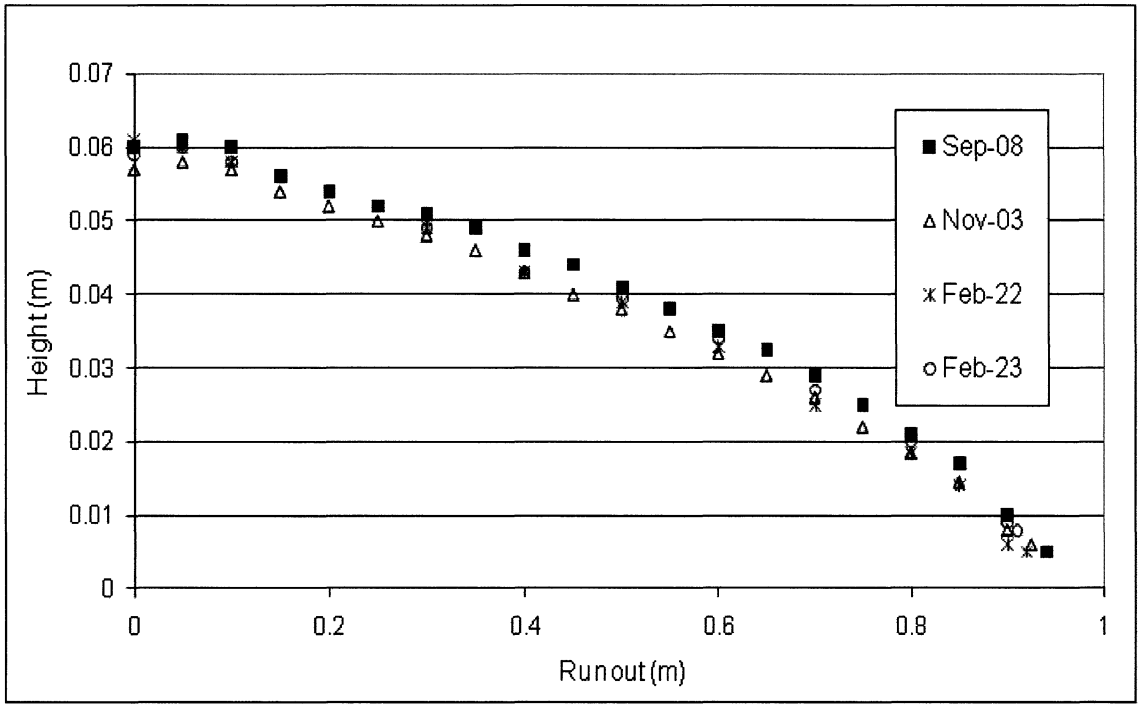

Figure 4.27: Repeatability of single layer flume tests at deposition rates of 30 LPM (Henriquez 2008)

The test with a flow rate of 1.6 LPM is best-fit with a yield stress of 30 Pa, which corresponds to the yield stress extrapolated from the slump test at 38% gravimetric water content (Figure 4.28). However, for the test with the slowest flow rate, 0.4 LPM, was best-fit to a yield stress of 40 Pa corresponding to the yield stress at lower water content (Figure 4.30), revealing the effects of settling on changes of rheological properties of the tailings.

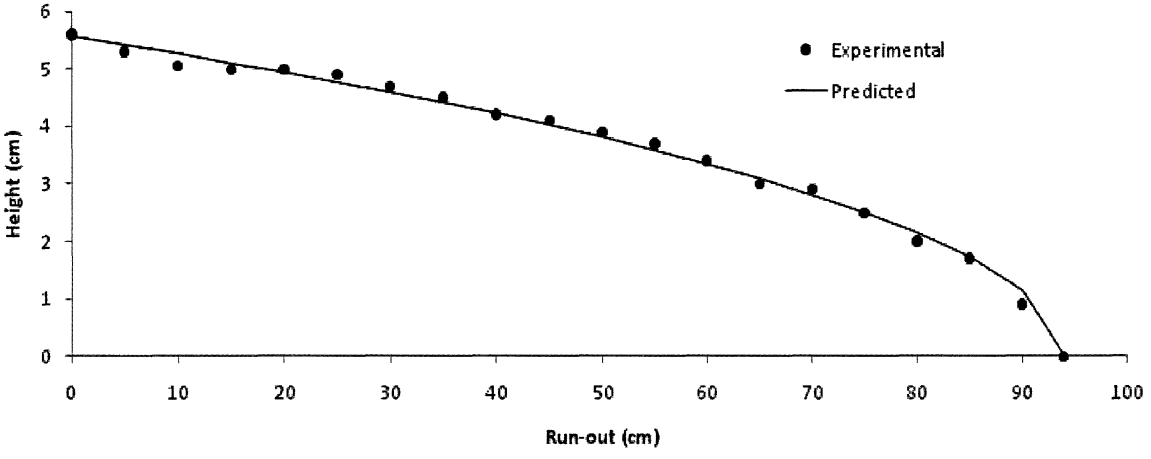

Figure 4.28: A single layer flow at 38% GWC with the deposition rate of 1.6 LPM (Test#1), all fitted with Equation 2.28 employing a 30 Pa yield stress

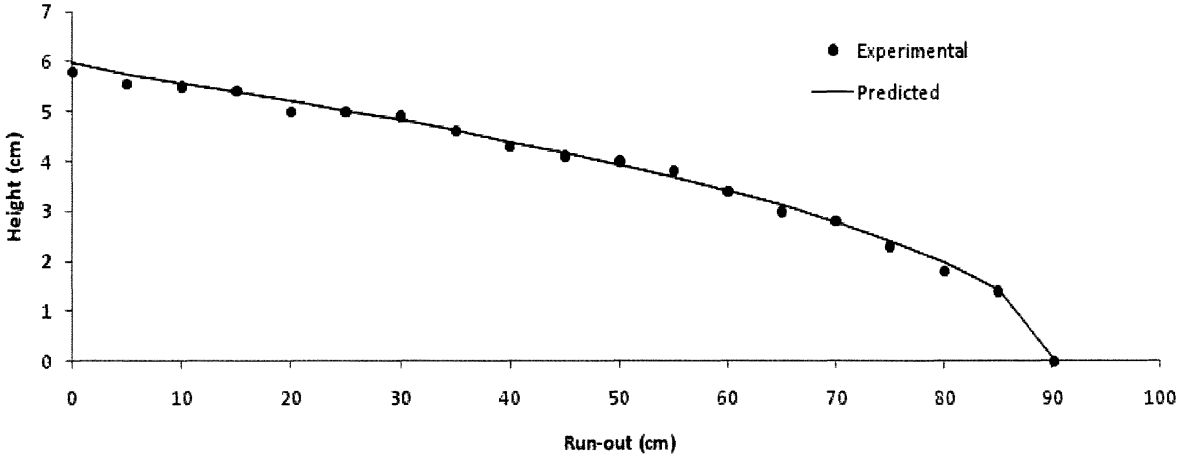

Figure 4.29: A single layer flow at 38% GWC with the deposition rate of 0.8 LPM (Test#2), all fitted with Equation 2.28 employing a 35 Pa yield stress.

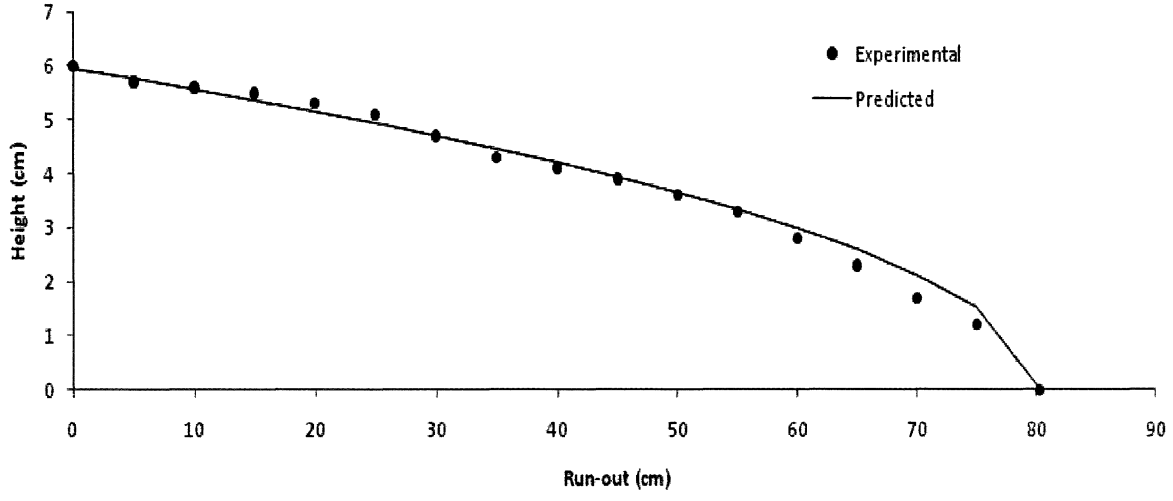

Figure 4.30: A single layer flow at 38% GWC with the deposition rate of 0.4 LPM (Test#3), all fitted with Equation 2.28 employing a 40 Pa yield stress.

4.4.2 Effects of settling on the stack's geometry

In order to further investigate the effects of settling, other tests were conducted while the deposition time was varied.

As mentioned earlier, flume tests were recorded by a high speed camera. The following figure is an example of the visualization of tailings deposited with the speed of 0.4LPM and at the gravimetric water content of 38%, while tailings were deposited in 30 minutes. To better illustrate the rheological changes samples were taken from different points of the flow for water content measurements of subsequent flume tests 10 minutes after deposition and after the tailings came to a stop. The result showed that the water content at the deposition point was 36.8%, and 39.4%, 40 cm from the deposition point, after 10 minutes (Figure 4.31).

The water content for the toe of the deposition was the highest (46.7%) and the lowest at the deposition point with the water content of 36.8% after the flow stopped. This is due to two factors, i) the flow unrolls like a carpet, the freshest tailings flowing over the older tailings to the toe, and ii) bleed water drains toward the toe in the flume tests. These two phenomenon result in the water content changes and as seen in section 4.2 the yield stress is very sensitive to changes in the water content, resulting in a profile which is steeper than expected. Figure 4.32 further confirmes this statement as the best fit was gained when a yield stress of 47 Pa was employed.

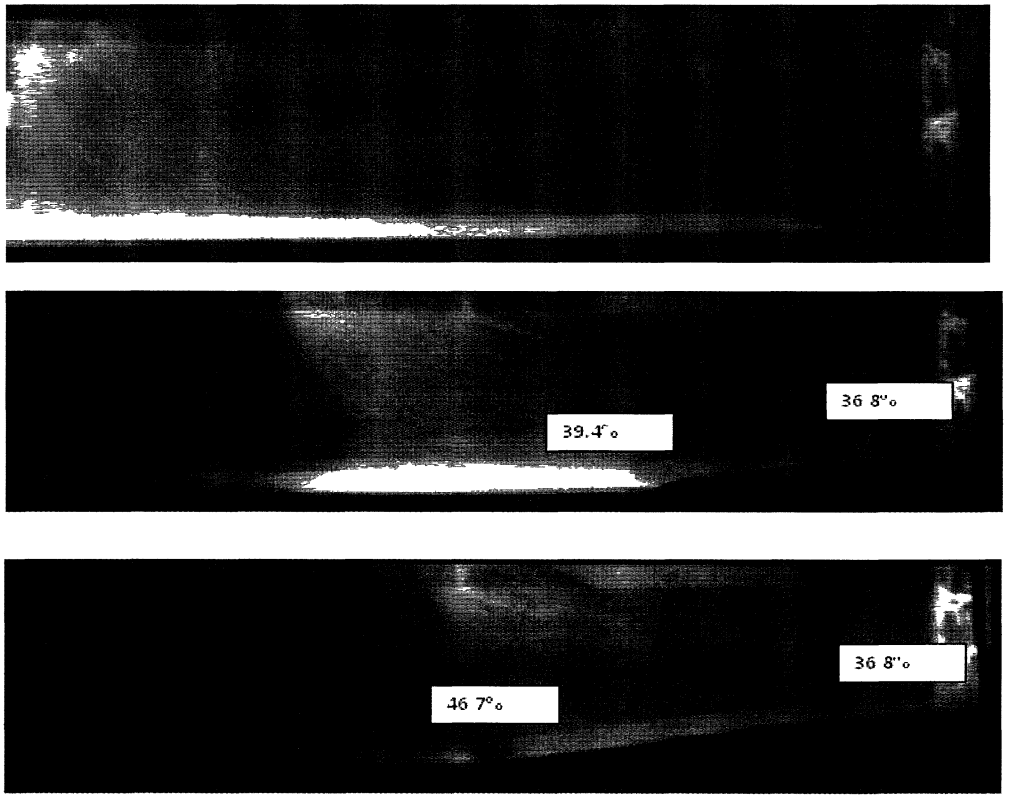

Figure 4.31: Visualization of a flume test where tailings where deposited at the 0.4 LPM and at 38% GWC at beginning, after 10 minutes and end of the test (Test#4) (numbers are the water content at different points)

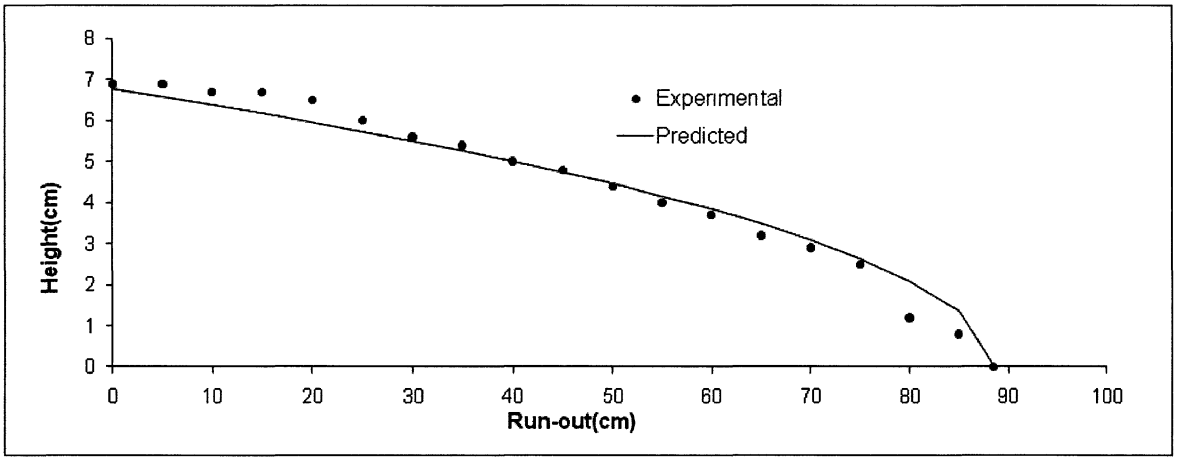

Figure 4.32: A single layer flow at 38% GWC with the deposition rate of 0.4 LPM and in 30 minutes (Test#4), all fitted with Equation 2.28 employing a 47 Pa yield stress

In the next test, Figure 4.33, the deposition time was increased to 40 minutes and the best fit was gained employing a yield stress of 52 Pa. Note that for all the tests where tailings were deposited at 38% GWC and with the slowest flow rate, longer deposition time resulted in a higher value for the yield stress as a result of giving the tailings more time for settling.

Figure 4.34 illustrates the changes in the yield stress as the tailings were deposited at 47% gravimetric water content and with the slowest speed. The LT equations were fit to the experimental data using a yield stress of 20 Pa, again higher the value from the slump test results.

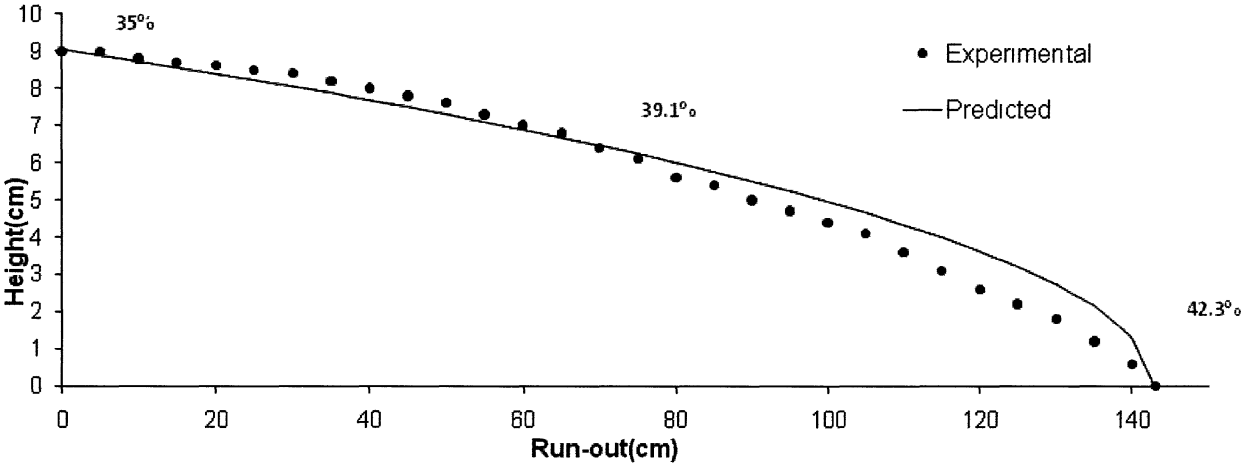

Figure 4.33: A single layer flow at 38% GWC with the deposition rate of 0.4 LPM and in 40 minutes (Test#5), all fitted with Equation 2.28 employing a 52 Pa yield stress.

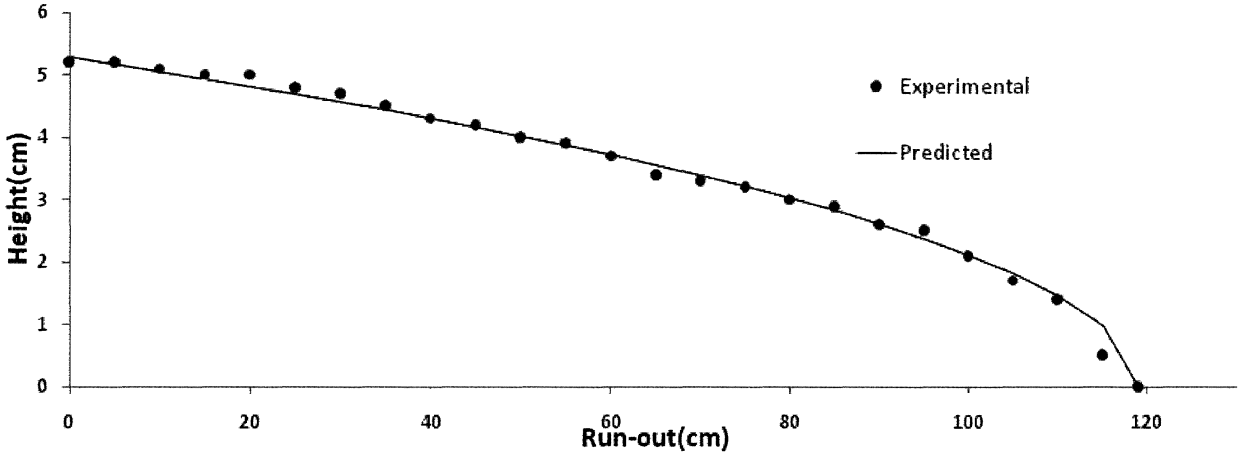

Figure 4.34: A single layer flow at 47% GWC with the deposition rate of 0.4 and in 30 minutes (Test#6), all fitted with Equation 2.28 employing a 20 Pa yield stress.

4.4.3 Flume test on successive layers

Flume test on successive layers were used to evaluate the effects of underlying desiccated layer on the changes in the rheological properties of the fresh layer. The fresh layer was always deposited at the rate of 0.4 LPM. It should be noted that before the new layer was poured the older layer was left to dry to significant values of suction (between 60 to 80 KPa). The water flux out of the flowing tailings into underlying desiccated tailings was tracked using tensiometers installed in the bottom layer.

Results from a multilayer deposition are illustrated in Figure 4.35 and Figure 4.36 where tailings were let to deposit in their natural form. The second layer was deposited at the speed 0.4 LPM after the first layer desiccated to a matric suction of 61 kPa . The evolution of suction in the older desiccated layer is shown in Figure 4.36. Tensiometers 1 and 4 were installed at the toe and deposition point, and tensiometers 2 and 3 were located in between with tensiometer 2 closest to the toe. Tailings were let to flow until they reached the toe of the desiccated layer. There is a very dramatic dissipation of matric suctions as the flow passes over each tensiometer. The flow takes 15 minutes (900 s) to be deposited even the matric suction at the toe is completely dissipated before the flow stops.

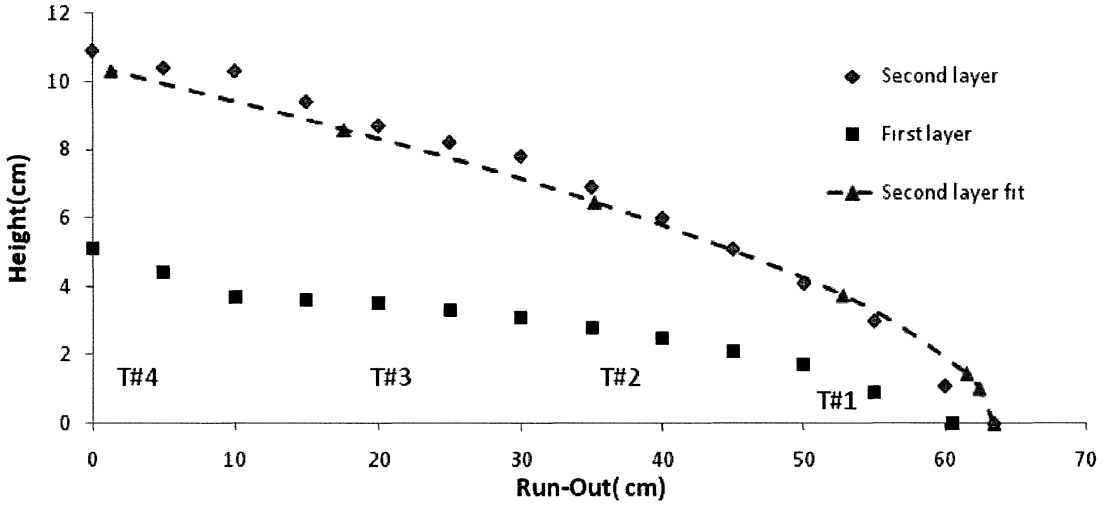

Figure 4.35: Deposition of second layer after the first layer is desiccated to a matric suction of 60 kPa by drying(Test#7). Second layer is best-fit to Equation 2.29, using a yield stress of 100 Pa

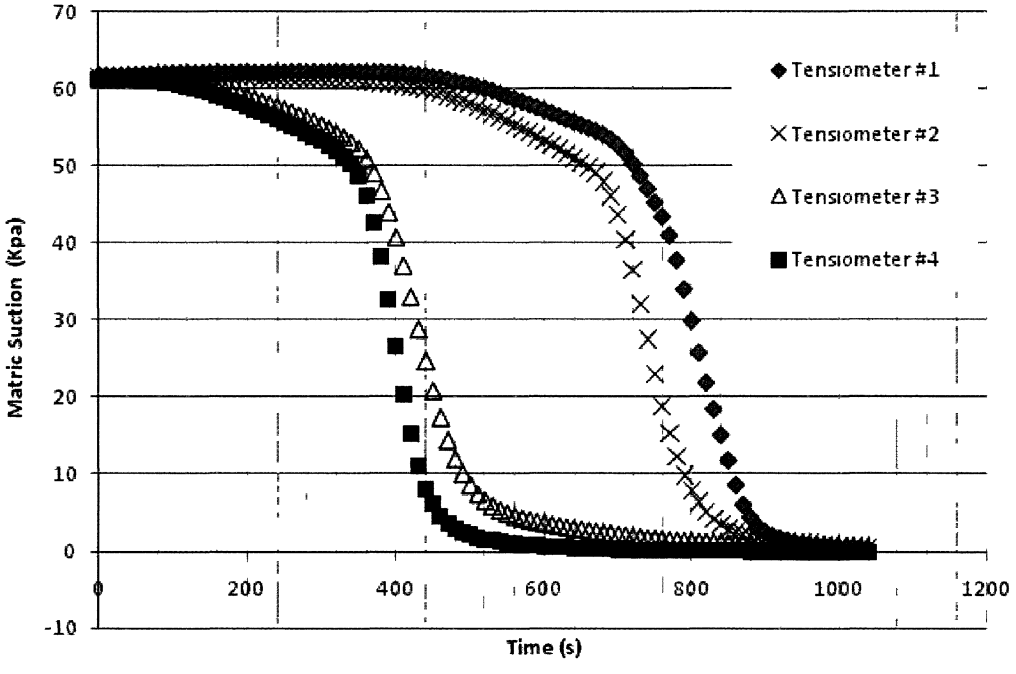

Figure 4.36: Evolution of matric suction in the older layer during deposition of the second layer over 900s (Test#7)

The second layer is fitted with Equation 2.29, the angle in Equation 2.29, which represents the underlying topography, is obtained by fitting the original layer's topography with a linear profile to estimate the slope. The best fit for Equation 2.29, shown in Figure 4.35 is with a yield stress of 100 Pa, over three times the yield stress of a fresh layer deposited over a short time period (30 Pa).

To further investigate the capacity of the underlying layer for soaking water out of the freshly deposited layer other tests were conducted in different conditions.

The following Figures (4.37 and 4.38) show the results from another flume test where tailings were deposited at the lowest speed and at around 39% GWC. This time tailings were deposited on a layer with longer run-out. Similar to the previous test the second layer was fitted with Equation 2.29. The best fit for Equation 2.29 was gained with a yield stress of 90 Pa, more than 4 times the yield stress from the slump test at the same water content and close to when the tailings were deposited at around 38% GWC but on less amount of tailings (the run-out was 160% greater than the previous test).

The water content at different locations is shown in Figure 4.37. The water content near the toe of the profile was 39.1%, much lower than expected, which is due to the capillary action by the underlying layer as the tailings were flowing.

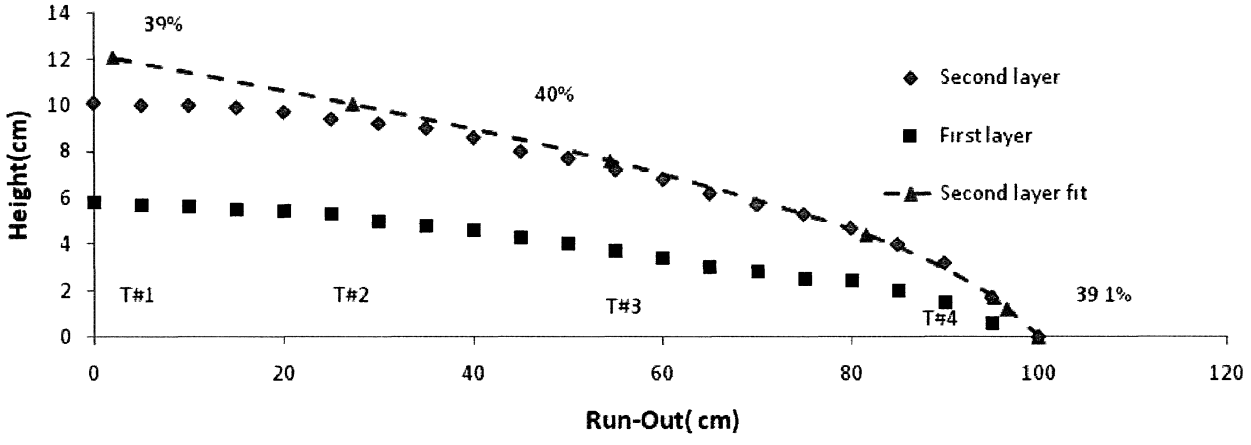

Figure 4 37 Deposition of second layer after the first layer is desiccated (Test#8) Second layer is best-fit to Equation 2 29, using a yield stress of 90 Pa

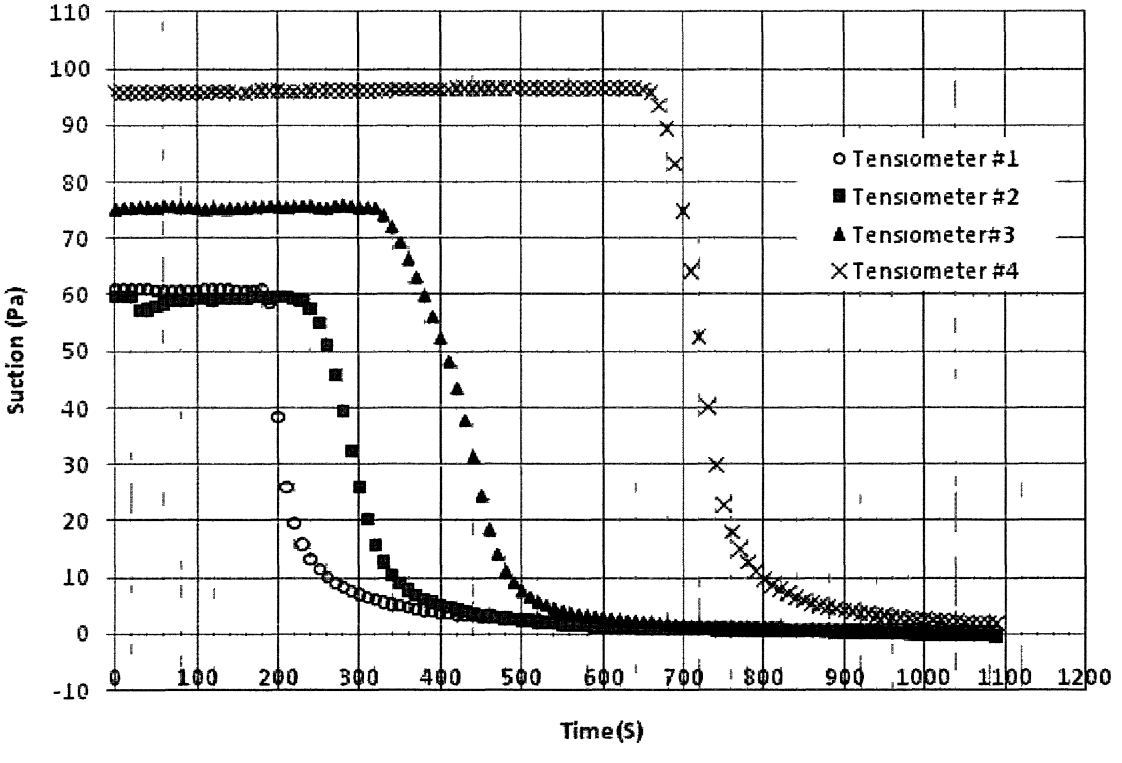

Figure 4 38 Evolution of matric suction in the older layer during deposition of the second layer (Test#8)

In the next test the effects of the degree of saturation of the underlying layer was investigated by letting the first layer dessicate up to higher matric suction (around 140 KPa). It can be observed from Figure 4.39 that this time the underneath layer had higher capacity for soaking water out of the freshly deposited layer as the best fit was gained with a yield stress of around 116 KPa. The tensiometer results are not reported as they all cavitated before the second layer was poured.

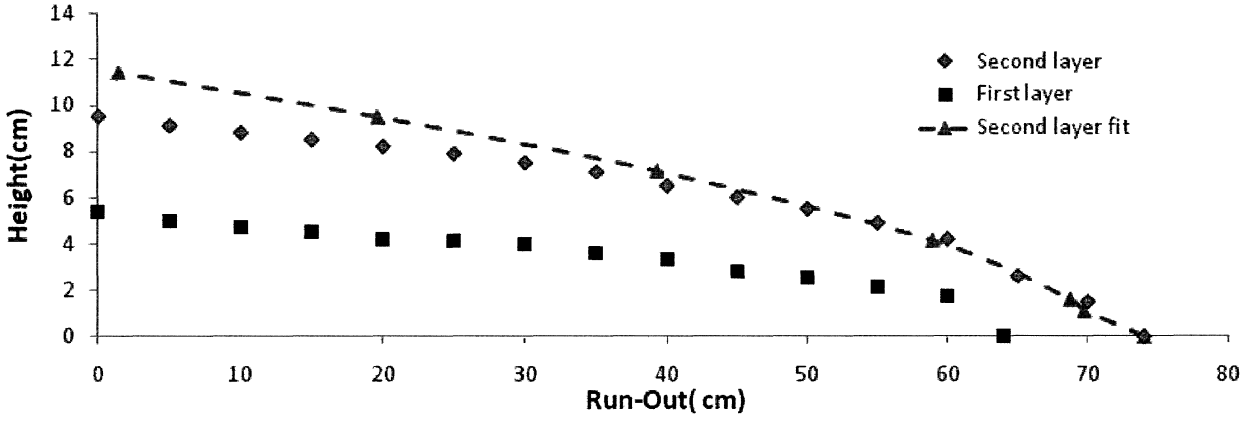

Figure 4.39: Deposition of second layer after the first layer is desiccated (Test#9)

Another test was conducted using the flume, where tailings at 38% GWC were deposited at the rate of 0.4 LPM on a flat desiccated layer of 150 cm long. After the first layer was desiccated to a matric suction of 80 kPa by drying the second layer was poured. Figures 4.40 through 4.42 show the different profile of the second layer as it was deposited.

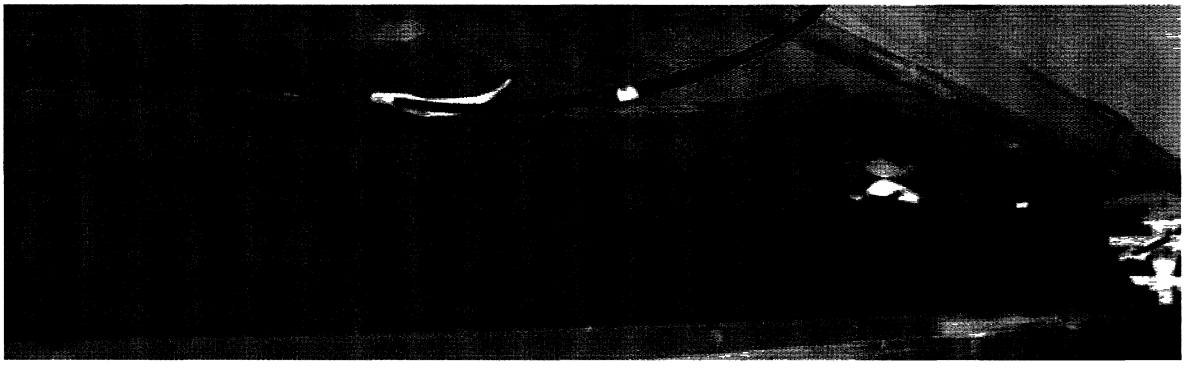

Figure 4.40: Top view of the flume test before deposition (the cracks show that the layer is highly dessicated (Test#10)

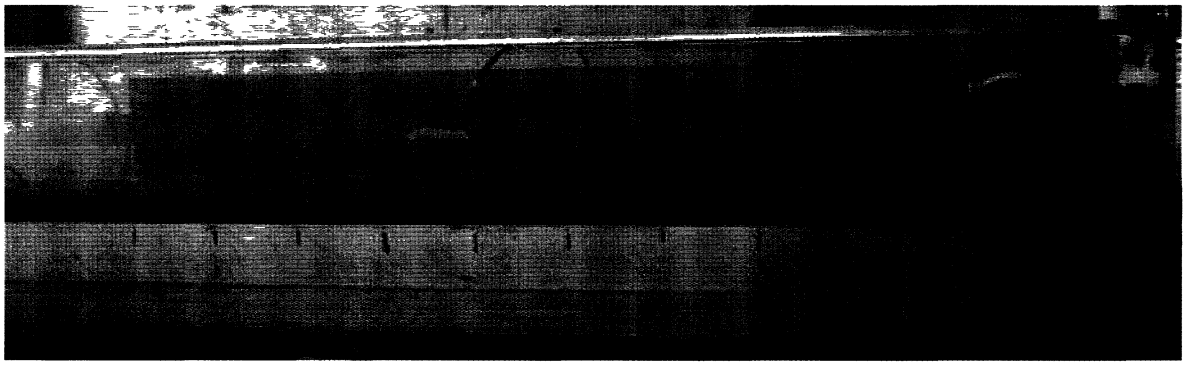

Figure 4.41: View from the side of the flume a few minutes into deposition (Test#10)

Figure 4.42: Top view of the flume test on a flat bed during deposition (Test#10)

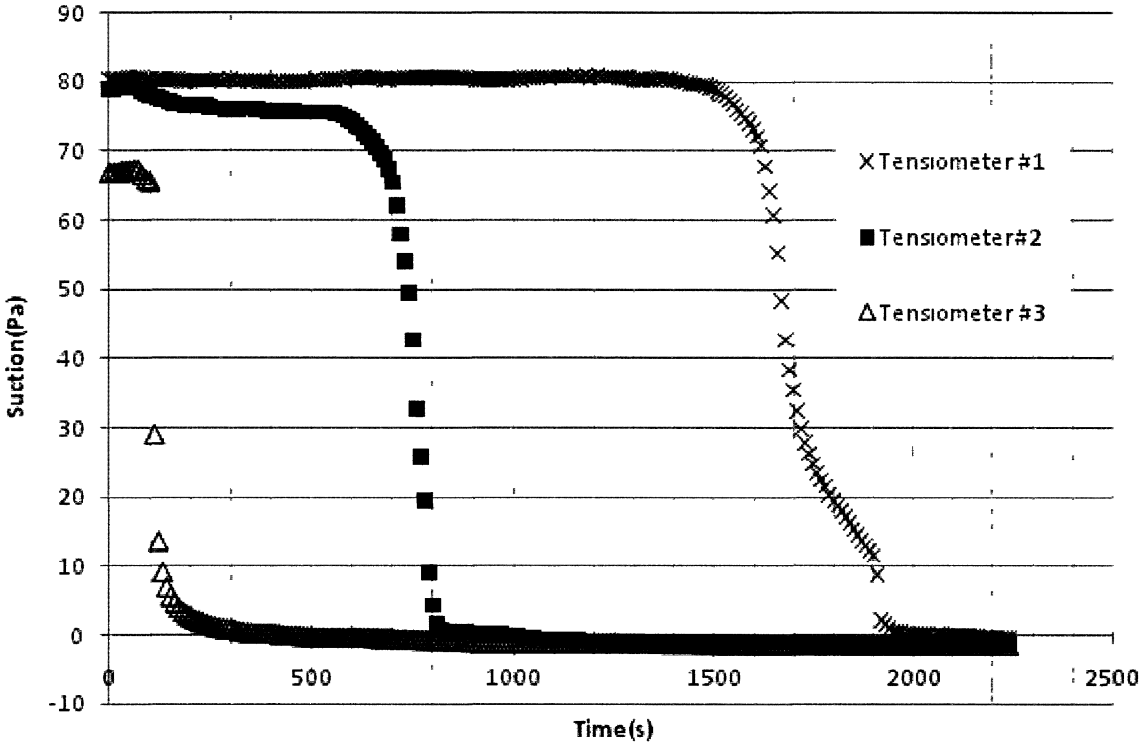

Figure 4.43: Evolution of matric suction (Test#10)

Figure 4.43 presents the evolution of the matric suction in the older layer during deposition. Tensiometers 1 and 3 were installed at the toe and deposition point, and tensiometers 2 in between these two. The flow took 35 minutes (2100 s) to reach the toe, again the matric suction at the toe is completely dissipated before the flow stops.

The second layer is fitted with Equation 2.28. The best fit for Equation 2.28, shown in (Figure 4.44) , is with a yield stress of 50 Pa, close to the yield stress gained from the tailings deposited on a flat bed in the flume.

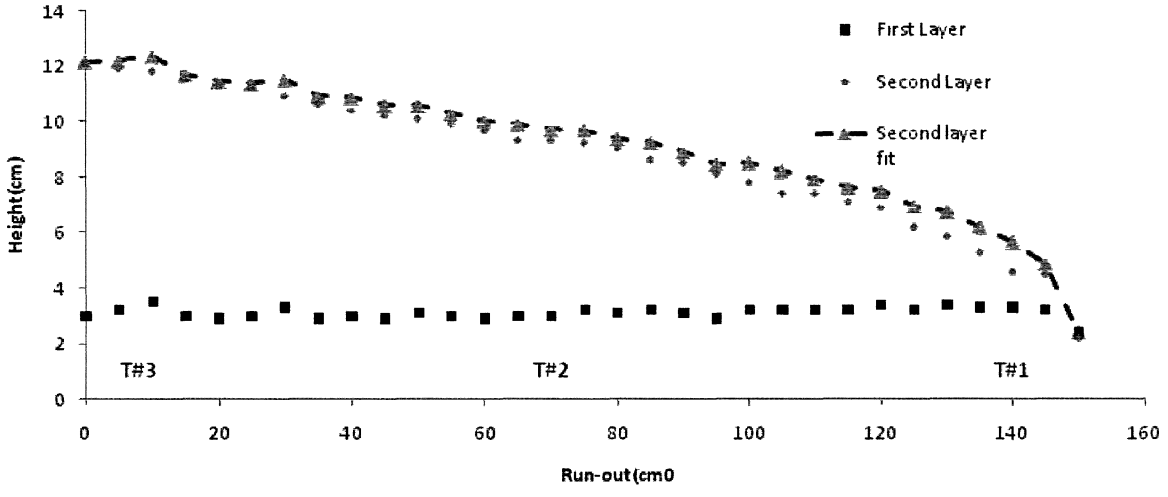

Figure 4.44: Deposition of second layer on a flat desiccated layer (Test#10). Second layer is best-fit to Equation 2.28, using a yield stress of 50 Pa

4.4.3.1 Flume test on sloping planes

Flume test of single layer was performed on a slope of 4.57° where tailings were deposited with the slowest speed (0.4 LPM) and at GWC of around 38%, the results are presented in Figure 4.45.

The profile was predicted using Equation 2.29 and the best fit was gained when a yield stress of 40 Pa was used. Note that the approximately the same volume of tailings were used as the test#7 (when tailings were deposited on a desiccated layer) and the sloped which was picked was that of the first layer (Figure 4.35). By comparing the results of these two tests the role of the capillary action is better understood. In the later test the flow resulted in a greater extent and lower slope; indicating that the underneath layer has a high potential of soaking the water out of

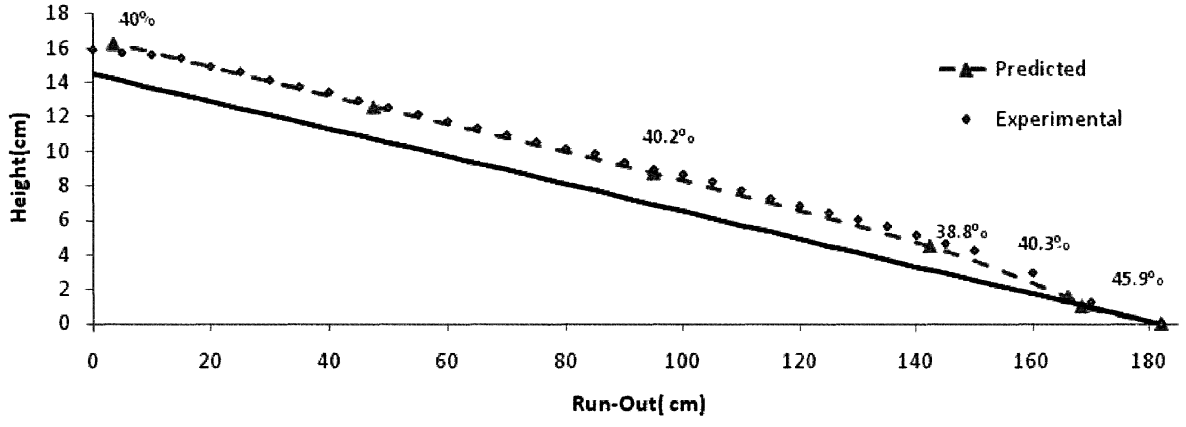

Figure 4.45: Flume test performed on an inclined bed with the slope of 4.57^0 (Test#11)

the freshly deposited tailings as they are flowing, giving them a higher strength.

4.4.3.2 Discussion of flume test results

The following table shows the summary of the single layer flume test results conducted at 38% GWC. The table shows the yield stress from fitting the Lubrication Theory equation for flow on a slope and on flat surface (Equation 2.28 and 2.29) to the experimental data and the deposition time for each test. The fourth column shows the water content of the tailings for half the deposition time from the settling curve at the same water content (Figure 4.3) and the yield stress for that particular water content according to the slump test data.

The yield stress values predicted from best fits of the data to the LT equations lie below the yield stress values determined if the rate of settling is similar to what occurs under static conditions. It may be that the kinetic energy in the tailings in

Best fit yield stress (Pa)	Flow rate(LPM)	Deposition time(s)	GWC from settling test	Yield stress from slump for GWC from settling test
30	1.6	200	37.63	32
35	0.8	400	36.94	41
40	0.4	710	36.37	48
47	0.4	1800	35.44	60
52	0.4	2340	35.17	65
40	0.4	900	36.13	50

Table 4.6: Summary of single layer flume test results

the flume are enough to delay settling. However, a similar trend was observed within these tests and the settling test: the yield stress increases with time of deposition, slowing down for longer deposition time (Figure 4.46).

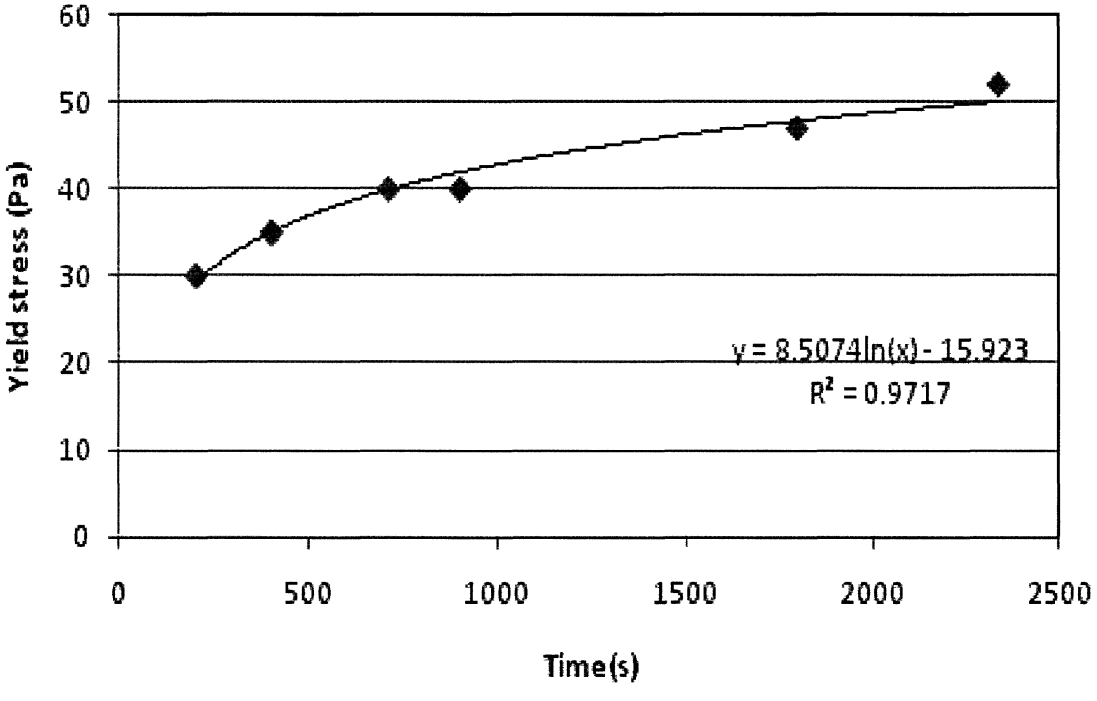

Figure 4.46: Best-fit yield stress versus deposition time for single layer tests

The following table summarizes the results from the multilayer deposition and the final water content for the second layers assuming the maximum capacity of the first layer for soaking water from the freshly deposited layer.

Best fit yield stress (Pa)	**Flow rate (LPM)**	**Deposition time(s)**	**Average matric suction (first layer)**	**GWC second layer (Capillary)**	**Yield stress from slump**
100	0.4	900	61	35.12	68
90	0.4	1100	70	35.97	50
50	0.4	2100	70	35.7	50
116	0.4	600	140	34.71	75

Table 4.7: Summary of double layer flume test results

The quantity of water transferred between the two layers is calculated using the difference between the initial water content of the bottom layer (measured or estimated from the wate-retention curve for freshly deposited tailings, in Figure 4.2), and the resaturated water content estimated using the water-retention curve for rewetted tailings (Figure 4.2). This quantity of water is then used to determine the change in water content of the fresh layer. The results indicate that the yield stress gained from the estimated change in water content by capillary action alone lies below the value from the yield stress gained by best fitting the data to LT equations. However, the above analysis may be too simplistic. Nevertheless, it is apparent that the water adsorption by the underlying layer can increase the yield stress as the tailings are flowing.

4.5 Pouring Test

In all of these tests the subsequent layer was deposited after a day where the underlying layer had dried to approximately 30%, therefore no appreciable suction developed. Note that the maximum deposition time was 400 s, compared to over 900 s for the flume tests, as a result the yield stress change is not significant and a value of 30 Pa was used in the predictions.

In the first test, for each layer 2500 mL of tailings were deposited with the speed of 0.4 LPM, where 11 layers were deposited. The first layers exhibited an axi-symmetric profile and could be very well-predicted in terms of the footprint and average angle using the lubrication theory (Figure 4.50). The curvature of the layers initially decreases, until the profile became almost linear. As the number of layers deposited increased the discrepancy between the profiles predicted using the lubrication theory increases with the experimental data. Later layers begin to exhibit a convex profile (Figures 4.51 and 4.52). This is similar to what is observed in the field in late deposition of thickened tailing (Addis and Cunningham, 2010). The type of dynamic flow that is exhibited at this point indicates that at least for part of the time during deposition the flow establish a high velocity channel until some point where the flow started to spread out near the bottom of the stack.

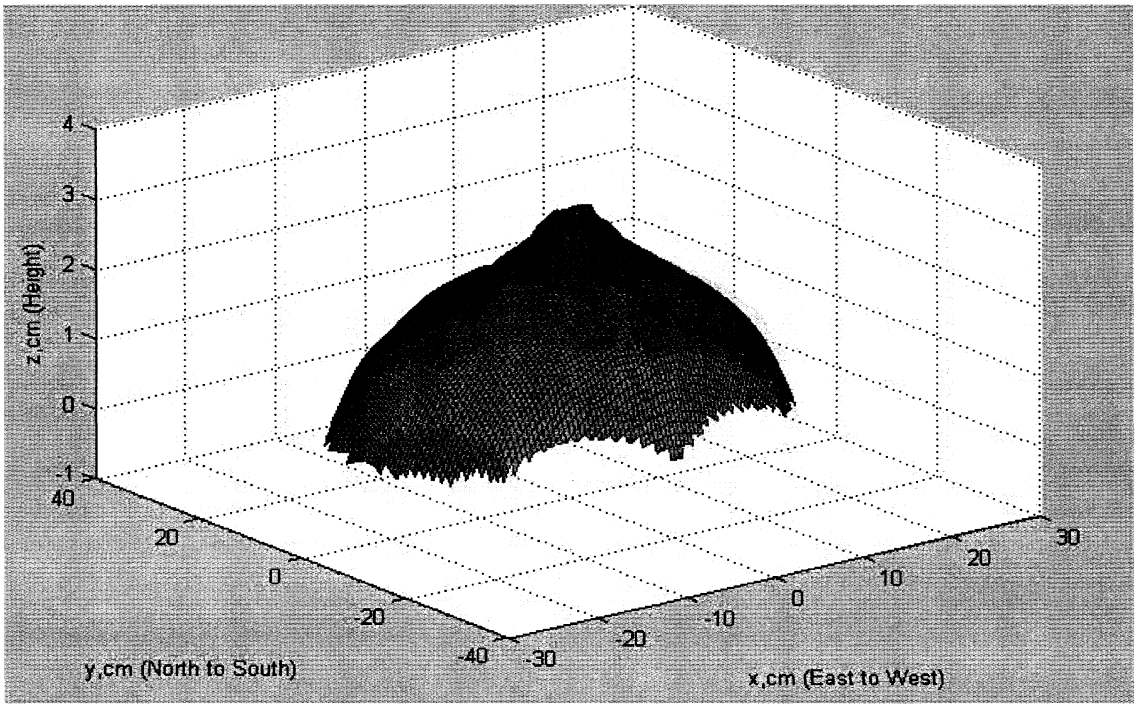

Figure 4.47: Experimental and predicted for layer 1 (0.4 LPM, 2500 ml)

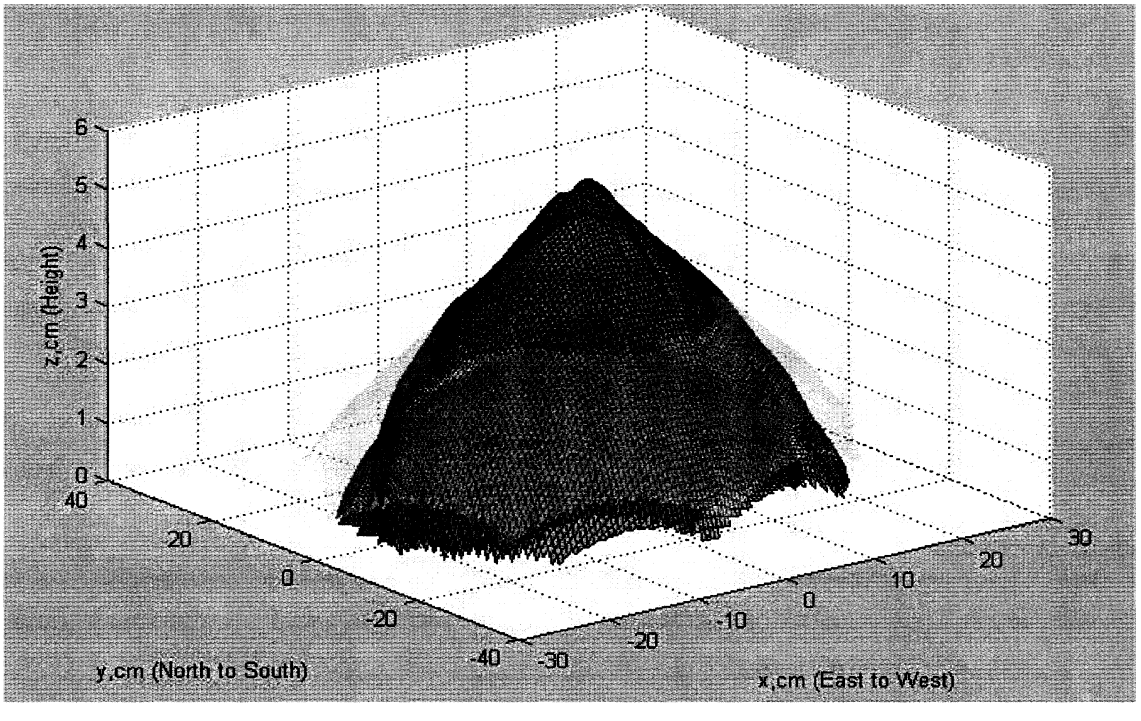

Figure 4.48: Layers 1 to 2, Prediction for layer 2 (0.4 LPM, 2500 ml)

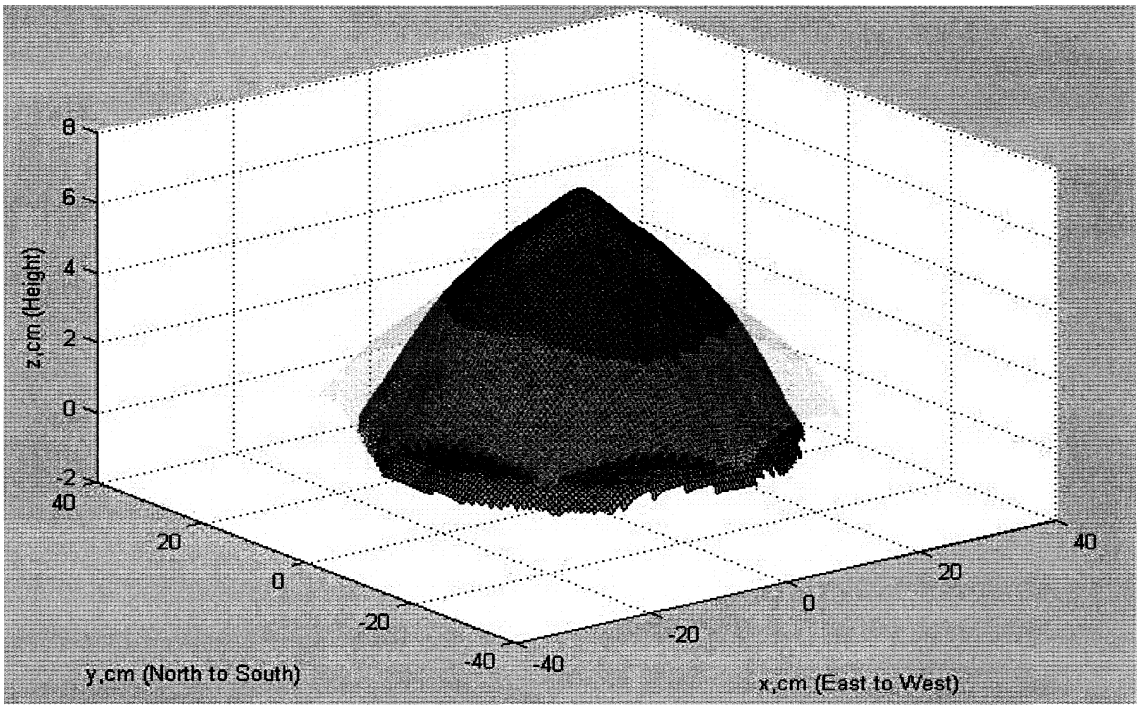

Figure 4.49: Layers 1 to 3, Prediction for layer 3 (0.4 LPM, 2500 ml)

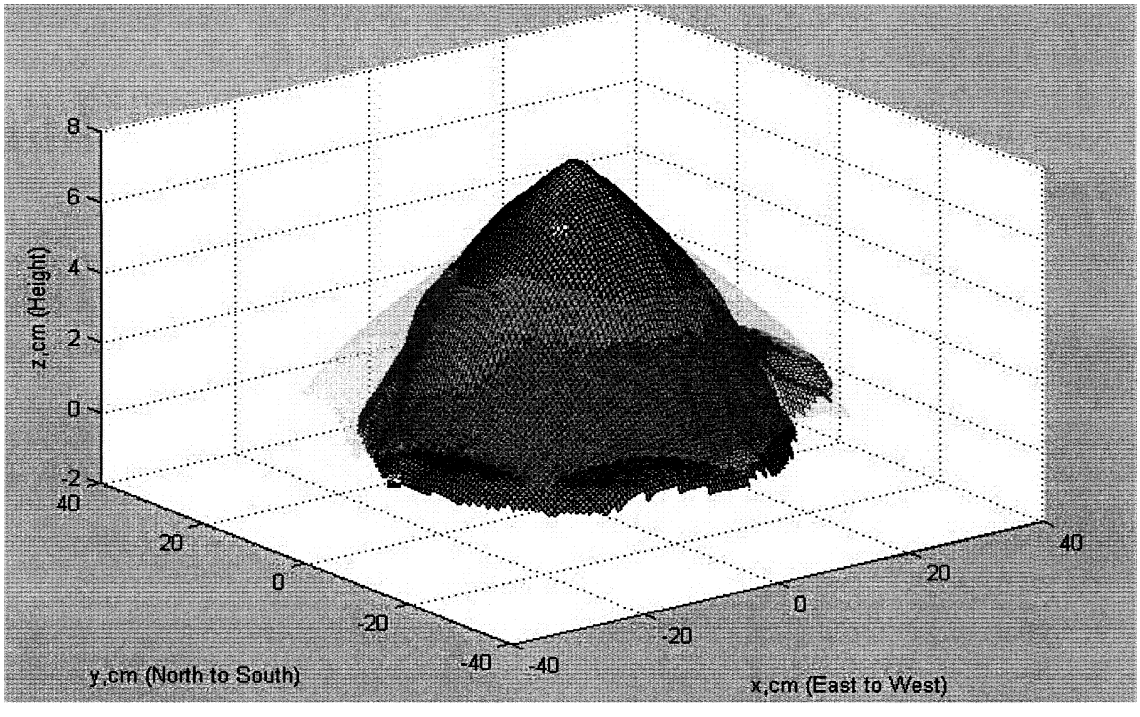

Figure 4.50: Layers 1 to 4, Prediction for layer 4 (0.4 LPM, 2500 ml)

Figure 4.51: Example of later geometry, plan view after 8 layers.

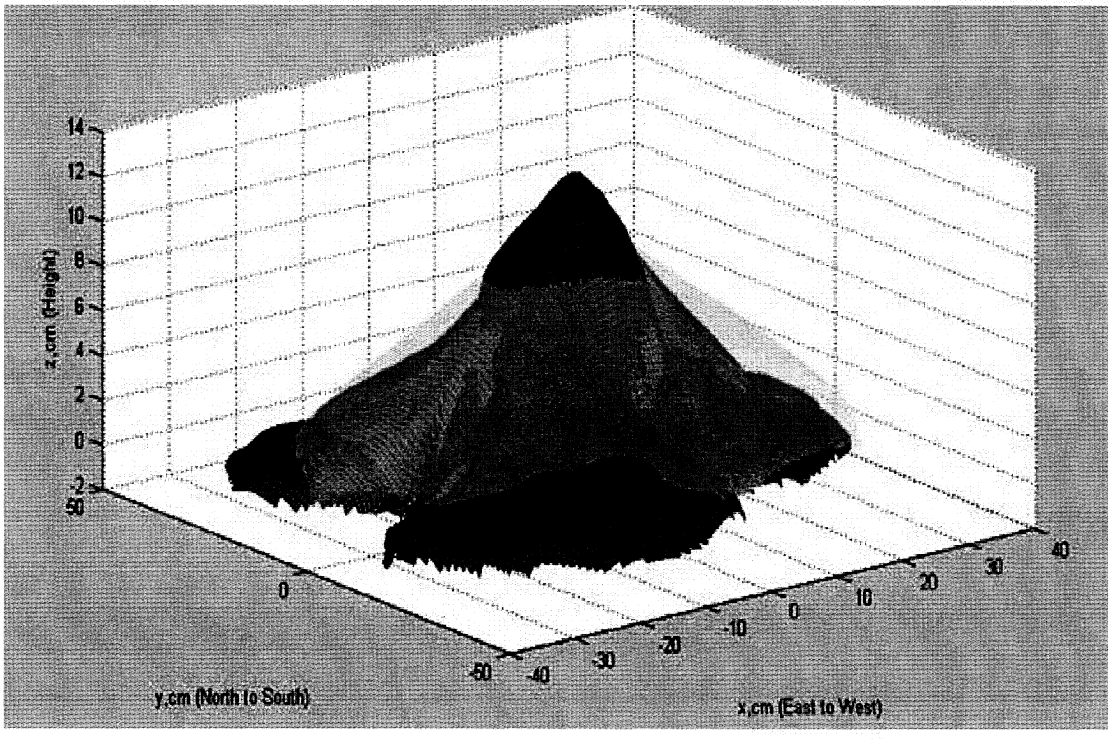

Figure 4.52: Layers 1 to 8, Prediction for layer 8 (0.4 LPM, 2500 ml)

Figure 4.53 shows the predicted and experimental values for the average angle for different volume of tailings for this test (speed of 0.4LPM). It can be seen that at the beginning there is a good correlation between the predicted and the experimental data; however, as the number of layers increased the slope predicted using the Lubrication Theory falls below the values from the experiment.

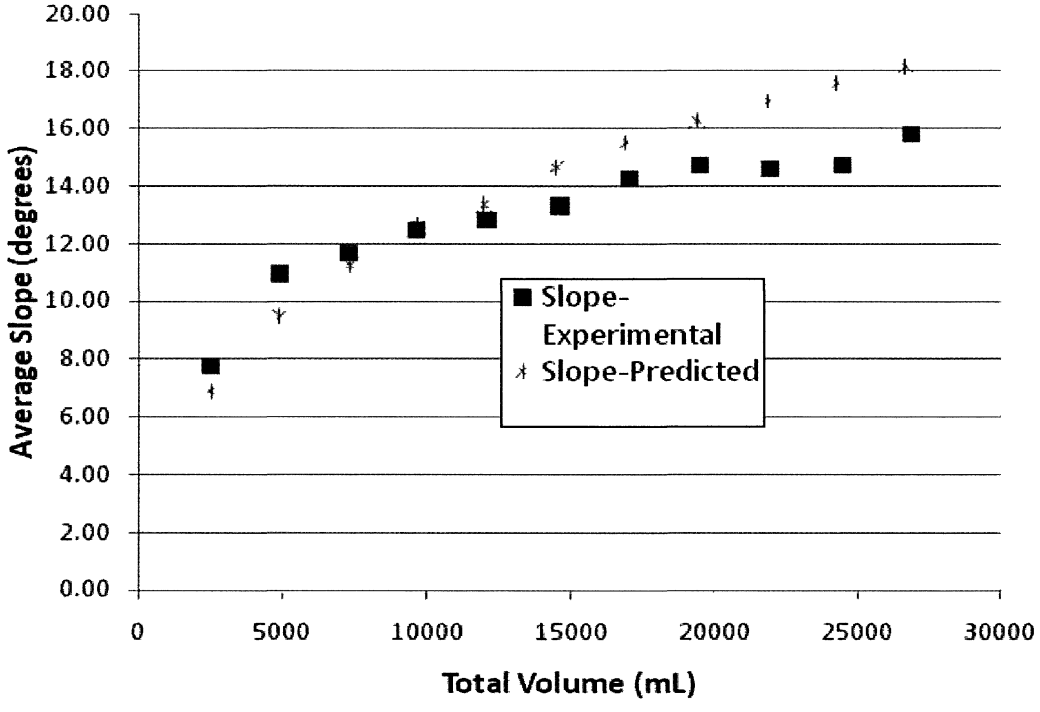

Figure 4.53: Predicted and experimental values for slope (0.4 LPM, 2500 ml)

Similar trend was observed when the tailings were deposited at higher speed (0.8 LPM), but with the same volume. The discrepancy between the predicted and experimental results occurred at the same angle (14^0).

4.6 Profile of tailings in the field

Figure 4.54 shows the profile of Bulyanhulu tailings in field, measured in the summer of 2005. The data were best-fit to Equation 2.29, assuming deposition from the top of a conical hill of 0.5 degree, employing a yield stress of 100 Pa.

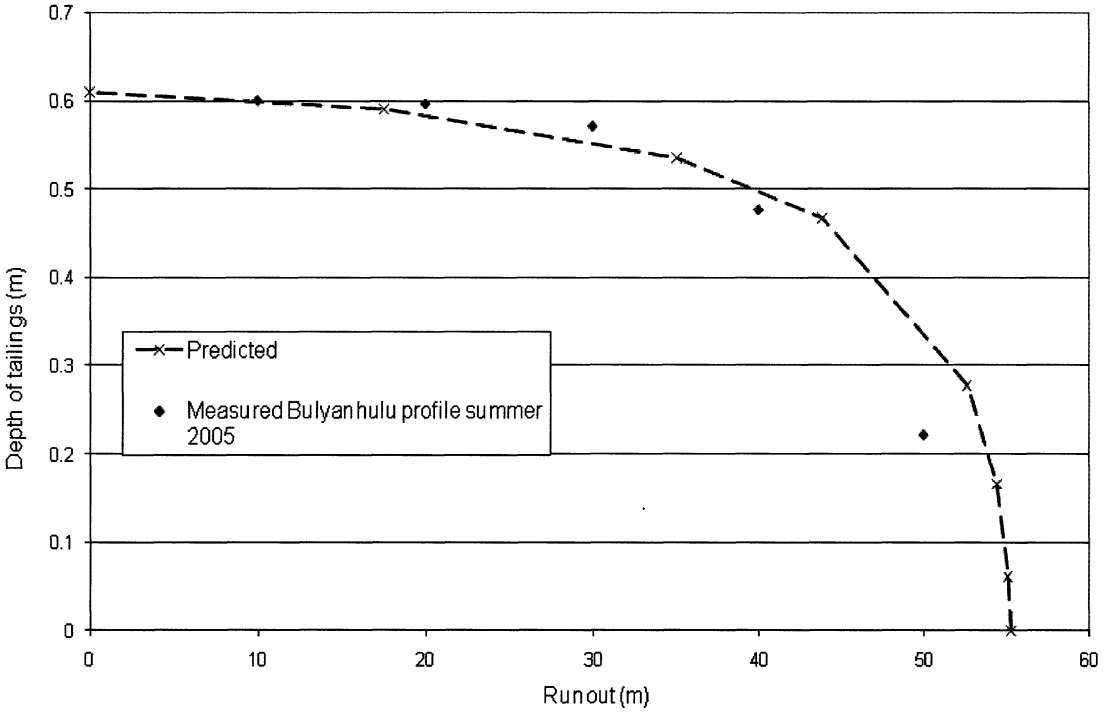

Figure 4.54: Profile of Bulyanhulu tailings in field (After Simms 2007)

Figures 4.55 presents the profile of multilayer tailings deposits obtained in the spring of 2001 in field. As can be observed from this figure, the initial layers show significant curvature. This curvature decreases as the number of layers increase, becoming linear in the later deposits. Similar behavior was observed during the pouring tests conducted in the laboratory (Figure 4.56).

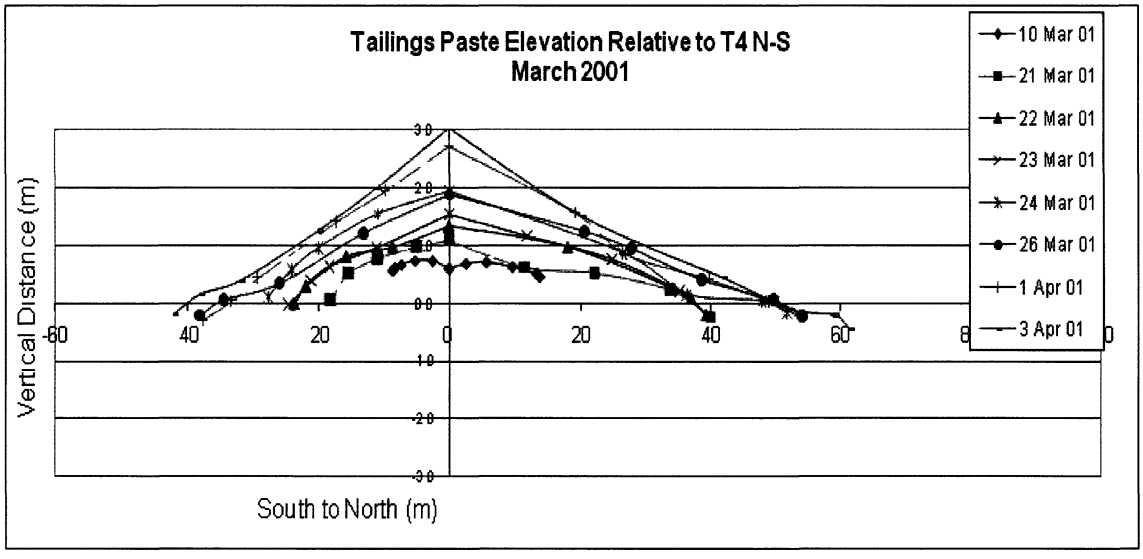

Figure 4 55 North-South profile of Bulyanhulu tailings in the field

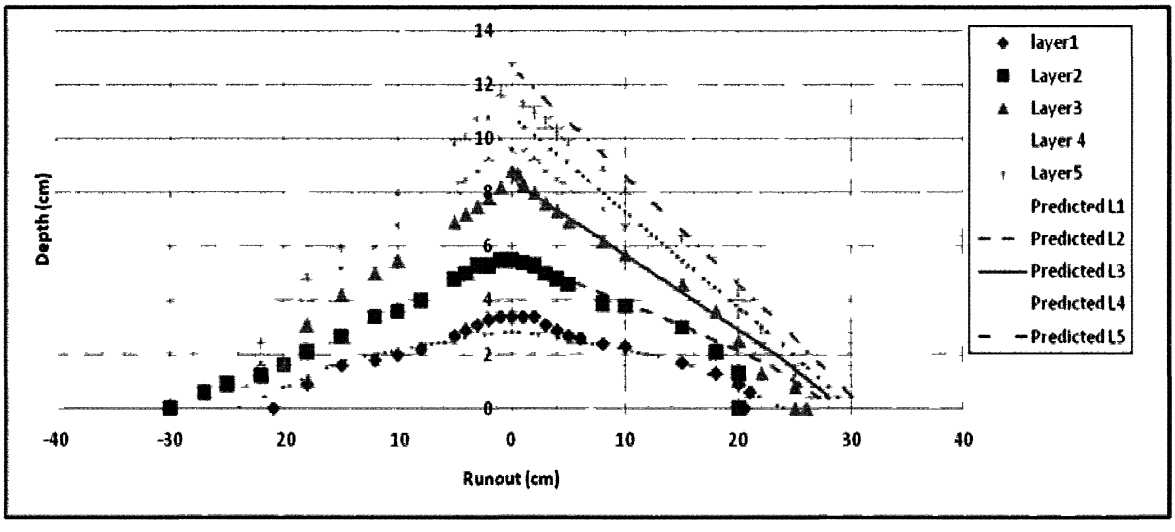

Figure 4 56 Pouring test conducted in laboratory

Chapter 5

Conclusion

5.1 Conclusion

The geometry of tailing stacks is in part influenced by the rheological behaviour of the tailings, as well as by depositional parameters such as flow rate. This research investigates the changes in the rheological properties of gold tailings after they exit the pipe during deposition.

To this end, three sets of tests were conducted. The rheological parameters of the gold tailings were determined through both direct and indirect measurements using an Anton Par Rheometer, model MCR301, with a vane fixture and the slump test. In addition, several flume tests at laboratory scale were performed where the tailings were deposited at different initial water content, flow rates on both flat and inclined surface. An effective yield stress was evaluated by fitting the Lubrication Theory

equations to the equilibrium profiles. Finally, pouring tests on 1m by 1m Plexiglas surface to investigate the applicability of the lubrication theory to multiple layer and three-dimensional geometry.

It was found that the slump test, stress relaxation, constant stress, and stress growth tests gave fairly consistent estimates of yield stress (30, 20, between 20 and 50, and 40 Pa for 38% GWC respectively). Constant stress tests showed that for any stress applied below 120 Pa, the vane would eventually stop, though substantial shearing of the sample might already have occurred. The indirect method did not seem to be an appropriate technique for estimating the true yield stress of the material, as neither the Bingham, Casson, or Herchel-Bulley adequately captured the shape of the measured flow curves.

The influence of settling during deposition, was evaluated by slowly depositing single layer flows in flume. For tests deposited with a certain deposition time, the best-fit yield stress agreed with the yield stress determined from the slump test. Beyond a certain deposition time, the tailings exhibited consistently higher yield stresses with longer deposition times. Yield stress could be correlated with deposition time using a logarithmic function. The rate of yield stress increase was somewhat less than what is observed in static settling tests.

The influence of adsorption of water by the underlying layer during deposition was investigated in a flume, by slowly depositing a fresh layer over a previously desiccated layer. The extent of desiccation was recorded using tentiometers installed in the

desiccated layer. Substantial increases in apparent yield stress were observed, above and beyond what one would expect from settling alone. The maximum yield stress observed in these tests was 116 Pa.

Multilayer Pouring tests, simulating 3-D tailings deposition, showed that LT theory agrees well with the overall angle for the first several layers. At a certain point, the tailings flow regime apparently changes, and the stack begins to exhibit a convex profile; steeper angle near the deposition point, and very flat angles near the edge of the footprint. The development of a convex profile is observed at many TT sites for later stages of deposition.

Generally, capillarity and the settling nature of highly thickened tailings are sufficient to result in "out of pipe" dewatering of tailings as the tailings flow. Significant increases in yield stress were detected for overland flow even without capillary action by the underlying layer. This shows that the effects of these two phenomena are important when it comes to managing surface deposition, and may be potentially used as an advantage by engineers to control a stacks footprint.

Chapter 6

Recommendations

6.1 Recommendations for future work

During the multilayer deposition tests (pour tests), it was observed that at a certain point the flow regime changed. Past this point, the LT equations were no longer applicable. It is recommended that the point at which this change in flow regime occurs could be quantified. It may be possible to determine appropriate Reynolds and Froude numbers to define this change in flow regime. A wide range of pour tests, for different layer volumes and pump speeds, are recommended.

It was shown that the yield stress increase during deposition was significant and it was a function of both settling and capillary action by underlying tailings. It is of significant practical interest to determine if there is a maximum value of yield stress that can be mobilized by these phenomena. Tests with longer run-outs would

be necessary to investigate the maximum yield stress gain. Such tests with longer run-outs, would also build confidence in the potential application of the LT equations to practice.

Bibliography

[1] Addis, P.C. and Cunningham, E.J. "Comparison of beaching slopes from two centrally discharging tailings storage facilities", *Proceedings of the 13th International Seminar on Paste and Thickened tailings*, Toronto, Canada, 2010.

[2] Annual Book of ASTM Standards. *Designation: C 143/C 143M-97 Standard Test Method for Slump of Hydraulic-Cement Concrete.* vol. 04.02, Concrete and Aggregate, pp. 89-91, 1998.

[3] Annual Book of ASTM Standards. *Designation: D 422-63 Standard test method for particle-size analysis of soils*, Philadelphia, PA, 1990.

[4] Blakey, B.C. and James, D.F. "Characterizing the rheology of laterite slurries ", *International Journal of Mineral Processing*, vol. 70, no. 1-4, pp. 23-39, 2003.

[5] Boger, D.V. "Rheology and the resource industries", *Chemical Engineering-Science*, vol. 464, no. 22, pp. 4525-4536, 2009.

[6] Cincilla, W.A., Landriault, D.A., and Verburg, R. "Application of paste technology to surface disposal of mineral wastes", *Proceeding of the 4th International Conference on Tailings and Mine Wastes 97*, Fort Collins, Colarado, USA, 343-356, 1997.

[7] Chalkley, M.E., Conard, B.R. Lakshmanan, V. I. and Wheeland, K.G. "Tailings and effluent management ", *International symposium on tailings and effluent management*, Pergamon Press, New York.vol. 20, pp.24, 1989

[8] Clarke, B. "Rheology of coarse settling suspensionsn", *Institution of Chemical Engineers – Transactions*, vol. 45, no. 6, pp. T251-T256, 1967

[9] Clayton, S., Grice, T.G., and Boger, D.V. "Analysis of the slump test for on-site yield stress measurement of mineral suspensions", *International Journal of Mineral Processing*, vol. 70, no. 1-4, pp.3 - 21, 2003.

[10] Coussot, P. and Proust, S. "Slow, unconfined spreading of a mudflow ", *Journal of Rheology*, vol. 40, no. 6, pp.1179 - 1189, 1996.

[11] Crowder, J.J. "Deposition, consolidation, and strength of a non-plastic tailings paste for surface disposal", Ph.D. Thesis, Department of Civil Engineering, University of Toronto, Toronto, Canada, 2004.

[12] Crowley, P.R. and Kitzes, A.S. "Rheological behavior of thorium oxide slurries in laminar flow", *Industrial and Engineering Chemistry*, vol. 49, no. 5, pp. 888 - 892, 1957.

[13] DIN (Deutsches Institude for Normung) 53019-2. 2001.

[14] Dunmula, A. and Simms, P. "Solute mass transport and atmospheric drying of high-density gold tailings", *Proceedings of the 13th International Seminar on Paste and Thickened tailings*, Toronto, Canada, 2010.

[15] Dzuy, N. Q. and Boger, D.V. "Yield stress measurement for concentrated suspensions", *Journal of Rheology*, vol. 27, no. 4, pp. 321 - 349, 1983.

[16] Engman, M., Sellgren, A., Sundquist, A., Wennberg, T., and Goldkuhl, I. "Users perspectives on the design of high density base metal tailings handling systems", *Proceedings of the eleventh tailings and mine waste conference*, Vail, Colorado, USA, pp. 45-54, 2004.

[17] Fisseha, B., Bryan, R., and Simms, P. " Evaporation, unsaturated flow, and oxidation in multilayer deposits of a gold paste tailings", *Proceedings of the 12th International Seminar on Paste and Thickened Tailings,* Via del Mar, Chile, April 21st -24th, 2009

[18] Fisseha, B., Bryan, R, and Simms, P. " Evaporation, unsaturated flow, and salt accumulation in multilayer deposits of a gold paste tailings",

ASCE Journal of Geotechnical and Geoenvironmental Engineering, In Press, doi:10.1061/(ASCE)GT.1943-5606.0000367, 2010.

[19] Fourie, A.B., Blight, G.E., and G. Papageorgiou "Static liquefaction as a possible explanation for the Merriespruit tailings dam failure", *Canadian Geotechnical Journal* , vol. 38, pp.707- 719, 2001.

[20] Fourie, A B. and Tshabalala, L. "Initiation of static liquefaction and the role of K_0 consolidation", *Canadian Geotechnical Journal,* vol. 42, no. 3, pp. 892-906, 2005.

[21] Gawu, S K.Y. and Fourie, A.B. "Assessment of the modified slump test as a measure of the yield stress of high-density thickened tailings", *Canadian Geotechnical Journal* , vol. 41, no. 1 pp.39-47, 2004.

[22] Hallborn, D.J. "The "lump" test", *Short Course, Rheology of Paste and Thickened Tilings*, 13th International Seminar on Paste and Thickened Tailings, Toronto, Canada, 2010

[23] Hallborn, D.J. "Pipe flow of homogeneous slurry", PHD Thesis, University of Biritish Columbia, Vancouver, Canada, 2008

[24] Hallborn, D.J. and Klein, B, "A physical model for yield plastic fluids", *Particle Science and Technology- An International Journal*, vol. 27, no. 1, 2009.

[25] Harris, J. "Rheology and Non-Newtonian Flow", Longman Inc., New York, USA, 1977

[26] Henriquez, J. and Simms, P. "Dynamic imaging and modeling of multilayer deposition of gold paste tailings", *Minerals Engineering*, vol. 22, no. 2, pp 128-139, 2009.

[27] Henriquez, J. "Dynamic imaging and modeling of gold paste tailings", M.A.Sc. Thesis, Department of Civil and Environmental Engineering, Carleton University, Ottawa, Canada, 2008.

[28] Houlihan, R.H., Mian, M.H. and Lord, E.R. "Oil sand tailings-technology development and regulations", *Proceeding of the 13th International Seminar on Paste and Thickened Tailings,* Toronto, Canada, 2010

[29] ICOLD and UNEP. *Bulletin121: Tailing dams-Risk of dangerous occurrences, Lesson learnt from practical experiences*, Paris, 144. 2001

[30] Jambor, J.L., Blowes, D.W. and Ritchie, A.I.M. "Environmental aspects of mine wastes ", Volume 31, Vancouver, British Columbia, 2003

[31] Jewell, R.J. and Fourie, A.B "Paste and Thickened Tailings-A guide ", Australian Centre for Geomechanics, Perth, Austrailia, 2006.

[32] Klein, B. and Hallborn, D.J., "Short Course: Rheology of paste and thickened tailings", *13th International Seminar on Paste and Thickened Tailings,* Toronto, Canada, 2010

[33] Kwak, M., James, D.F., and Klein, K.A. "Flow behavior of tailing paste for surface disposal", *Journal of Mineral Processing*, vol. 77, no. 3, pp. 139-1535, 2005.

[34] Leong, Y. and Boger, D.V. "Surface chemistry effects on concentrated suspension rheology", *Journal of colloid and interface science,* vol. 136, no. 1, pp. 249-258, 1990.

[35] Lideell, P.V. and Boger, D.V. "Yield stress measurement with the vane ", *Journal of Non-Newtonian Fluids Mechanics* vol. 63, no. 2-3, pp. 235-261, 1996.

[36] Liu, K.F. and Mei, C.C. "Approximate equations for the slow spreading of a thin sheet of Bingham plastic fluid", *Physics of Fluids A: Fluids Dynamics.* vol. 2, no. 1, pp. 30-36, 1990.

[37] MAC 2009, Mining Association of Canada Annual Report. Retrieved from Newsroom, the Mining ASSOCIATION OF Canada Web site: *http : //www.mining.ca/www/media − lib/MAC − Documents/Annual − Reports/*2009 − *annual − report − en.pdf*, 2009.

[38] Matthews, J.G., Shaw, W.H., Mackinnon, M.D., and Cuddy, R.G. "Development of Composite Tailings Technology at Syncrude", *International Journal of Surface Mining, Reclamation, and Environmental* , vol. 16, no. 1, pp. 147 - 157, 2002.

[39] McPhail, G. "Prediction of the beaching characteristics of hydraulically placed tailings", PhD Dissertation submitted to the University of the Witwatersrand, Johannesburg, SA, 1995

[40] Mpofu, P., Addai-Mensah, J., and Ralston, J. "Flocculation and dewatering behaviour of smectite dispersions: effect of polymer structure type", *Minerals Engineering* , vol. 17, pp.411 - 423, 2003.

[41] Newson, T.A. and Fahey, M. "Measurement of evaporation from saline tailings storages", *Engineering Geology.* vol. 70,no. 3-4 pp. 217-233, 2003.

[42] Nguyen Q. D. and Boger D. V. "Application of rheology to solving tailings disposal problems", *International Journal of Mineral Processing* , vol. 54, no. 3-4, pp.217-233, 1998.

[43] O'Kane, M., Wilson, G. W. and Barbour, S.L., "Instrumentation and monitoring of an engineered soil cover system for mine waste rock", *IEEE Canadian Geotechnical Journal,* Vol. 35, no. 5, pp. 828-846, 1998.

[44] Oxenford, J. and Lord, E.R. "Canadian Experience in the application of paste and thickened tailings for surface disposal", *Proceedings of the ninth international seminar on paste and thickened tailings*, Limerick, Ireland, pp. 93-105, 2006.

[45] Pashias, N., Boger D.V., Summers J., and D.J. Glenister, "A fifty centrheometer for yield stress measurement", *Journal of Geophysical Research*, vol. 101, no. B11, pp.217- 229, 1996.

[46] Pirouz, B. and Williams, M.P.A. " Prediction of non-segregating thickened tailings beach slopes a new method", *Proceedings of the Tenth International Seminar on Paste and Thickened Tailings*, Perth, Australia, March 13th 15th, pp. 315327, 2007.

[47] Price, W.A. "Challenges posed by metal leaching and acid rock drainage ", *Environmental aspects of mine wastes*, J. L. Jambor. Blowes, A.I.M Ritchie. 2003.

[48] Qiu, Y. and Sego, D.C. "Laboratory properties of mine tailings ", *Canadian Geotechnical Journal* , vol. 38, no. 1, pp.183-190, 2001.

[49] Robinsky, E. "Tailings disposal by the thickened discharge method for improved economy and environmental control", *Proceedings of 2nd Int. Tailing Symp., Argall, G.(ed.), Miller Freeman, San Francisco* pp. 75 - 95, 1979.

[50] Rowe, R. K., Quigley, R. M., and Booker, J. R. "Clayey barrier systems for waste disposal facilities ", London, Spon 1995.

[51] Scola, J.C. and Landriault, D. " An evaluation of high dewatered tailings disposal application in large scale mining operation in Chiles Atacama Desert ", *Proceeding of the 10th International Seminar on paste and Thickened tailings*, Australian Centre for Geomechanics, Perth, Australia, 329-335, 2007

[52] Shields, D.H. "Innovations in Tailings Disposal", *Canadian Geotechnical Journal,* vol. 12, no. 3, pp. 320-325, 1975.

[53] Shuttleworth, J.A., Thomson, B.J., and Wates, J.A. "Surface disposal at Bulyanhulu practical lessons learned", *6th International Conference on Paste and Thickened tailings*, Santiago, Chile, 2005

[54] Simms, P. "On the relation between laboratory flume tests and deposition angles of high density tailings", *Proceedings of the 10th International Seminar on Paste and Thickened tailings*, Australian Centre for Geomechanics, Perth, Australia, 329-335, 2007.

[55] Simms, P., Dumula, A., Fisseha, B. and Bryan, R. "Generic modeling of desiccation for cyclic deposition of thickened tailings to maximize density and to minimize oxidation", *Proceedings 13th International Seminar on Paste and Thickened tailings*, Toronto, Canada, 2010.

[56] Simms, P., Grabinsky M.W., and Zhan, G. "Modelling evaporation of paste tailings fom the Bulyanhulu mine", *Canadian Geotechnical Journal* , vol. 44, pp. 1417-1432. 2007

[57] Sofra, F. and Boger, D.V. "Environmental rheology for waste minimization in the minerals industry", *Chemical engineering Journal* , vol. 86, no. 3, pp.319-330, 2002.

[58] Sofra, F. and Boger, D.V. "Slope prediction for thickened tailings and pastes", *Proceeding of the Eighth International Conference on Tailings and Mine waste*, Fort Collins. Balkema, Rotterdam, pp.75- 83, 2001.

[59] Tanner, R. "Engineering Rheology ", Second Edition. Oxford University Press Inc., New York, USA, 2000.

[60] Tailing Performance Criteria and Requirement for Oil sands Mining Schemes."Energy Resources Conservation Board ", Directive(074) 2009.

[61] Ter-Stepanian, G. "Settling of tailings ", *proceeding of the seventh international conference on tailings and mine waste management*, colarado, usa, 2000.

[62] Theriault, J., Frostiak, J. and Welch D. "Surface disposal of paste tailings at the Bulyanhulu gold mine, Tanzania ", *Proceedings of Mining and the Environment III Conference, Sudbury 2003*, Mining and the Environment, Sudbury, Ontario, Canada, 2003.

[63] Vick, S. G. "Planning, design, and analysis of tailing dams", John Wiley and sons, USA, 1990.

[64] White, F.M. "Fluid mechanics", McGraw-Hill, New York, USA, 1986

[65] Wilson, G. W., Fredlund, D.G and Barbour, S.L. "The effect of soil suction on evaporative fluxes from soil surfaces ", *Canadian Geotechnical Journal* , vol. 34, no. 1, pp.145-155, 1997.

[66] Wilson, K. C., Addie, G. R., Sellgren, A. and Clift, R. "Slurry Transport Using Centrifugal Pumps ", Third edition, 2006.

[67] Wright, P.G. "The variation of viscosity with temperature", *Physics Education*, vol. 12, no. 5, pp. 323-325, 1977

[68] Yanful, E.K., Samad, M. and Mian, H. "Shallow Water Cover Technology for Reactive Sulphide Tailings Management", *Geotechnical News,* Vol. 22, no. 31, pp. 42-51, 2004.

[69] Yuhi, M. and Mei, C.C. "Slow spreading of fluid mud over a conical surface", *Journal of Fluid Mechanics,* Vol. 519, pp. 337-358, 2004.